Acta Oceanologica Sinica
Founded in 1982, monthly publication
Academic Journal with Top International Influence in China (Top 5%)
Impact factor: 1.369
CAS ranking: oceanography 2

# Virtual Edition for South China Sea

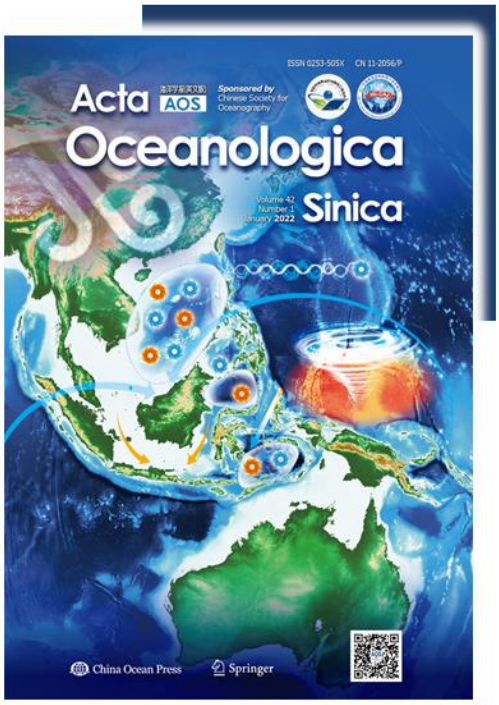


Special Topic for The South China Sea Annual Meeting 2021

As a marginal sea of the western Pacific, the South China Sea (SCS) sits in the corridor of the East Asian Monsoon and pathway of Pacific typhoons. There are active multi-scale dynamical and biogeochemical processes worth pursuing. The three-layer circulation with active mesoscale eddies provides the basic dynamic environment for processes in the SCS. The variations in the Pacific and Indian Oceans change the circulation in the SCS through the atmospheric bridge and the ocean channels. Furthermore, energetic submesoscale fronts, waves, and turbulent mixing occur and play crucial roles in the biogeochemical processes in the SCS.

The South China Sea Annual Meeting (SCSAM) 2022 will be held on December 3–4 online by Jiangxi Normal University, focusing on academic exchanges of the new research results and progresses in the interdisciplinary multi-scale processes in the SCS. The SCSAM 2022 is the ninth international workshop of the series, which started in April 2013 and renamed as SCSAM in 2018 (see details on Page 75).

# Acta Oceanologica Sinica

## Subject Index to 2020.11-2023.01 South China Sea

**CONTENTS**

点击题目
链接摘要

### The South China Sea Annual Meeting 2021 (Vol. 42 No.1)



### The South China Sea Annual Meeting 2020 (Vol. 41 No. 7)

## The South China Sea Annual Meeting 2019 (Vol. 39 No.11)

## Natural gas geology in the South China Sea (Vol. 40 No.2)

## Physical Oceanography, Marine Meteorology and Marine Physics

## Marine Chemistry



## Marine Geology

## Marine Biology



## Ocean Engineering



## Marine Technology

## Marine Information Science



## News and Views

*Acta Oceanol. Sin.*, 2023
https://doi.org/10.1007/s13131-022-2091-4
http://www.aosocean.com
E-mail: ocean2@hyxb.org.cn

# Nitrate isotope dynamics in the lower euphotic-upper mesopelagic zones of the western South China Sea

Zixuan Li[1], Chao Xu[1], Minfang Zheng[1], Mengya Chen[1], Yusheng Qiu[1], Hantao Zhou[1], Min Chen[1], Run Zhang[1]*

[1] College of Ocean and Earth Sciences, Xiamen University, Xiamen 361102, China

Received 31 January 2022; accepted 12 July 2022



**Abstract**

The dual isotopes (N and O) of nitrate were measured using a denitrifier bacterial method in the western South China Sea (WSCS) during September 2015 to elucidate key information during N transformation in the lower euphotic zone (LEZ)-upper mesopelagic zone (UMZ, down to 500 m in this study) continuum, which is a vital sub-environment for marine N cycle and sequestration of atmospheric $CO_2$ as well. The N isotopic composition ($\delta^{15}N$) of nitrate generally decreased from 500 m toward the base of the euphotic zone (~100 m), reaching a value of ~4.6‰ (vs. air $N_2$) at the base of the LEZ, suggesting the imprint of remineralization (nitrification) of isotopically light N from atmospheric source. The $\delta^{15}N$ and $\delta^{18}O$ of nitrate only generally conform to a 1:1 line at 50 m and 75 m, suggesting that nitrate assimilation is a dominant process to shape nitrate isotope signature in this light-limited and relatively N-replete lower part of the euphotic zone. The fractionation factors of N and O isotopes during nitrate fractionation ($^{15}\varepsilon_{ASSIM}$, $^{18}\varepsilon_{ASSIM}$) using a steady-state model were estimated to be 4.0‰±0.3‰ and 5.4‰±0.3‰, respectively. The occurrence of nitrification at the base of the LEZ and most of the UMZ is corroborated by the decoupling of $\delta^{15}N$ and the oxygen isotopic composition ($\delta^{18}O$) of nitrate. Our results will provide insights for better understanding N cycle in the South China Sea from a perspective of present and past.

**Key words:** N and O isotopes, nitrate assimilation, nitrification, western South China Sea

**Citation:** Li Zixuan, Xu Chao, Zheng Minfang, Chen Mengya, Qiu Yusheng, Zhou Hantao, Chen Min, Zhang Run. 2023. Nitrate isotope dynamics in the lower euphotic-upper mesopelagic zones of the western South China Sea. Acta Oceanologica Sinica, doi: 10.1007/s13131-022-2091-4

## 1 Introduction

The availability of nitrogen (N) nutrients in the surface ocean acts as an important control on primary production and the sequestration of atmospheric $CO_2$ in the ocean (Sigman et al., 2010). In low latitude oligotrophic oceans, N is commonly a limiting factor for primary production in the euphotic zone due to limited input nitrate from subsurface under highly stratified condition of the upper water column (Moore et al., 2013). Besides, $N_2$ fixation and atmospheric deposition also play a complementary role by providing new N for the ecosystem and thus contribute to the export of organic matter out of the euphotic zone (Karl et al., 1997). Post formation in the euphotic zone, a portion of the organic N, largely in the form of sinking particle N, will be exported downward undergo remineralization at intermediate depth and recycle back to nitrate pool (Kao et al., 2012).

For the stratified oligotrophic regimes, a layered structure of euphotic zones with respect to the rates of chemical scavenging and elemental transport may be a general and ubiquitous feature globally (Cai et al., 2008; Dore and Karl, 1996; Dore et al., 2008). It had been elucidated by $^{234}Th$:$^{238}U$ disequilibria that the oceanic stratified euphotic zone can separated into two layers, i.e., an upper oligotrophic zone (UEZ) contributing to majority of the primary production but low net export, and a lower eutrophic zone (LEZ) contributing less to primary production but has much more intense scavenging (Coale and Bruland, 1987). Indeed, the oligotrophic regions are featured by remineralization-intensive ecosystems where most of the organic matter there is recycled rapidly especially for the UEZ (Karl et al., 2021). Thus, the LEZ acts as the interface connecting the UEZ and the upper portion of the mesopelagic zone (UMZ), within which key microbial remineralization and nutrient recycling reactions occur with the degradation of sinking particulate organic material (Peters et al., 2018).

The LEZ-UMZ continuum is a key sub-environment for understanding N cycle in the ocean at least for the following reasons. First, in the UEZ dissolved inorganic N (DIN) is depleted, while in the LEZ there is usually a non-negligible concentration of unused nitrate left (like in the South China Sea (SCS)) (Zhang et al., 2020). Hence, any variability in N assimilation will have the potential to affect the net export of N and its isotopic composition ($\delta^{15}N$). Second, relative to UEZ, LEZ is much more influenced directly by nutrient injections from the bordering UMZ. Last but not least, LEZ is characterized by low ambient light intensity but elevated nitrate concentration, and a non-negligible fraction of primary production occurring in the LEZ of the oligotrophic regimes (e.g., ~20% at Station ALOHA in the North Pacific Subtropical Gyre; Karl et al., 2021). Considering that the index of carbon export efficiency, i.e., e-ratio (particulate carbon export at export interface/depth-integrated primary production), is typically low in oligotrophic oceanic regions (e.g., ~0.052 at Sta-

Foundation item: The National Natural Science Foundation of China under contract Nos 42076042 and 41721005; the Science and Technology Basic Resources Investigation Program of China under contract No. 2017FY201403.
*Corresponding author, E-mail: zhangrun@xmu.edu.cn

*Acta Oceanol. Sin.*, 2023
https://doi.org/10.1007/s13131-022-2101-6
http://www.aosocean.com
E-mail: ocean2@hyxb.org.cn

# Distribution and risk assessment of heavy metals in surface sediments of coastal mudflats on Leizhou Peninsula, China

Tingting Li[1, 2, 3*], Lili Jia[3], Xin Zhu[3], Min Xu[1], Xinchang Zhang[4, 5]

[1] Key Laboratory of Ocean and Marginal Sea Geology, South China Sea Institute of Oceanology, Chinese Academy of Sciences, Guangzhou 510301, China

[2] University of Chinese Academy of Sciences, Beijing 100049, China

[3] Guangdong Geological Survey Institute, Guangzhou 510080, China

[4] State Key Laboratory of Isotope Geochemistry, Guangzhou Institute of Geochemistry, Chinese Academy of Sciences, Guangzhou 510640, China

[5] CAS Center for Excellence in Deep Earth Science, Guangzhou 510640, China

Received 23 May 2022; accepted 13 September 2022



**Abstract**

Mudflats play a vital role in maintaining the dynamic balance between sea and land. To understand the characteristics, sources, and pollution risks of six heavy metals (As, Cd, Cr, Cu, Hg, and Pb) in the coastal mudflats on the Leizhou Peninsula, 257 surface sediment samples were studied using mathematical statistics, correlation analysis, and factor analysis. The results show that the overall concentrations of these heavy metals are low although there are several high abnormal points in the local areas. The strong correlation between these heavy metals indicates that the sources of some of the metals are similar, yet their elemental combinations in different cities (counties) varied. According to the calculated enrichment factor (EF), anthropogenic activity-induced heavy metals were determined in order of decreasing influence: As, Cd, Pb, Cr, Cu, and Hg. The low EF values of Hg indicate that it is not present as a contaminant in the study area, while low values of Cr and Cu from the Lianjiang City suggest that these two metals were also attributed to natural sources. The presence of As, Cd, Cr, Cu, and Pb from the remaining cities (counties) should be influenced by anthropogenic activities. The overall potential ecological risk index indicates that the ecological risks posed by the six analyzed heavy metals to the Leizhou Peninsula mudflats, in order of decreasing risk, are Cd, As, Hg, Pb, Cu, and Cr. It is noteworthy that only Cd in Lianjiang City demonstrated substantial ecological risk. Other examined heavy metals in other cities of the study area showed slight ecological risk.

**Key words:** mudflats, heavy metals, ecological risk assessment, source identification, Leizhou Peninsula

**Citation:** Li Tingting, Jia Lili, Zhu Xin, Xu Min, Zhang Xinchang. 2023. Distribution and risk assessment of heavy metals in surface sediments of coastal mudflats on Leizhou Peninsula, China. Acta Oceanologica Sinica, doi: 10.1007/s13131-022-2101-6

## 1 Introduction

Mudflats are found in the tidal zone where strong land-sea interactions exist. They are influenced by multiple factors such as tides, waves, rivers, geological formations, and climate change, and play a vital role in maintaining the dynamic balance between sea and land. The mudflat environmental changes are closely related to coastal economic development and social progress, and have a big significance in maintaining regional and global ecosystem balance (Bastami et al., 2014; Cui et al., 2016; Gao et al., 2016; Kulkarni et al., 2018). Mudflats are also the primary sources, sinks, and converters of various pollutants, playing a critical role in the prevention and control of water pollution as well as elemental cycling (Gao et al., 2012; Wang et al., 2013; Wu et al., 2014).

Environmental pollution has led to increasing degradation of ecosystem service functions in coastal mudflat wetlands. As typical cumulative pollutants, heavy metal elements have substantial biological toxicity and pose persistent threats to human health and the ecological environment (Cai et al., 2003, 2019a, 2019b; Tang et al., 2008; Chen et al., 2015; Zhang et al., 2019; Wang et al., 2020). Though many human and material resources have been invested in the study of heavy metal elements in mudflats, China remains behind other developed countries in responding to this issue. In 1986, China conducted the first national survey of coastal zone and seabed resources (Xi, 2004). Since 2002, the China Geological Survey has conducted environmental geochemical studies of heavy metals in various media such as soil, rock, sediment, and atmospheric fallout on a national scale (Xi, 2007). This has also involved the study of heavy metals in the coastal zone (Xi, 2005). The State Oceanic Administration of China conducted a special study on the pre-evaluation of an offshore marine comprehensive survey, which covered the investigation of heavy metals in offshore sediments (Jiang et al., 2015; Chai et al., 2019; Huang et al., 2020). However, these previous

Foundation item: The Guangdong, Guizhou, Hunan and Jiangxi 1:250,000 land quality geochemical survey under contract No. DD20160327-04; the National Natural Science Foundation of China under contract No. U1911202; the Guangdong Basic and Applied Basic Research Foundation under contract No. 2021A1515011547; the Guangzhou Basic and Applied Basic Research Foundation under contract No. 202102020465.

*Corresponding author, E-mail: tingtingliscsio@126.com

*Acta Oceanol. Sin.*, 2023
https://doi.org/10.1007/s13131-022-2045-x
http://www.aosocean.com
E-mail: ocean2@hyxb.org.cn

# The influence of lipid-extraction on the $\delta^{13}C$ of mesopelagic and demersal fish in the South China Sea: modification and application of lipid normalization models

Linyu Wang[1], Fuqiang Wang[1, 2], Zuozhi Chen[3], Ying Wu[1]*

[1] State Key Laboratory of Estuarine and Coastal Research, East China Normal University, Shanghai 200241, China

[2] Pilot National Laboratory for Marine Science and Technology (Qingdao), Qingdao 266237, China

[3] South China Sea Fisheries Research Institute, Chinese Academy of Fishery Sciences, Guangzhou 100141, China

Received 31 December 2021; accepted 6 April 2022



**Abstract**

Mesopelagic fish, the most important daily vertically migrating community in the oceans, are characterized by high lipid content which may obscure the interpretation of stable isotopes analysis. Demersal fish, which are important consumers in the food web dominated by mesopelagic fish, also have a high lipid content. Here we collected 127 fish samples from the South China Sea and evaluated the effect of lipid contents on $\delta^{13}C$ of mesopelagic and demersal fish. In lipid-extracted mesopelagic fish, the C/N content ratio (<5.5) shows a clear correlation with $\Delta\delta^{13}C$ (the offset of bulk and lipid-extracted $\delta^{13}C$ values), especially in non-migratory and semi-migratory species; these values were less correlation in demersal fish. Based on our results, we suggest that mesopelagic and demersal fish in different regions of the South China Sea should be studied separately using appropriate correction models and less fit for the traditional model. Moreover, the C/N content ratio should be used cautiously for establishing the lipid normalization model, especially for the fish in migratory mesopelagic fish and demersal fish. Our results also reveal that mesopelagic fish across nearby regions could be analyzed together. The new models described here can be applied in future studies of mesopelagic and demersal fish in the South China Sea.

**Key words:** mesopelagic fish, demersal fish, lipid normalization model, C/N content ratio, lipid content, $\delta^{13}C$, South China Sea

**Citation:** Wang Linyu, Wang Fuqiang, Chen Zuozhi, Wu Ying. 2023. The influence of lipid-extraction on the $\delta^{13}C$ of mesopelagic and demersal fish in the South China Sea: modification and application of lipid normalization models. Acta Oceanologica Sinica, doi: 10.1007/s13131-022-2045-x

## 1 Introduction

Mesopelagic fish dominate (in number and biomass) among open ocean teleostean fish. Most mesopelagic fish exhibit the behavioral trait of daily vertical migration through the water as a refuge against predators during the day and in pursuit of food at night (Olivar et al., 2012; Sutton, 2013). These fish play substantial roles in the active carbon transport process in the water column by carrying ingested zooplankton downward to deeper zones. Thus, these fish are a key factor in the open ocean food-webs and carbon flux (Irigoien et al., 2014). To satisfy the energy requirement for daily vertical migration, mesopelagic fish have a higher content of lipids, with indispensable functions in energy store and buoyancy (Catul et al., 2011; Hudson et al., 2014; Stowasser et al., 2009b; Wang et al., 2019a). Moreover, other mesopelagic fish groups, including non-migrant planktivores, and piscivores, and semi-migrant piscivores, are also essential in indirect carbon transport (Jónasdóttir et al., 2015). Mesopelagic fish also play an important role in marine food webs by providing food resources for the demersal fish (Richards et al., 2019).

Stable isotopes have been used to investigate the trophic ecology of mesopelagic fish in several regions (Eduardo et al., 2021). The carbon isotope content ratio ($^{13}C$:$^{12}C$), typically notated as $\delta^{13}C$, provides a time-integrated measure of carbon transfer to a consumer from their diet (Park et al., 2018; Peterson and Fry, 1987; Post, 2002). However, lipid $\delta^{13}C$ values are more likely to be depleted than carbon discrimination during synthesis and storage, resulting in more negative $\delta^{13}C$ values (DeNiro and Epstein, 1977; Newsome et al., 2010, 2018). The dietary sources revealed by $\delta^{13}C$ without lipid extraction are obscure due to the high lipid content in mesopelagic fish. Therefore, it is crucial to eliminate the effect of lipid content on the $\delta^{13}C$ value in these fish (Wang et al., 2019b). Whether it is appropriate to unify the existing models has not been studied (Cherel et al., 2010; Colaço et al., 2013; Fanelli et al., 2011; McClain-Counts et al., 2017; Olivar et al., 2019; Richards et al., 2019; Valls et al., 2014). Considering that mesopelagic fish tend to have high lipid content, we must cautiously eliminate lipid effects on $\delta^{13}C$ (Catul et al., 2011).

To eliminate the lipid effect and avoid time-consuming chemical extraction, the lipid normalization model has been recommended as the main method of sample standardization (Weldrick et al., 2019). There are two principal models typically used in studying the relationship between $\delta^{13}C$ and C/N content

Foundation item: the National Natural Science Foundation of China under contract Nos 42090043 and 41876074; the National Basic Research Program (973 Program) of China under contract No. 2014CB441502.
*Corresponding author, E-mail: wuying@sklec.ecnu.edu.cn

*Acta Oceanol. Sin.*, 2023
https://doi.org/10.1007/s13131-022-2097-y
http://www.aosocean.com
E-mail: ocean2@hyxb.org.cn

# Declined trends of chlorophyll *a* in the South China Sea over 2005–2019 from remote sensing reconstruction

Tianhao Wang[3], Yu Sun[4, 5], Hua Su[4, 5], Wenfang Lu[1, 2*]

[1] School of Marine Sciences, Sun Yat-Sen University, Zhuhai 519000, China

[2] Southern Marine Science and Engineering Guangdong Laboratory (Zhuhai), Zhuhai 519000, China

[3] State Key Laboratory of Marine Environmental Science, College of Ocean and Earth Sciences, Xiamen University, Xiamen 361102, China

[4] Key Laboratory of Spatial Data Mining and Information Sharing of Ministry of Education, Fuzhou University, Fuzhou 350108, China

[5] National & Local Joint Engineering Research Center of Satellite Geospatial Information Technology, Fuzhou University, Fuzhou 350108, China

Received 27 January 2022; accepted 15 August 2022



**Abstract**

Chlorophyll *a* concentration (CHL) is an important proxy of the marine ecological environment and phytoplankton production. Long-term trends in CHL of the South China Sea (SCS) reflect the changes in the ecosystem's productivity and functionality in the regional carbon cycle. In this study, we applied a previously reconstructed 15-a (2005–2019) CHL product, which has a complete coverage at 4 km and daily resolutions, to analyze the long-term trends of CHL in the SCS. Quantile Regression was used to elaborate on the long-term trends of high, median, and low CHL values, as an extended method of conventional linear regression. The results showed downward trends of the SCS CHL for the 75th, 50th, and 25th quantile in the past 15 a, which were –0.004 0 mg/(m$^3$·a) (–1.62% per year), –0.002 3 mg/(m$^3$·a) (–1.10% per year), and –0.001 9 mg/(m$^3$·a) (–1.01% per year). The negative trends in winter (November to March) were more prominent than those in summer (May to September). In terms of spatial distribution, the downward trend was more significant in regions with higher CHL. These led to a reduced standard deviation of CHL over time and space. We further explored the influence of various dynamic factors on CHL trends for the entire SCS and two typical systems (winter Luzon Strait (LZ) and summer Vietnam Upwelling System (SV)) with single-variate linear regression and multivariate random forest analysis. The multivariate analysis suggested the CHL trend pattern can be best explained by the trends of wind speed and mixed-layer depth. The divergent importance of controlling factors for LZ and SV can explain the different CHL trends for the two systems. This study expanded our understanding of the long-term changes of CHL in the SCS and provided a reference for investigating changes in the marine ecosystem.

**Key words:** chlorophyll *a* concentration, quantile trends, remote sensing reconstruction, South China Sea

**Citation:** Wang Tianhao, Sun Yu, Su Hua, Lu Wenfang. 2023. Declined trends of chlorophyll *a* in the South China Sea over 2005–2019 from remote sensing reconstruction. Acta Oceanologica Sinica, doi: 10.1007/s13131-022-2097-y

## 1 Introduction

Phytoplankton is the basis of the food chain in the ocean. It affects sea-surface carbon dioxide through photosynthesis. Chlorophyll-*a* (CHL) is one of the most important indicators of the phytoplankton biomass (Behrenfeld and Falkowski, 1997), and is often used to represent primary productivity. CHL also serves as a tracer of the physical dynamics of the ocean (Lévy et al., 2018). Studying CHL variability not only helps understand the energy flow (Longhurst et al., 1995) and material cycles in the marine ecosystem (Keiner and Yan, 1998; Aumont et al., 2002), but also promotes the research of carbon cycles (Boon and Duineveld, 1998) and supports the estimation of $CO_2$ concentration (Chen et al., 2011). The long-term variabilities and trends of CHL are key components of climate studies, such as the studies of the El Niño-Southern Oscillation (Feng and Zhu, 2012), sea-level rise (Wilson and Adamec, 2001), and other global issues (Huynh et al., 2020; Grémillet et al., 2008; Kouketsu et al., 2016).

The South China Sea (SCS) is the largest marginal sea in the western Pacific Ocean. The topography of the SCS varies greatly, with broad shelves and a deep basin larger than 5 000 m. The SCS is a semi-enclosed sea basin that connects to the Pacific Ocean and the Indian Ocean through Luzon Strait and the Malacca Strait, respectively. In addition to the water exchange with the open ocean, there is also abundant runoff input into the SCS (Liu et al., 2010, 2013). The SCS has distinct biogeochemical regimes consisting of an oligotrophic basin and river-dominated shelves (Dai et al., 2022). As a representative marginal sea and a weak source of $CO_2$ to the atmosphere (Dai et al., 2013), the ecosystem of the SCS has been paid broad attention. The changes in the SCS ecosystem can lead to changes in the capacity of carbon pumps (Lu et al., 2018a), altering the regional carbon cycle (Wang et al., 2021a) and other ecosystem functionalities. With the development of satellite remote sensing (Carder et al., 1999; Doney et al., 2009), opportunities were provided to reveal multi-scale variabil-

Foundation item: The National Natural Science Foundation of China under contract No. 41906019.
*Corresponding author, E-mail: luwf6@sysu.edu.cn

*Acta Oceanol. Sin.*, 2022, Vol. 41, No. 7, P. 1–12
https://doi.org/10.1007/s13131-022-2013-5
http://www.aosocean.com
E-mail: ocean2@hyxb.org.cn

# Circulation in the South China Sea is in a state of forced oscillation: Results from a simple reduced gravity model with a closed boundary

Rui Xin Huang[1], Hui Zhou[2, 3, 4*]

[1] Woods Hole Oceanographic Institution, Woods Hole, Massachusetts 02543, USA

[2] Key Laboratory of Ocean Circulation and Waves, Institute of Oceanology, Chinese Academy of Sciences, Qingdao 266071, China

[3] Laboratory for Ocean Dynamics and Climate, Pilot National Laboratory for Marine Science and Technology (Qingdao), Qingdao 266237, China

[4] University of Chinese Academy of Sciences, Beijing 100049, China

Received 10 June 2021; accepted 26 November 2021



**Abstract**

The South China Sea (SCS) is a narrow semi-enclosed basin, ranging from 4°–6°N to 21°–22°N meridionally. It is forced by a strong annual cycle of monsoon-related wind stress. The Coriolis parameter $f$ increases at least three times from the southern basin to the northern basin. As a result, the basin-cross time for the first baroclinic Rossby wave in the southern part of the basin is about 10-times faster than that in the northern part, which plays the most vitally important role in setting the circulation. At the northernmost edge of SCS, the first baroclinic Rossby wave takes slightly less than 1 year to move across the basin, however, it takes only 1–2 months in the southernmost part. Therefore, circulation properties for a station in the model ocean are not solely determined by the forcing at that time instance only; instead, they depend on the information over the past months. The combination of a strong annual cycle of wind forcing and large difference of basin-cross time for the first baroclinic Rossby wave leads to a strong seasonal cycle of the circulation in the SCS, hence, the circulation is dominated by the forced oscillations, rather than the quasi-steady state discussed in many textbooks.The circulation in the SCS is explored in detail by using a simple reduced gravity model forced by seasonally varying zonal wind stress. In particular, for a given time snap the western boundary current in the SCS cannot play the role of balancing mass transport across each latitude nor balancing mechanical energy and vorticity in the whole basin. In a departure from the steady wind-driven circulation discussed in many existing textbooks, the circulation in the SCS is characterized by the imbalance of mechanical energy and vorticity for the whole basin at any part of the seasonal cycle. In particular, the western boundary current in the SCS cannot balance the mass, mechanical energy, and vorticity in the seasonal cycle of the basin. Consequently, the circulation near the western boundary cannot be interpreted in terms of the wind stress and thermohaline forcing at the same time. Instead, circulation properties near the western boundary should be interpreted in terms of the contributions due to the delayed wind stress and the eastern boundary layer thickness. In fact, there is a clear annual cycle of net imbalance of mechanical energy and vorticity source/sink. Results from such a simple model may have important implications for our understanding of the complicated phenomena in the SCS, either from *in-situ* observations or numerical simulations.

**Key words:** South China Sea, ocean circulation, annual cycle, first baroclinic Rossby wave propagation, western boundary current, forced ossilation

**Citation:** Huang Rui Xin, Zhou Hui. 2022. Circulation in the South China Sea is in a state of forced oscillation: Results from a simple reduced gravity model with a closed boundary. Acta Oceanologica Sinica, 41(7): 1–12, doi: 10.1007/s13131-022-2013-5

## 1 Introduction

The circulation in South China Sea (SCS) shares many important characters with the circulation in the world oceans. Circulation in the SCS can be separated into two components, the wind-driven circulation and the thermohaline circulation. Our study in this note is focused on the wind-driven circulation, which has been studied in many previous publications (Wyrtki, 1961; Shaw et al., 1999; Chu et al., 1999; Qu, 2000; Fang et al., 2002; Yang et al., 2002; Gan et al., 2006; Wang et al., 2006).

One of the most important characters of the wind-driven circulation in the SCS is that the strong annual cycle related to the South Asia monsoon. In fact, wind stress in the SCS can completely reverse its direction during a typical annual cycle. The time evolution during the annual cycle is an important aspect of

Foundation item: The Strategic Priority Research Program of the Chinese Academy of Sciences under contract No. XDB42000000; the National Natural Science Foundation of China under contract No. 41876009.
*Corresponding author, E-mail: zhouhui@qdio.ac.cn

*Acta Oceanol. Sin.*, 2022, Vol. 41, No. 7, P. 13–25
https://doi.org/10.1007/s13131-021-1954-4
http://www.aosocean.com
E-mail: ocean2@hyxb.org.cn

# Vertical velocity and transport in the South China Sea

Yaohua Zhu[1, 2, 3], Dingqi Wang[1, 4], Yonggang Wang[1, 2, 3], Shujiang Li[1, 2, 3], Tengfei Xu[1, 2, 3], Zexun Wei[1, 2, 3*]

[1] First Institute of Oceanography, and Key Laboratory of Marine Science and Numerical Modeling, Ministry of Natural Resources, Qingdao 266061, China

[2] Laboratory for Regional Oceanography and Numerical Modeling, Pilot National Laboratory for Marine Science and Technology (Qingdao), Qingdao 266237, China

[3] Shandong Key Laboratory of Marine Science and Numerical Modeling, Qingdao 266061, China

[4] College of Oceanic and Atmospheric Sciences, Ocean University of China, Qingdao 266100, China

Received 4 August 2021; accepted 12 October 2021



**Abstract**

Deep water in the South China Sea is renewed by the cold and dense Luzon Strait overflow. However, from where and how the deep water upwells is poorly understood yet. Based on the Hybrid Coordinate Ocean Model reanalysis data, vertical velocity is derived to answer these questions. Domain-integrated vertical velocity is of two maxima, one in the shallow water and the other at depth, and separated by a layer of minimum at the bottom of the thermocline. Further analysis shows that this two-segmented vertical transport is attributed to the vertical compensation of subsurface water to the excessive outflow of shallow water and upward push of the dense Luzon Strait overflow, respectively. In the abyssal basin, the vertical transport increases upward from zero at the depth of 3 500–4 000 m and reaches a maximum of $1.5\times10^6$ m$^3$/s at about 1 500 m. Deep water upwells mainly from the northeastern and southwestern ends of the abyssal basin and off the continental slopes. To explain the upward velocity arising from slope breaks, a possible mechanism is proposed that an onshore velocity component can be derived from the deep western boundary current above steep slopes under bottom friction.

**Key words:** vertical velocity, vertical transport, Luzon Strait overflow, South China Sea

**Citation:** Zhu Yaohua, Wang Dingqi, Wang Yonggang, Li Shujiang, Xu Tengfei, Wei Zexun. 2022. Vertical velocity and transport in the South China Sea. Acta Oceanologica Sinica, 41(7): 13–25, doi: 10.1007/s13131-021-1954-4

## 1 Introduction

The South China Sea (SCS) covers an area of $3.5\times10^6$ km$^2$, including $1.68\times10^6$ km$^2$ on continental shelves, $1.26\times10^6$ km$^2$ on slopes and $0.55\times10^6$ km$^2$ in the abyssal basin below 3 000 m (Fig. 1). In view of the 200 m isobath, it is a semienclosed oceanic basin (Wang, 1986). The SCS connects to the western Pacific through its sole deepwater renewal channel, the Luzon Strait, with the deepest sill at about 2 400 m. Below the depth of 1 500 m, the density on both sides of the Luzon Strait bifurcates, and water is denser on the Pacific side than that on the SCS side. As a result, there exists a persistent pressure gradient across the Luzon Strait, driving a so-called Luzon Strait deepwater overflow from the Pacific into the SCS (Nitani, 1972; Qu et al., 2006; Li and Qu, 2006; Zhao et al., 2014; Zhang et al., 2015). The bifurcation depth of water density, about 1 500 m, is thus considered as the upper interface of the Luzon Strait overflow. After the dense Pacific water sinks into the SCS through the gaps in the Heng-Chun Ridge, the abyssal water in the SCS is renewed and must upwell somewhere. Then, scientific questions arise. At what depth and from where the abyssal water upwells? What is the causal mechanism?

Vertical velocity in the SCS has been studied as an important index of regional upwelling and downwelling. Among previous studies, Chai et al. (2001) analyzed formation of upwelling in the nearshore areas and Gan et al. (2013) focused on dynamics of the intensified downwelling over a widened northern SCS continental shelf. Xie et al. (2012), Jing et al. (2015) and Xie et al. (2017) investigated the vertical circulation and its dynamics on the continental shelf east of Hainan Island. Qu (2000) and Qu et al. (2007) discussed offshore upwelling in the upper layer using historical temperature profiles, while Chao et al. (1996), Shu et al. (2014), and Cai and Gan (2020) analyzed vertical velocity in the deep layer using numerical models. Until now, an overall look of the vertical velocity and associated transport in the SCS basin scale is not in focus yet, however, it is an important part of vertical circulation and also links the layered horizontal circulation. Our objective of this study is to reveal the spatial pattern of vertical velocity and structure of vertical transport. Further, we devote to the mechanism how the vertical velocity arises from the abyssal basin, and mechanism how the vertical transport is forced. Finally, we analyze the role of vertical velocity and vertical transport, and then diagram the three-dimensional circulation in the SCS.

The rest of the paper is organized as follows. In Section 2, we describe the method and validate the data used in this study. Section 3 is devoted to the vertical velocity and mechanism of the vertical transport in the thermocline. Section 4 focuses on the vertical velocity and transport in the deepwater cell. A possible mechanism of upward velocity in the abyssal basin is proposed in Section 5, followed by a summary and conclusions in Section 6.

Foundation item: The National Key Research and Development Program of China under contract No. 2019YFC1408400; the National Natural Science Foundation of China under contract Nos 41876029, 41821004 and 41776042.
*Corresponding author, E-mail: weizx@fio.org.cn

*Acta Oceanol. Sin.*, 2022, Vol. 41, No. 7, P. 26–41
https://doi.org/10.1007/s13131-022-2014-4
http://www.aosocean.com
E-mail: ocean2@hyxb.org.cn

# High-resolution simulation of upper-ocean submesoscale variability in the South China Sea: Spatial and seasonal dynamical regimes

Haijin Cao[1, 2*], Xin Meng[2], Zhiyou Jing[3], Xiaoxiao Yang[2]

[1] Key Laboratory of Marine Hazards Forecasting of Ministry of Natural Resources, Hohai University, Nanjing 210024, China

[2] College of Oceanography, Hohai University, Nanjing 210024, China

[3] State Key Laboratory of Tropical Oceanography, South China Sea Institute of Oceanology, Chinese Academy of Sciences, Guangzhou 510301, China

Received 22 July 2021; accepted 18 November 2021



**Abstract**

Submesoscale processes in marginal seas usually have complex generating mechanisms, highly dependent on the local background flow and forcing. This numerical study investigates the spatial and seasonal differences of submesoscale activities in the upper ocean of the South China Sea (SCS) and the different dynamical regimes for sub-regions. The spatial and seasonal variations of vertical vorticity, horizontal convergence, lateral buoyancy gradient, and strain rate are analyzed to compare the submesoscale phenomenon within four sub-regions, the northern region near the Luzon Strait (R1), the middle ocean basin (R2), the western SCS (R3), and the southern SCS (R4). The results suggest that the SCS submesoscale processes are highly heterogeneous in space, with different seasonalities in each sub-region. The submesoscale activities in the northern sub-regions (R1, R2) are active in winter but weak in summer, while there appears an almost seasonal anti-phase in the western region (R3) compared to R1 and R2. Interestingly, no clear seasonality of submesoscale features is shown in the southern region (R4). Further analysis of Ertel potential vorticity reveals different generating mechanisms of submesoscale processes in different sub-regions. Correlation analyses also show the vertical extent of vertical velocity and the role of monsoon in generating submesoscale activities in the upper ocean of sub-regions. All these results suggest that the sub-regions have different regimes for submesoscale processes, e.g., Kuroshio intrusion (R1), monsoon modulation (R2), frontal effects (R3), topography wakes (R4).

**Key words:** submesoscale, South China Sea, high-resolution simulation, spatial difference, seasonal difference

**Citation:** Cao Haijin, Meng Xin, Jing Zhiyou, Yang Xiaoxiao. 2022. High-resolution simulation of upper-ocean submesoscale variability in the South China Sea: Spatial and seasonal dynamical regimes. Acta Oceanologica Sinica, 41(7): 26–41, doi: 10.1007/s13131-022-2014-4

## 1 Introduction

Upper-ocean submesoscale processes, with horizontal scales of a few to tens of kilometers and time scales of a few days, are ubiquitous in the ocean and have strong impacts on the oceanic flows. A number of studies have revealed that submesoscale processes play a key role in the restratification of mixed layer (ML) (Boccaletti et al., 2007; Fox-Kemper et al., 2008; Bachman et al., 2017), oceanic vertical transport of salt, heat, biogeochemical productivity (Mahadevan and Tandon, 2006; Lévy et al., 2012; Zhong and Bracco, 2013; Rosso et al., 2014; Siegelman et al., 2020), and energy transfer to smaller scales (Capet et al., 2008; Cao et al., 2021). Understanding these effects is crucial to the upper-ocean mixing (Yang et al., 2017), planktonic ecosystem (Lévy et al., 2018), and oceanic energy cycle (Dong et al., 2020; Cao et al., 2021). Some other studies through numerical simulations (Sasaki et al., 2014; Brannigan et al., 2015; Rocha et al., 2016; Wang et al., 2018; Zhang et al., 2020) and observations (Callies et al., 2015; Thompson et al., 2016; Yu et al., 2019) have shown that the upper-ocean submesoscale processes undergo a clear seasonal cycle depending on the local background flow and forcing. Submesoscale physics are ubiquitous but highly heterogeneous in space and time.

Strong, dense submesoscale processes can be generated in regions where the lateral buoyancy gradient or strain rate is strong. The former can provide sufficient potential energy (fronts) that catalyzes instabilities with energy transfer to smaller scales, and the latter is favorable for generating submesoscale fronts (known as submesoscale frontogenesis). The two processes frequently occur in or near western boundary currents (D'Asaro et al., 2011; Shcherbina et al., 2013), in the Southern Ocean (Adams et al., 2017), and in marginal seas (e.g., the South China Sea, hereafter referred to as SCS; Zhang et al., 2020). Physically, these effects arise from a series of submesoscale instabilities that extract energy from the background flow (Haine and Marshall, 1998).

In the open ocean, the seasonality of submesoscale activities

Foundation item: The National Key Research and Development Program of China under contract No. 2017YFA0604104; the National Natural Science Foundation of China under contract Nos 42176004, 92058201 and 41776040; the Fundamental Research Funds for the Central Universities under contract No. B220202050.

*Corresponding author, E-mail: h.cao@hhu.edu.cn

*Acta Oceanol. Sin.*, 2022, Vol. 41, No. 7, P. 42–53
https://doi.org/10.1007/s13131-021-1971-3
http://www.aosocean.com
E-mail: ocean2@hyxb.org.cn

# Submesoscale-enhanced filaments and frontogenetic mechanism within mesoscale eddies of the South China Sea

Ruixi Zheng[1, 2], Zhiyou Jing[1, 3*]

[1] State Key Laboratory of Tropical Oceanography, South China Sea Institute of Oceanology, Chinese Academy of Sciences, Guangzhou 510301, China

[2] University of Chinese Academy of Sciences, Beijing 100049, China

[3] Southern Marine Science and Engineering Guangdong Laboratory (Guangzhou), Guangzhou 511458, China

Received 12 June 2021; accepted 5 October 2021



**Abstract**

Submesoscale activity in the upper ocean has received intense studies through simulations and observations in the last decade, but in the eddy-active South China Sea (SCS) the fine-scale dynamical processes of submesoscale behaviors and their potential impacts have not been well understood. This study focuses on the elongated filaments of an eddy field in the northern SCS and investigates submesoscale-enhanced vertical motions and the underlying mechanism using satellite-derived observations and a high-resolution (~500 m) simulation. The satellite images show that the elongated highly productive stripes with a typical lateral scale of ~25 km and associated filaments are frequently observed at the periphery of mesoscale eddies. The diagnostic results based on the 500 m-resolution realistic simulation indicate that these submesoscale filaments are characterized by cross-filament vertical secondary circulations with an increased vertical velocity reaching $O$(100 m/d) due to submesoscale instabilities. The vertical advections of secondary circulations drive a restratified vertical buoyancy flux along filament zones and induce a vertical heat flux up to 110 W/m$^2$. This result implies a significant submesoscale-enhanced vertical exchange between the ocean surface and interior in the filaments. Frontogenesis that acts to sharpen the lateral buoyancy gradients is detected to be conducive to driving submesoscale instabilities and enhancing secondary circulations through increasing the filament baroclinicity. The further analysis indicates that the filament frontogenesis detected in this study is not only derived from mesoscale straining of the eddy, but also effectively induced by the subsequent submesoscale straining due to ageostrophic convergence. In this context, these submesoscale filaments and associated frontogenetic processes can provide a potential interpretation for the vertical nutrient supply for phytoplankton growth in the high-productive stripes within the mesoscale eddy, as well as enhanced vertical heat transport.

**Key words:** submesoscale process, vertical exchange, frontogenesis, South China Sea

**Citation:** Zheng Ruixi, Jing Zhiyou. 2022. Submesoscale-enhanced filaments and frontogenetic mechanism within mesoscale eddies of the South China Sea. Acta Oceanologica Sinica, 41(7): 42–53, doi: 10.1007/s13131-021-1971-3

## 1 Introduction

Mesoscale eddies with a typical horizontal scale of approximately 100 km greatly contribute to the transports of heat, mass, and biogeochemical tracers in the open ocean (Bryden and Brady, 1989; Chelton et al., 2011a; Dong et al., 2014; Zhang et al., 2014; McGillicuddy, 2016). However, the upwelling induced by mesoscale eddies may only account for 20%–30% of new production (Martin, 2003; McGillicuddy et al., 2003). Meanwhile, submesoscale-induced vertical advection is considered as an important process that fills the gap in vertical transport (Lévy et al., 2001; Omand et al., 2015; Mahadevan, 2016). Submesoscale motions characterized by $O$(1) Rossby and Richardson numbers can induce large vertical velocities, which can be one order of magnitude greater than that of mesoscale eddies, thereby efficiently enhancing vertical exchanges in the upper ocean (Klein and Lapeyre, 2009; Klymak et al., 2016; Su et al., 2020).

Submesoscale activities are ubiquitous in the eddy-active northern South China Sea (SCS), shown by recent simulations and observations (Dong and Zhong, 2020; Lin et al., 2020; Zheng et al., 2020). In this region, most of the eddies travel southwestward along the continental slope with a propagation speed close to that of baroclinic Rossby waves, before they die near the Xisha Islands (Wang et al., 2008; Chen et al., 2011; Nan et al., 2011). These energetic eddies provide favorable conditions for the occurrence of submesoscale behavior (Lapeyre and Klein, 2006; Dong and Zhong, 2018; Zhang et al., 2020). Submesoscale-permitting observations and simulations suggest that the vertical transport induced by submesoscale ageostrophic processes is at least one order of magnitude larger than mesoscale eddies in winter (Zhong et al., 2017). Moreover, *in-situ* microstructure observations show that the elevated turbulent dissipation rate at the eddy periphery is closely connected with the enhancement of

Foundation item: The National Natural Science Foundation of China under contract Nos 92058201, 41776040, 41830538 and 41949907; the Talents Team Project of Southern Marine Science and Engineering Guangdong Laboratory (Guangzhou) under contract No. GML2019ZD0303; the Program of Chinese Academy of Sciences under contract Nos ZDBS-LY-DQC011, ZDRW-XH-2019-2, XDA15020901 and ISEE2021PY01.
*Corresponding author, E-mail: jingzhiyou@scsio.ac.cn

*Acta Oceanol. Sin.*, 2022, Vol. 41, No. 7, P. 54–64
https://doi.org/10.1007/s13131-021-1952-6
http://www.aosocean.com
E-mail: ocean2@hyxb.org.cn

# Variability of the deep South China Sea circulation derived from HYCOM reanalysis data

Yaohua Zhu[1, 2, 3], Guojiao Cao[4], Yonggang Wang[1, 2, 3], Shujiang Li[1, 2, 3], Tengfei Xu[1, 2, 3], Dingqi Wang[1, 5], Fei Teng[1, 2, 3], Zexun Wei[1, 2, 3*]

[1] First Institute of Oceanography, and Key Laboratory of Marine Science and Numerical Modeling, Ministry of Natural Resources, Qingdao 266061, China

[2] Laboratory for Regional Oceanography and Numerical Modeling, Pilot National Laboratory for Marine Science and Technology (Qingdao), Qingdao 266237, China

[3] Shandong Key Laboratory of Marine Science and Numerical Modeling, Qingdao 266061, China

[4] Navigation College, Jiangsu Maritime Institute, Nanjing 211100, China

[5] College of Oceanic and Atmospheric Sciences, Ocean University of China, Qingdao 266100, China

Received 22 July 2021; accepted 26 August 2021



**Abstract**

This study aims to investigate variability of the deep South China Sea (SCS) circulation using the Hybrid Coordinate Ocean Model (HYCOM) global reanalysis product. The results reveal that annual cycle is a dominant component in the deep SCS circulation. Meanwhile, the boundary circulation strength is the weakest in January and peaks between June and September. The eastern and southern boundary currents strengthen/weaken one to three months earlier than that in the western and northern boundaries. Vector Empirical Orthogonal Functions (VEOF) analysis results reveal that semiannual and intraseasonal fluctuations are significant components, of which the spatial patterns are mainly confined in the northern and western boundary areas as well as the southwestern sub-basin. Wavelet analysis results show the strength of significant fluctuation varies year to year. Trend analysis results indicate a decadal weakening in the deep SCS circulation. An anomalous anticyclonic circulation, 50–70 km apart from the slope break, tends to weaken the cyclonic boundary circulation in the western and northern boundaries as well as the southwestern sub-basin. This trend is similar to the observed decadal weakening in the North Atlantic deep circulation. Thus, the findings of this study reveal that the variation of the deep SCS circulation has a remarkable response to the climate change. The mechanisms responsible for the variation are worth pursuing if more observations are available.

**Key words:** South China Sea, variability of deep circulation, HYCOM data, VEOF analysis, wavelet analysis

**Citation:** Zhu Yaohua, Cao Guojiao, Wang Yonggang, Li Shujiang, Xu Tengfei, Wang Dingqi, Teng Fei, Wei Zexun. 2022. Variability of the deep South China Sea circulation derived from HYCOM reanalysis data. Acta Oceanologica Sinica, 41(7): 54–64, doi: 10.1007/s13131-021-1952-6

## 1 Introduction

The South China Sea (SCS) is the largest marginal sea in the tropical western Pacific. Below 200 m depth, the deep SCS basin is semi-enclosed (Wyrtki, 1961). It connects with the western Pacific through its sole deepwater renewal channel, the Luzon Strait. Oriented northeast–southwest and confined into a diamond-shaped region, the deep SCS basin can be divided into the northeastern (NE), northwestern (NW), southwestern (SW), southeastern (SE) and central sub-basins. In the middle, the Xisha Islands, Zhongsha Islands and Huangyan Island (i.e., Scarborough Shoal) combine an east-westward chain of islands and seamounts across the central basin, separating the central basin into the northern and southern central sub-basins (Fig. 1). The circulation pattern in the two central sub-basins may differ as deep water exchange is partially impeded by this island chain (Zhu et al., 2019).

The deep circulation in the SCS is driven by the Luzon Strait deepwater overflow below the depth of 1 500 m from the western Pacific, which is forced by a persistent pressure gradient across the Luzon Strait (Qu et al., 2006; Li and Qu, 2006; Zhao et al., 2014; Zhang et al., 2015). The time-mean circulation in the deep SCS basin is known as cyclonic inferred from observations (Wang, 1986; Qu et al., 2006; Li and Qu, 2006; Shao et al., 2007; Wang et al., 2011; Zhu et al., 2017a) and simulated by numerical models (Chao et al., 1996; Yuan, 2002; Lan et al., 2013; Xie et al., 2013; Xiao et al., 2013; Wang and Zhao, 2013; Shu et al., 2014; Xu and Oey, 2014; Gan et al., 2016a, b).

Nevertheless, being the difficulty in study of the deep SCS circulation, its variability is still not clear due to lack of long-term and large-scale observations. Hitherto, a few pioneering works were engaged in the variability of deep circulation by means of seasonal mean climatology of current velocities. Among them, the numerical simulation of Lan et al. (2015) and Gan et al. (2016a, b) suggested a stronger circulation in summer than that in winter. Zheng et al. (2021) also found the southwestward boundary currents are strong in summer and autumn but insig-

Foundation item: The National Key Research and Development Program of China under contract No. 2019YFC1408400; the National Natural Science Foundation of China under contract Nos 41876029 and 41821004.
*Corresponding author, E-mail: weizx@fio.org.cn

*Acta Oceanol. Sin.*, 2022, Vol. 41, No. 7, P. 65–77
https://doi.org/10.1007/s13131-021-1975-z
http://www.aosocean.com
E-mail: ocean2@hyxb.org.cn

# Objective array design for three-dimensional temperature and salinity observation: Application to the South China Sea

Mengxue Qu[1, 2, 3], Zexun Wei[1, 2, 3], Yanfeng Wang[1, 2, 3], Yonggang Wang[1, 2, 3], Tengfei Xu[1, 2*]

[1] First Institute of Oceanography, and Key Laboratory of Marine Science and Numerical Modeling, Ministry of Natural Resources, Qingdao 266061, China

[2] Laboratory for Regional Oceanography and Numerical Modeling, Pilot National Laboratory for Marine Science and Technology (Qingdao), Qingdao 266237, China

[3] Shandong Key Laboratory of Marine Science and Numerical Modeling, Qingdao 266061, China

Received 31 May 2021; accepted 3 September 2021



**Abstract**

In this study, a moored array optimization tool (MAOT) was developed and applied to the South China Sea (SCS) with a focus on three-dimensional temperature and salinity observations. Application of the MAOT involves two steps: (1) deriving a set of optimal arrays that are independent of each other for different variables at different depths based on an empirical orthogonal function method, and (2) consolidating these arrays using a *K*-center clustering algorithm. Compared with the assumed initial array consisting of 17 mooring sites located on a 3°×3° horizontal grid, the consolidated array improved the observing ability for three-dimensional temperature and salinity in the SCS with optimization efficiencies of 19.03% and 21.38%, respectively. Experiments with an increased number of moored sites showed that the most cost-effective option is a total of 20 moorings, improving the observing ability with optimization efficiencies up to 26.54% for temperature and 27.25% for salinity. The design of an objective array relies on the ocean phenomenon of interest and its spatial and temporal scales. In this study, we focus on basin-scale variations in temperature and salinity in the SCS, and thus our consolidated array may not well resolve mesoscale processes. The MAOT can be extended to include other variables and multi-scale variability and can be applied to other regions.

**Key words:** optimal array design, observation system simulation experiment, South China Sea, empirical orthogonal function, *K*-center clustering

**Citation:** Qu Mengxue, Wei Zexun, Wang Yanfeng, Wang Yonggang, Xu Tengfei. 2022. Objective array design for three-dimensional temperature and salinity observation: Application to the South China Sea. Acta Oceanologica Sinica, 41(7): 65–77, doi: 10.1007/s13131-021-1975-z

## 1 Introduction

Oceanography depends on observations. Accurate and sufficient observations are the essential prerequisites for revealing ocean phenomena, understanding ocean variability, and improving ocean prediction skills. The continuous measurement of ocean variables at fixed stations, such as a moored buoy array or subsurface mooring array (collectively referred to as moored or mooring array hereafter), is one of the most important approaches to collect long-term time series of the three-dimensional data on ocean temperature, salinity, and velocity. Although the ideal number of moored array sites is "the more the better", available sites, however, could never be adequate to cover the investigated domain due to costly instruments required for each site in reality. Therefore, it is important to determine the optimum array design using a limited number of station sites. The site locations in an optimum array design should be the most "representative" of the area of interest and would thus yield the best estimation or prediction of oceanic characteristics (Lermusiaux, 2007; Zhang et al., 2020).

One way of determining an optimum array design is by conducting an observation system simulation experiment (OSSE) (Masutani et al., 2010). The OSSE approach was first used in the meteorological community to assess potential improvements in numerical weather prediction with additional observations involved and was later widely used to design the meteorological station network (Arnold and Dey, 1986). The application of OSSEs in physical oceanography has been promoted by an increase in ocean observation. Examples include optimal designs of a tide gauge array (McIntosh, 1987), tropical Atlantic mooring array (Hackert et al., 1998), monitoring array for the North Atlantic meridional overturning (Hirschi et al., 2003), tropical Indian Ocean mooring array (Ballabrera-Poy et al., 2007; Oke and Schiller, 2007; Sakov and Oke, 2008), Pacific Ocean mooring array (Zhang and Bellingham, 2008; Liu et al., 2018b), and mooring arrays for regional and coastal seas (Frolov et al., 2008; Yildirim et al., 2009; Fu et al., 2011; Xue et al., 2011; Zhang et al., 2019; Geng et al., 2020). The OSSEs have also been employed to assess the ability of a moorings observing system in monitoring the intraseasonal variability of currents in the northwestern tropical Pacific Ocean (Liu et al., 2018a). In addition, several investigations have used OSSEs to propose an optimum sampling design for hybrid instruments and platforms, e.g., glider-mooring ob-

Foundation item: The National Key Research and Development Program of China under contract No. 2019YFC1408400; the National Natural Science Foundation of China under contract No. 41876029.
*Corresponding author, E-mail: xutengfei@fio.org.cn

*Acta Oceanol. Sin.*, 2022, Vol. 41, No. 7, P. 78–83
https://doi.org/10.1007/s13131-022-2032-2
http://www.aosocean.com
E-mail: ocean2@hyxb.org.cn

# Rapid environmental assessment in the South China Sea: Improved inversion of sound speed profile using remote sensing data

Ke Qu[1], Binbin Zou[2]*, Jianbo Zhou[3]

[1] College of Electronics and Information Engineering, Guangdong Ocean University, Zhanjiang 524088, China

[2] Shanghai Acoustics Laboratory, Chinese Academy of Sciences, Shanghai 201815, China

[3] School of Marine Science and Technology, Northwestern Polytechnical University, Xi'an 710072, China

Received 12 June 2021; accepted 21 April 2022



**Abstract**

Complex perturbations in the profile and the sparsity of samples often limit the validity of rapid environmental assessment (REA) in the South China Sea (SCS). In this paper, the remote sensing data were used to estimate sound speed profile (SSP) with the self-organizing map (SOM) method in the SCS. First, the consistency of the empirical orthogonal functions was examined by using *k*-means clustering. The clustering results indicated that SSPs in the SCS have a similar perturbation nature, which means the inverted grid could be expanded to the entire SCS to deal with the problem of sparsity of the samples without statistical improbability. Second, a machine learning method was proposed that took advantage of the topological structure of SOM to significantly improve their accuracy. Validation revealed promising results, with a mean reconstruction error of 1.26 m/s, which is 1.16 m/s smaller than the traditional single empirical orthogonal function regression (sEOF-r) method. By violating the constraints of linear inversion, the topological structure of the SOM method showed a smaller error and better robustness in the SSP estimation. The improvements to enhance the accuracy and robustness of REA in the SCS were offered. These results suggested a potential utilization of REA in the SCS based on satellite data and provided a new approach for SSP estimation derived from sea surface data.

**Key words:** South China Sea, sound speed profile empirical orthogonal function, self-organizing maps

**Citation:** Qu Ke, Zou Binbin, Zhou Jianbo. 2022. Rapid environmental assessment in the South China Sea: Improved inversion of sound speed profile using remote sensing data. Acta Oceanologica Sinica, 41(7): 78–83, doi: 10.1007/s13131-022-2032-2

## 1 Introduction

The core objective of rapid environmental assessment (REA) is to provide environmental nowcasts for operational activity in any arbitrary region of the global ocean. As a thorough understanding of variations in the sound speed profile (SSP) can help enhance the performance of sonar in civil and military applications, the rapid assessment of the SSP has become a focus of research in the area. However, as SSP measurement with broad spatiotemporal coverage is extremely time-consuming and laborious, it is almost impossible to obtain the 3D structure of the sound speed via *in situ* measurements. Although the water column is optically opaque, remote sensing is the only platform that can provide real-time observations of the ocean at a large scale. Therefore, it is feasible to obtain rapid assessments of the SSP using remote sensing data.

The thermal expansion and contraction of the water column, and conduction of heat on the surface of water form an intrinsic link between the parameters of the surface and profiles of the subsurface. Therefore, related research has focused on the sea level (SL) and the sea surface temperature (SST). Carnes confirmed the relationship between remote sensing data (SL and SST) and subsurface profiles in the Gulf Stream (Carnes et al., 1990), and then estimated the subsurface profiles of the Northwest Pacific and Northwest Atlantic Oceans by using single empirical orthogonal function regression (sEOF-r) (Carnes et al., 1994). As the empirical orthogonal function (EOF) and linear regression can significantly improve the efficiency of inversion, sEOF-r has been widely used in REA models, such as the US Navy's forecasting system for the ocean (Fox et al., 2002). In the framework of sEOF-r, the vertical spatial and temporal characteristics of the oceanographic profile can be calculated by using remote sensing data in linear empirical relationships between the parameters of the surface and the subsurface (Meijers et al., 2011). A celebrated instance is that of the Modular Ocean Data Assimilation System (MODAS), which provides a dynamic climatology that can be used to obtain the height and temperature of the sea surface to predict underwater structures by constructing synthetic profiles generated by regression analysis (Rahaman et al., 2016). The SSP has also been reconstructed directly via sEOF-r (Chen et al., 2018).

In recent years, machine learning theory has been introduced to problems similar to the above. Since machine learning is a universal framework to solve for the inherent characteristics of the training set, nonlinear relationships between parameters of the surface and subsurface can be extracted without any assumption about the vertical structure of the water column. Hjelmervik

Foundation item: The Natural Science Foundation of Guangdong Province under contract No. 2022A1515011519; the National Natural Science Foundation of China under contract No. 11904290.
*Corresponding author, E-mail: zoubb@mail.ioa.ac.cn

*Acta Oceanol. Sin.*, 2020, Vol. 39, No. 11, P. 1–12
https://doi.org/10.1007/s13131-020-1671-4
http://www.hyxb.org.cn
E-mail: hyxbe@263.net

# Dynamical analysis of submesoscale fronts associated with wind-forced offshore jet in the western South China Sea

Xiaolong Huang[1, 2], Zhiyou Jing[1, 3, 4]*, Ruixi Zheng[1, 2], Haijin Cao[5]

[1] State Key Laboratory of Tropical Oceanography, South China Sea Institute of Oceanology, Chinese Academy of Sciences, Guangzhou 510301, China

[2] University of Chinese Academy of Sciences, Beijing 100049, China

[3] Southern Marine Science and Engineering Guangdong Laboratory (Guangzhou), Guangzhou 511458, China

[4] Innovation Academy of South China Sea Ecology and Environmental Engineering, Chinese Academy of Sciences, Guangzhou 510301, China

[5] College of Oceanography, Hohai University, Nanjing 210024, China

Received 13 April 2020; accepted 8 July 2020



**Abstract**

This study investigates the submesoscale fronts and their dynamic effects on the mean flow due to frontal instabilities in the wind-driven summer offshore jet of the western South China Sea (WSCS), using satellite observations, a 500 m-resolution numerical simulation, and diagnostic analysis. Both satellite measurements and simulation results show that the submesoscale fronts occupying a typical lateral scale of $O$(~10) km are characterized with one order of Rossby (*Ro*) and Richardson (*Ri*) numbers in the WSCS. This result implies that both geostrophic and ageostrophic motions feature in these submesoscale fronts. The diagnostic results indicate that a net cross-frontal Ekman transport driven by down-front wind forcing effectively advects cold water over warm water. By this way, the weakened local stratification and strong lateral buoyancy gradients are conducive to a negative Ertel potential vorticity (PV) and triggering frontal symmetric instability (SI) at the submesoscale density front. The cross-front ageostrophic secondary circulation caused by frontal instabilities is found to drive an enhanced vertical velocity reaching $O$(100) m/d. Additionally, the estimate of the down-front wind forcing the Ekman buoyancy flux (EBF) is found to be scaled with the geostrophic shear production (GSP) and buoyancy flux (BFLUX), which are the two primary energy sources for submesoscale turbulence. The large values of GSP and BFLUX at the fronts suggest an efficient downscale energy transfer from larger-scale geostrophic flows to the submesoscale turbulence owing to down-front wind forcing and frontal instabilities. In this content, submesoscale fronts and their instabilities substantially enhance the local vertical exchanges and geostrophic energy cascade towards smaller-scale. These active submesoscale processes associated density fronts and filaments likely provide new physical interpretations for the filamentary high chlorophyll concentration and frontal downscale energy transfer in the WSCS.

**Key words:** submesoscale fronts, enhanced vertical velocity, energy transfer, offshore jet, western South China Sea

**Citation:** Huang Xiaolong, Jing Zhiyou, Zheng Ruixi, Cao Haijin. 2020. Dynamical analysis of submesoscale fronts associated with wind-forced offshore jet in the western South China Sea. Acta Oceanologica Sinica, 39(11): 1–12, doi: 10.1007/s13131-020-1671-4

## 1 Introduction

Upper ocean circulation, significantly influenced by atmospheric forcing consists of motions of a broad range of scales (Wunsch and Ferrari, 2004; Thomas and Taylor, 2010). The submesoscale fronts, which constitute an asymmetrical atmospheric forcing (e.g., down-front wind forcing and surface cooling), can be frequently detected from high-resolution satellite observations (Zheng et al., 2008; Liu et al., 2015; Liu and Levine, 2016). These elongated fronts are dynamically characterized by $O$(1) Rossby number (*Ro*) and Richardson number (*Ri*). In addition, they possess a typical lateral scale of $O$(1–10) km and a time scale of $O$(hour–day) (Thomas et al., 2008). For such space and time scales, the assumption of geostrophy is no longer valid (Gula et al., 2014; McWilliams, 2017, 2019). Thus, dynamic processes involved in submesoscale fronts or filaments include both geostrophic and ageostrophic motions. Furthermore, the ageostrophic processes associated with the submesoscale instabilities can produce significant divergent flows and stir up a large vertical velocity, thus substantially contributing to the enhanced vertical fluxes of heat, buoyancy, nutrient, and momentum in the upper oceans (Mahadevan and Tandon, 2006; Su et al., 2018; Zhang et al., 2019). The frontal instabilities at submesoscales have been detected to be able to extract kinetic energy (KE) from the larger-scale geostrophic flows, and cascade energy towards

Foundation item: This work is supported by the Chinese Academy of Sciences under contract Nos ZDBS-LY-DQC011, ZDRW-XH-2019-2 and ISEE2018PY05; the Southern Marine Science and Engineering Guangdong Laboratory (Guangzhou) under contract No. GML2019ZD0303; the National Natural Science Foundation of China under contract Nos 41776040 and 92058201; the Pilot National Laboratory for Marine Science and Technology (Qingdao) under contract No. OCFL-201804; the State Key Laboratory of Tropical Oceanography under contract No. LTO1907; the Guangzhou Science and Technology Project under contract No. 201904010420.
*Corresponding author, E-mail: jingzhiyou@scsio.ac.cn

*Acta Oceanol. Sin.*, 2020, Vol. 39, No. 11, P. 13–20
https://doi.org/10.1007/s13131-020-1621-1
http://www.hyxb.org.cn
E-mail: hyxbe@263.net

# Influence of two inlets of the Luzon overflow on the deep circulation in the northern South China Sea

Muping Zhou[1, 2, 3], Changlin Chen[2, 4*], Yunwei Yan[3, 4], Wenhu Liu[2]

[1] College of Ocean and Earth Science, Xiamen University, Xiamen 361102, China

[2] Department of Atmospheric and Oceanic Sciences & Institute of Atmospheric Sciences, Fudan University, Shanghai 200438, China

[3] State Key Laboratory of Satellite Ocean Environment Dynamics, Second Institute of Oceanography, Ministry of Natural Resources, Hangzhou 310012, China

[4] Southern Marine Science and Engineering Guangdong Laboratory (Zhuhai), Zhuhai 519000, China

Received 21 January 2020; accepted 2 April 2020



**Abstract**

An inverse reduced-gravity model is used to simulate the deep South China Sea (SCS) circulation. A set of experiments are conducted using this model to study the influence of the Luzon overflow through the two inlets on the deep circulation in the northern SCS. Model results suggest that the relative contribution of these inlets largely depends on the magnitude of the input transport of the overflow, but the northern inlet is more efficient than the southern inlet in driving the deep circulation in the northern SCS. When all of the Luzon overflow occurs through the northern inlet the deep circulation in the northern SCS is enhanced. Conversely, when all of the Luzon overflow occurs through the southern inlet the circulation in the northern SCS is weakened. A Lagrangian trajectory model is also developed and applied to these cases. The Lagrangian results indicate that the location of the Luzon overflow likely has impacts upon the sediment transport into the northern SCS.

**Key words:** inlets, Luzon overflow, deep circulation, northern South China Sea

**Citation:** Zhou Muping, Chen Changlin, Yan Yunwei, Liu Wenhu. 2020. Influence of two inlets of the Luzon overflow on the deep circulation in the northern South China Sea. Acta Oceanologica Sinica, 39(11): 13–20, doi: 10.1007/s13131-020-1621-1

## 1 Introduction

The South China Sea (SCS) is the largest semi-enclosed marginal sea in the northwestern Pacific, bounded by the Luzon Island to the east, Kalimantan Island to the south, Vietnam to the west, and China to the north (Fig. 1a). The deepest water is confined within a bowl-shaped trench with a maximum depth of around 5 560 m (Wyrtki, 1961). The Luzon Strait is the only deep channel connecting the deep SCS water with the open ocean (Qu et al., 2006; Tian and Qu, 2012). Because the Luzon Strait has a sill depth of around 2 400 m, the deep SCS basin is completely isolated below 2 400 m.

The deep circulation in the SCS is characterized by a cyclonic gyre with a strong deep western boundary current (DWBC, Fig. 1a). This deep SCS circulation pattern and the DWBC were reported by Qu et al. (2006) from World Ocean Database and Wang et al. (2011) from the U.S. Navy Generalized Digital Environment Model (GDEM) data, the existence of DWBC was further verified by Zhou et al. (2017) from *in-situ* mooring observations, and to some extent captured by numerical simulations (Lan et al., 2013, 2015; Wang et al., 2018).

The deep circulation in the SCS results from the interaction between multi-scale dynamic processes and the complex topography (Qu, 2002; Qu et al., 2006; Tian et al., 2006; Tian et al., 2009; Chang et al., 2010; Wang et al., 2011; Lan et al., 2013; Zhao et al., 2014; Lan et al., 2015; Shu et al., 2016; Wang et al., 2016, 2018, 2019; Yang et al., 2016). Many studies have suggested that the Luzon overflow, which is comprised of the relatively cold and high-density Pacific Ocean water sinks to the SCS after it crosses the Luzon Strait, is one of the most important factors in determining the deep circulation in the SCS (Wyrtki, 1961; Qu et al., 2006; Li and Qu, 2006; Wang et al., 2011; Lan et al., 2013; Zhao et al., 2014). Based on all available hydrographic data from the World Ocean Database 2001, Qu et al. (2006) suggested that the overflow through the Luzon Strait has a notable impact on the circulation and water property distributions in the deep SCS. Through a set of sensitivity experiments using an ocean general circulation model, Lan et al. (2013) revealed that the Luzon overflow controls the formation of the deep cyclonic gyre in the SCS.

Based on *in-situ* observations, the Luzon overflow has two primary inlets (Fig. 1b). The northern inlet has an average volume transport of ~$0.7\times10^6$ $m^3/s$, while the southern inlet has an average volume transport of ~$0.9\times10^6$ $m^3/s$ (Zhao et al., 2014). In addition, it has been shown that the transport across both inlets possesses significant intraseasonal variations in the 20–60 d band and seasonal variations in the 100–360 d band (Zhao et al., 2014; Zhou et al., 2014; Ye et al., 2019). To the best of our knowledge, the role that the overflows from two inlets play in driving the SCS deep circulation has not been studied. Furthermore, previous studies have shown that the deep SCS circulation also has a significant impact on the sediment transport over the northern

Foundation item: The Foundation of China Ocean Mineral Resources R&D Association under contract No. DY135-E2-2-02; the National Natural Science Foundation of China under contract Nos 91428206, 41976028 and 41806019.
*Corresponding author, E-mail: chencl@fudan.edu.cn

*Acta Oceanol. Sin.*, 2020, Vol. 39, No. 11, P. 21–32
https://doi.org/10.1007/s13131-020-1677-y
http://www.hyxb.org.cn
E-mail: hyxbe@263.net

# Surface water exchanges in the Luzon Strait as inferred from Lagrangian coherent structures

Zhehao Zheng[1], Wei Zhuang[1, 2*], Jianyu Hu[1, 2], Zelun Wu[1, 3], Changjian Liu[4]

[1] State Key Laboratory of Marine Environmental Science, College of Ocean and Earth Sciences, Xiamen University, Xiamen 361102, China

[2] Southern Marine Science and Engineering Guangdong Laboratory (Zhuhai), Zhuhai 519082, China

[3] Joint Center for Ocean Remote Sensing, University of Delaware-Xiamen University, Newark, DE 19716, USA

[4] South China Sea Marine Survey and Technology Center, Ministry of Natural Resources, Guangzhou 510300, China

Received 1 May 2020; accepted 10 August 2020



**Abstract**

This study presents a Lagrangian view of upper water exchanges across the Luzon Strait based on the finite-time Lyapunov exponents (FTLE) fields computed from the surface geostrophic current. The Lagrangian coherent structures (LCSs) extracted from the FTLE fields well identify the typical flow patterns and eddy activities around the Luzon Strait. In addition, they reveal the intricate transport paths and fluid domains, which are validated by the tracks of satellite-tracked surface drifters and cannot be visually recognized in the velocity maps. The FTLE fields indicate that there are mainly four types of transport patterns near the Luzon Strait; among them, the Kuroshio northward-flowing "leaping" pattern and the clockwise rotating "looping" pattern occur more frequently than the "leaking" pattern of the direct Kuroshio branch into the SCS and the "outflowing" pattern from the SCS to the Pacific. The eddy shedding events of the Kuroshio at the Luzon Strait are further analyzed, and the importance of considering LCSs in estimating transport by eddies is highlighted. The anticyclonic eddy (ACE) shedding cases reveal that ACEs mainly originate from the looping paths of Kuroshio and thus could effectively trap the Kuroshio water before eddy detachments. LCSs provide useful information to predict the positions of the upstream waters that finally enter the ACEs. In contrast, LCS snapshots indicate that during the formation of cyclonic eddies (CEs), most CEs are not connected with the pathways of Kuroshio water. Hence, the contribution of CEs to the surface water exchanges from the Pacific into the SCS is tiny.

**Key words:** Lagrangian coherent structures (LCSs), Kuroshio, Luzon Strait, transport pathways, particle tracking

**Citation:** Zheng Zhehao, Zhuang Wei, Hu Jianyu, Wu Zelun, Liu Changjian. 2020. Surface water exchanges in the Luzon Strait as inferred from Lagrangian coherent structures. Acta Oceanologica Sinica, 39(11): 21–32, doi: 10.1007/s13131-020-1677-y

## 1 Introduction

The Kuroshio is the poleward western boundary current of the North Pacific subtropical gyre. It mainly originates from the westward flowing North Equatorial Current, which bifurcates at the eastern coast of the Philippine Archipelago. The Kuroshio then flows northeastward, passing by the Luzon Strait, Taiwan Island, and Ryukyu Islands.

The South China Sea (SCS), which is the largest semienclosed marginal sea in the northwestern Pacific, is characterized by East Asian monsoon climate and a complex geometry (Fig. 1). A number of straits connect the SCS with the adjacent waters. Among these straits, the Luzon Strait is the only deep (>2 200 m) passage, and it is also the major oceanic pathway between the SCS and the Pacific Ocean. Over several decades, it has been observed that when the Kuroshio passes by the Luzon Strait, a portion of the warm and salty Pacific water enters the SCS (Shaw, 1991; Qu et al., 2000; Zhu et al., 2019). In the sense of annual mean, the inflow through the Luzon Strait partially flows out of the SCS through the Karimata and Mindoro Straits, forming the so-called SCS throughflow that is important for the heat and salt budgets of the SCS basin (Qu et al., 2005, 2006; Wang et al., 2006; Fang et al., 2009; Gordon et al., 2012; Wei et al., 2019).

With regard to the upper layer, both the historical hydrographic data and the surface drifter trajectories indicate notable seasonality of surface water exchange through the Luzon Strait (Shaw, 1991; Centurioni et al., 2004). The surface Kuroshio intrusion into the SCS is the largest in winter, followed by that in spring and in autumn; however, there is still no consensus on whether the water exchange in summer flows westward into the SCS or eastward into the northwestern Pacific Ocean (Shaw, 1991; Chu and Li, 2000). High-resolution satellite images reveal that the surface Kuroshio path in the Luzon Strait shows significant transient features and appears to be closely related to the nearby eddy activities (Yuan et al., 2006; Nan et al., 2011; Qiu et al., 2019; Zheng et al., 2019). Further, the unstable nature of the Kuroshio intrusion has been verified by model simulations (Metzger and Hurlbert, 2001; Xue et al., 2004), and the intruding path can be roughly divided into three types: the looping path, leaping path, and leaking path (Nan et al., 2011, 2015). Because of the complexity of the dynamic environment and the nondeterministic nature of flow pattern around the Luzon Strait, the variability of flow trajectories and the relevant dynamics are still not well

Foundation item: The National Key Research and Development Program of China under contract No. 2016YFA0601201; the National Natural Science Foundation of China under contract Nos 91858202, 91958203, 41730533 and 41776003.
*Corresponding author, E-mail: wzhuang@xmu.edu.cn

*Acta Oceanol. Sin.*, 2020, Vol. 39, No. 11, P. 33–43
https://doi.org/10.1007/s13131-020-1673-2
http://www.hyxb.org.cn
E-mail: hyxbe@263.net

# Effects of tidal currents on winter wind waves in the Qiongzhou Strait: a numerical study

Peng Bai[1, 2], Zheng Ling[2], Cong Liu[3]*, Junshan Wu[4], Lingling Xie[1, 2]

[1] Marine Resources Big Data Center of South China Sea, Southern Marine Science and Engineering Guangdong Laboratory (Zhanjiang), Zhanjiang 524025, China

[2] Guangdong Province Key Laboratory for Coastal Ocean Variation and Disaster Prediction, College of Ocean and Meteorology, Guangdong Ocean University, Zhanjiang 524088, China

[3] Ocean College, Zhejiang University, Zhoushan 316021, China

[4] East China Sea Bureau of Ministry of Natural Resources, Shanghai 200137, China

Received 30 April 2020; accepted 11 June 2020



**Abstract**

Effects of currents on winter wind waves in the tide-dominated Qiongzhou Strait (QS) were numerically evaluated via employing the coupled ocean-atmosphere-wave-sediment transport (COAWST) modeling system. Validations showed satisfactory model performance in simulating the intense tidal currents in the QS. Different effects of sea level variations and tidal currents on waves were examined under the maximum eastward (METC) and westward (MWTC) tidal currents. In the east entrance area of the QS, the positive sea levels under the MWTC deepened the water depth felt by waves, benefiting the further propagation of wave energy into the inner strait and causing increased wave height. The METC and the MWTC could both enhance the wave height in the east entrance area of the QS, mainly through current-induced convergence and wavenumber shift, respectively. By current-induced refraction, the METC (MWTC) triggered counterclockwise (clockwise) rotation in peak wave directions in the northern part of the QS while clockwise (counterclockwise) rotation in the southern part.

**Key words:** Qiongzhou Strait, COAWST, significant wave height, peak wave direction

**Citation:** Bai Peng, Ling Zheng, Liu Cong, Wu Junshan, Xie Lingling. 2020. Effects of tidal currents on winter wind waves in the Qiongzhou Strait: a numerical study. Acta Oceanologica Sinica, 39(11): 33–43, doi: 10.1007/s13131-020-1673-2

## 1 Introduction

Wave-current interaction represents one of the dominant driving forces in coastal shallow seas, during which process wave dynamics can be considerably modified. When currents are present, the effective wind vector driving the waves is the subtraction of the current vector from the wind vector (Wolf and Prandle, 1999; Fan et al., 2009). Currents can exert refraction, modification of bottom stress, steepening, current-induced breaking, and blocking effects on the waves (Vincent, 1979; Wolf and Prandle, 1999; Ris et al., 1999; Ardhuin et al., 2012). Through Doppler shift, currents change the wave frequency and thereby the phase speed (Tolman, 1990; Wolf and Prandle, 1999). Moreover, the variations of the sea level can also modify wave characteristics by changing the water depth felt by waves (Tolman, 1990; Wolf and Prandle, 1999; Pleskachevsky et al., 2009).

Many efforts have emphasized the significance of currents' effects on the waves, particularly under strong currents condition. In the southern North Sea, numerical investigation of Osuna and Monbaliu (2004) revealed that differences in significant wave heights ($H_s$) and mean periods due to currents could reach up to about 0.2 m and 1 s when currents speed up to 1 m/s. Following currents could reduce the wave height since the wave group propagates faster and therefore wave energy is dispersed (Fan et al., 2009); conversely, wave energy would be concentrated and $H_s$ could be increased when waves encounter opposite currents (Warner et al., 2010). During a storm event, storm-driven strong currents could lead to the variations of $H_s$ up to 0.6 m in the semi-enclosed Gulf of Venice (Benetazzo et al., 2013). In the tide dominated estuary investigated by Bolaños et al. (2014), wave period as well as $H_s$ was modulated predominantly by the time-varying water depth, meanwhile, current-induced Doppler shift could exert a prime effect on wave period. Generally, taking currents' effects on waves into consideration could improve the performance of wave models, for instance, Guillou (2017) highlighted that introduction of tidal forcing into the wave model lead to ~30% variations of $H_s$ by current-induced refraction, and therefore significantly improved the wave simulation; Rapizo et al. (2017) demonstrated that wave models tend to overestimate wave height on opposing currents, and introducing current-enhanced wave dissipation into the wave model considerably improved the simulation of wave height and mean wave period.

The Qiongzhou Strait (QS) is a 30-km wide tide-dominated busy shipping lane between the Leizhou Peninsula and the Hainan Island (Fig. 1), it is a key passage linking the Beibu Gulf and

Foundation item: The Fund of Southern Marine Science and Engineering Guangdong Laboratory (Zhanjiang) under contract No. ZJW-2019-08; the Program for Scientific Research Start-up Funds of Guangdong Ocean University under contract No. 101302/R18001; the National Natural Science Foundation of China under contract No. 41776034; the First-class Discipline Plan of Guangdong Province under contract No. CYL231419012.
*Corresponding author, E-mail: liucong175@gmail.com

*Acta Oceanol. Sin.*, 2020, Vol. 39, No. 11, P. 44–51
https://doi.org/10.1007/s13131-020-1667-0
http://www.hyxb.org.cn
E-mail: hyxbe@263.net

# Mooring observed mode-2 internal solitary waves in the northern South China Sea

Liang Chen[1, 2, 3*], Xuejun Xiong[1, 2, 3*], Quanan Zheng[4], Yeli Yuan[1, 2, 3], Long Yu[1, 2, 3], Yanliang Guo[1, 2, 3], Guangbing Yang[1, 2, 3], Xia Ju[1, 2, 3], Jia Sun[1, 2, 3], Zhenli Hui[1, 2, 3]

[1] First Institute of Oceanography, Ministry of Natural Resources, Qingdao 266061, China

[2] Founctional Laboratory for Regional Oceanography and Numerical Modeling, Pilot National Laboratory for Marine Science and Technology (Qingdao), Qingdao 266237, China

[3] Laboratory for Regional Oceanography and Numerical Modeling, Pilot National Laboratory for Marine Science and Technology (Qingdao), Qingdao 266237, China

[4] Department of Atmospheric and Oceanic Science, University of Maryland, College Park, Maryland 20742, USA

Received 20 January 2020; accepted 5 May 2020



**Abstract**

The mode-2 internal solitary waves (ISWs) generated by mode-2 internal tide (IT) are identified by mooring observations in the northern South China Sea (SCS) from 2016 to 2017. Two mode-2 ISWs with a re-appearance period of 24.9 h observed on 29 and 30 July 2016 are characterized by type-b ISWs. They occurred when the isotherms compressed obviously in the vertical direction. Modal decomposition of IT horizontal currents shows that the vertical compression of the isotherms is mainly caused by diurnal mode-2 IT. The analysis of the role of the density stratification reveals that a deeper and thinner pycnocline is favorable for generation of mode-2 ISWs rather than pycnocline intensity. By comparing the mode-2 nonlinear, dispersion coefficients and the Ursell numbers calculated based on the stratification associated with different kinds of ITs with the observation results, it is shown that the diurnal mode-2 IT plays a crucial role in the generation of the mode-2 ISWs. When the diurnal mode-2 IT interacts with the semidiurnal IT and causes a deeper and thinner pycnocline, the mode-2 ISWs are easily excited.

**Key words:** mode-2 internal solitary waves, South China Sea, internal tide, mooring observation

**Citation:** Chen Liang, Xiong Xuejun, Zheng Quanan, Yuan Yeli, Yu Long, Guo Yanliang, Yang Guangbing, Ju Xia, Sun Jia, Hui Zhenli. 2020. Mooring observed mode-2 internal solitary waves in the northern South China Sea. Acta Oceanologica Sinica, 39(11): 44–51, doi: 10.1007/s13131-020-1667-0

## 1 Introduction

Previous investigations have shown that the internal solitary waves (ISWs), with large amplitudes and strong current velocities, are broadly distributed in the stratified coastal ocean and marginal seas (Jackson, 2007; Zhao et al., 2006; Stanton and Ostrovsk, 1998; Apel et al., 1985; Osborne and Burch, 1980). The South China Sea (SCS), in particular the northern SCS, is one of ocean areas where the energetic ISWs occur frequently (Wang et al., 2013; Zheng, 2017; Chen et al., 2018). In terms of the wave modes, the observed ISWs in the northern SCS could be categorized as two types, i.e., the first baroclinic mode (mode-1) and the second baroclinic mode (mode-2) (Yang et al., 2004; Chen et al., 2019). Mode-1 ISWs are characterized by only one extreme value of the vertical displacement of isotherms in the whole water column. Mode-2 ISWs typically show upward (downward) displacement of isotherms in the upper (lower) water column and three layers of currents from the uppermost to bottommost portions of a wave (Yang et al., 2010). In recent years, mode-2 ISWs in the northern SCS have been observed and reported (Yang et al., 2004; 2009; Ramp et al., 2012). According to mooring observations, Yang et al. (2009) found that mode-2 ISWs on the upper continental slope of the northern SCS occur occasionally in summer, and more frequently in winter, implying that their occurrence may be associated with the seasonal change of local stratification. Ramp et al. (2015) observed a profusion of mode-2 ISWs during 5–16 August 2011 by two cruises. They found that the waves cannot persist very far from the underwater ridge and likely do not contribute to the SCS transbasin wave phenomenon. Most recently, Chen et al. (2019) revealed a high occurrence frequency of mode-2 ISWs (including 21 mode-2 ISWs) on the northwestern SCS shelf slope west of Dongsha Atoll in December 2016, and reported an extreme mode-2 ISW with maximum upward and downward amplitudes of 73 m and 91 m, respectively. This implies that the mode-2 ISWs present in the SCS and are not difficult to be observed. Although the amplitudes and current velocities of mode-2 ISWs are smaller than those of the mode-1

Foundation item: The National Science and Technology Major Project under contract No. 2016ZX05057015; the National Natural Science Foundation of China (NSFC) under contract Nos 41376038, 40406009, 41806123 and 41506038; the NSFC-Shandong Joint Fund for Marine Science Research Centers under contract No. U1606405; the National Program on Global Change and Air-Sea Interaction under contract Nos GASI-03-01-01-02, GASI-02-IND-STSsum and GASI-IPOVAI-01-05; the Public Science and Technology Research Funds Projects of Ocean under contract No. 200905024; the National Key Scientific Instrument and Equipment Development Projects under contract No. 2012YQ12003908.
*Corresponding author, E-mail: chenliang@fio.org.cn; xiongxj@fio.org.cn

*Acta Oceanol. Sin.*, 2020, Vol. 39, No. 11, P. 52–68
https://doi.org/10.1007/s13131-020-1670-5
http://www.hyxb.org.cn
E-mail: hyxbe@263.net

# Kuroshio intrusion in the Luzon Strait in an eddy-resolving ocean model and air-sea coupled model

Qian Yang[1, 2], Hailong Liu[1, 2*], Pengfei Lin[1, 2], Yiwen Li[1, 2]

[1] State Key Laboratory of Numerical Modeling for Atmospheric Sciences and Geophysical Fluid Dynamics, Institute of Atmospheric Physics, Chinese Academy of Sciences, Beijing 100029, China

[2] College of Earth Sciences, University of Chinese Academy of Sciences, Beijing 100049, China

Received 13 June 2020; accepted 23 July 2020



**Abstract**

The Kuroshio intrusion in a quasi-global eddy-resolving model (LICOMH) and a fully air-sea coupled model (LICOMHC) was evaluated against observations. We found that the Kuroshio intrusion was exaggerated in the former, while biases were significantly attenuated in the latter. Luzon Strait transport (LST) in winter was reduced from $-8.8\times10^6$ m$^3$/s in LICOMH to $-6.0\times10^6$ m$^3$/s in LICOMHC. Further analysis showed that different LST values could be explained by different large-scale and local surface wind stresses and the eddies east to the Luzon Strait as well. The relatively stronger cyclonic eddies in LICOMH northeast of the Luzon Island led to weak Kuroshio transport and strong intrusion through the Luzon Strait. The summed transport of all three factors was approximately $2.0\times10^6$ m$^3$/s, which was comparable with the difference in LST between the two experiments. The EKE budget showed that strong EKE transport and the baroclinic transformation term led to strong cyclonic eddies east of the Kuroshio in LICOMH, while surface winds contributed little to the differences in the eddies.

**Key words:** Kuroshio intrusion, South China Sea, eddy-resolving model, air-sea coupled model

**Citation:** Yang Qian, Liu Hailong, Lin Pengfei, Li Yiwen. 2020. Kuroshio intrusion in the Luzon Strait in an eddy-resolving ocean model and air-sea coupled model. Acta Oceanologica Sinica, 39(11): 52–68, doi: 10.1007/s13131-020-1670-5

## 1 Introduction

The Luzon Strait (LS), located between the Luzon Island and the Taiwan Island, is a primary gap of the South China Sea (SCS) that forms a connection with the western North Pacific. The Kuroshio, the northward western boundary current of the subtropical gyre of the North Pacific, commonly intrudes westward into the SCS through the LS via various pathways. Sometimes, the intrusion may induce a loop current in the LS, and Kuroshio water flows out of the SCS through the northern part of the LS. The Kuroshio intrusion not only affects stratification (Metzger and Hurlburt, 1996; Qu et al., 2000; Xu and Su, 2000), circulation (Metzger and Hurlburt, 1996; Qu et al., 2000; Xu and Su, 2000; Tian et al., 2006), and mesoscale eddies (Sun et al., 2016) in the northern SCS but also affects the mass, heat and salt budgets of the whole SCS basin (Metzger and Hurlburt, 1996; Qu et al., 2000; Xu and Su, 2000).

Recently, some major features of the Kuroshio intrusion have been gradually identified due to an increasing number of *in situ* measurements, high resolution satellite data and numerical products, including intrusion types (Hu et al., 2000; Caruso et al., 2006; Nan et al., 2011a; Nan et al., 2015; Huang et al., 2016), water exchange in the LS (Lan et al., 2004; Tian et al., 2006; Shu et al., 2014), and interactions between the Kuroshio and mesoscale processes (Yuan et al., 2006; Sheu et al., 2010; Zhao and Luo, 2010; Nan et al., 2011b; Lu and Liu, 2013; Lien et al., 2014; Chang et al., 2015; Nan et al., 2015; Kuo et al., 2017). The Kuroshio intrusion into the SCS also has multiscale variability, ranging from seasonal (Qu et al., 2000, 2004; Xu and Su, 2000; Lan et al., 2004; Yang et al., 2013; Huang et al., 2017) to interannual (Kim et al., 2004; Qu et al., 2004; Wang et al., 2006a; Wu, 2013) to decadal (Nan et al., 2013) timescales. All relevant works prior to 2014 were well documented in the review paper by Nan et al. (2015).

The Kuroshio intrusion is usually estimated by Luzon Strait transport (LST) in the upper 400 m or 1 000 m (Qu et al., 2004; Nan et al., 2013) water layer from 18.5°N to 22.0°N along 120.75°E due to the relatively large number of observations. However, LST cannot describe which path the Kuroshio intrusion takes in the northern SCS. Hu et al. (2000) and Caruso et al. (2006) concluded that there were four and five types of paths, respectively. Nan et al. (2011a) and Nan et al. (2015) recently proposed an area-average geostrophic vorticity method (based on satellite data in the southwestern region of Taiwan) to classify the Kuroshio intrusion. Three different types were identified: the leaping path, the looping path and the leaking path. Huang et al. (2016, 2017) further refined the method into two subindices, called the double index (DI). These methods have been effective for identifying Kuroshio intrusion paths in both observational and modeling studies (Nan et al., 2013; Huang et al., 2017).

In addition to observational studies, many theoretical and numerical models have also been used to study the Kuroshio in-

Foundation item: The National Key R&D Program for Developing Basic Sciences under contract Nos 2018YFA0605703, 2016YFC1401401 and 2016YFC1401601; the Strategic Priority Research Program of Chinese Academy of Sciences under contract No. XDB42010404; the National Natural Science Foundation of China under contract Nos 41976026, 41776030, 41931183, 41931182 and 41576026.

*Corresponding author, E-mail: lhl@lasg.iap.ac.cn

*Acta Oceanol. Sin.*, 2020, Vol. 39, No. 11, P. 69–81
https://doi.org/10.1007/s13131-020-1676-z
http://www.hyxb.org.cn
E-mail: hyxbe@263.net

# Spatial structure of turbulent mixing of an anticyclonic mesoscale eddy in the northern South China Sea

Yongfeng Qi[1†], Chenjing Shang[2†], Huabin Mao[1, 3*], Chunhua Qiu[4], Changrong Liang[1], Linghui Yu[1], Jiancheng Yu[5], Xiaodong Shang[1]

[1] State Key Laboratory of Tropical Oceanography, South China Sea Institute of Oceanology, Chinese Academy of Sciences, Guangzhou 510301, China

[2] Shenzhen Key Laboratory of Marine Bioresources and Eco-environmental Science, College of Life Science and Oceanography, Shenzhen University, Shenzhen 518060, China

[3] Ocean College, Zhejiang University, Zhoushan 316021, China

[4] The Center for Coastal Ocean Science and Technology, School of Marine Sciences, Sun Yat-sen University, Guangzhou 510275, China

[5] State Key Laboratory of Robotics, Shenyang Institute of Automation, Chinese Academy of Sciences, Shenyang 110016, China

Received 23 June 2020; accepted 10 August 2020



**Abstract**

Upper turbulent mixing in the interior and surrounding areas of an anticyclonic eddy in the northern South China Sea (SCS) was estimated from underwater glider data (May 2015) in the present study, using the Gregg-Henyey-Polzin parameterization and the Thorpe-scale method. The observations revealed a clear asymmetrical spatial pattern of turbulent mixing in the anticyclonic eddy area. Enhanced diffusivity (in the order of $10^{-3}$ $m^2/s$) was found at the posterior edge of the anticyclonic mesoscale eddy; on the anterior side, diffusivity was one order of magnitude lower on average. This asymmetrical pattern was highly correlated with the eddy kinetic energy. Higher shear variance on the posterior side, which is conducive to the triggering of shear instability, may be the main mechanism for the elevated diffusivity. In addition, the generation and growth of sub-mesoscale motions that are fed by mesoscale eddies on their posterior side may also promote the occurrence of strong mixing in the studied region. The results of this study help improve our knowledge regarding turbulent mixing in the northern SCS.

**Key words:** mesoscale eddy, turbulent mixing, South China Sea, GHP parameterization, Thorpe-scale method

**Citation:** Qi Yongfeng, Shang Chenjing, Mao Huabin, Qiu Chunhua, Liang Changrong, Yu Linghui, Yu Jiancheng, Shang Xiaodong. 2020. Spatial structure of turbulent mixing of an anticyclonic mesoscale eddy in the northern South China Sea. Acta Oceanologica Sinica, 39(11): 69–81, doi: 10.1007/s13131-020-1676-z

## 1 Introduction

The South China Sea (SCS) is the largest semi-enclosed marginal sea in the northwestern Pacific Ocean. Its large-scale currents are driven by the East Asian monsoon (Xie et al., 2003). It has been reported that the SCS experiences a range of multiscale dynamical processes including wind- and density-driven circulation (Qu, 2000; Wang et al., 2011), strong internal waves (Alford et al., 2015; Huang et al., 2016), enhanced turbulent mixing (Tian et al., 2009; Liang et al., 2017), and energetic mesoscale eddies (Wang et al., 2003; Zhang et al., 2013; Qiu et al., 2019b). Among these processes, mesoscale eddies with strong kinetic energies play an important role in the dynamics across a range of scales (Chelton et al., 2011) and are a key transport mechanism of oceanic material (Zhang et al., 2014).

Mesoscale eddies in the northern SCS have received much attention in the past few decades, which is evident in both hydrographic datasets and satellite sea-level anomaly data (Li et al., 1998; Li and Pohlmann, 2002; Yuan et al., 2007; Chow et al., 2008; Wang et al., 2003, 2008; Chen et al., 2011; Chu et al., 2014; Zhang et al., 2016; Qiu et al., 2019b). Previous studies have examined eddy structures, eddy life-cycles (in terms of their origination, shifts, development, and decay), and the associated transport of energy and matter in the northern SCS (Wang et al., 2005; Nan et al., 2015; Zhang et al., 2016; Zheng et al., 2017; Qiu et al., 2019a). The prevailing dynamical paradigm is that the oceanic eddies are

Foundation item: The National Key R&D Plan of China under contract Nos 2017YFC0305904, 2017YFC0305804 and 2016YFC1401404; the National Natural Science Foundation of China under contract Nos 41876023, 41630970, 41806037, 41706137 and 41806033; the Guangdong Science and Technology Project under contract Nos 2019A1515111044, 2018A0303130047 and 2017A030310332; the Guangzhou Science and Technology Project under contract No. 201707020037; the Natural Science Foundation of Shenzhen University under contract No. 2019078; the Dedicated Fund for Promoting High-quality Economic Development in Guangdong Province (Marine Economic Development Project) under contract No. GDOE[2019]A03; the Independent Research Project Program of State Key Laboratory of Tropical Oceanography under contract Nos LTOZZ1902 and LTO1909.
*Corresponding author, E-mail: maohuabin@scsio.ac.cn
†These authors contributed equally to this work.

*Acta Oceanol. Sin.*, 2020, Vol. 39, No. 11, P. 82–90
https://doi.org/10.1007/s13131-020-1669-y
http://www.hyxb.org.cn
E-mail: hyxbe@263.net

# Variations of mesoscale eddy SST fronts based on an automatic detection method in the northern South China Sea

Chunhua Qiu[1, 2*], Juan Ouyang[1], Jiancheng Yu[3], Huabin Mao[4], Yongfeng Qi[4], Jiaxue Wu[1, 2*], Danyi Su[1]

[1] School of Marine Sciences, Sun Yat-sen University, Guangzhou 510275, China

[2] Southern Marine Science and Engineering Guangdong Laboratory (Zhuhai), Zhuhai 519020, China

[3] State Key Laboratory of Robotics, Shenyang Institute of Automation, Chinese Academy of Sciences, Shenyang 110016, China

[4] State Key Laboratory of Tropical Oceanography, South China Sea Institute of Oceanology, Chinese Academy of Sciences, Guangzhou 510301, China

Received 15 June 2020; accepted 22 July 2020



**Abstract**

SST fronts at the mesoscale eddy edge (ME fronts) were investigated from 2007–2017 in the northern South China Sea (NSCS) based on an automatic method using satellite sea level anomaly (SLA) and SST data. The relative probabilities between the number of anticyclonic/cyclonic ME fronts (AEF/CEF) and the number of anticyclones/cyclones reached 20%. The northeastern and southwestern parts of these anticyclones had more fronts than the northwestern and southeastern parts, although CEFs were nearly equally distributed in all directions. The number of ME fronts had remarkable seasonal variations, while the eddy kinetic energy (EKE) showed no seasonal variations. The total EKE at the ME fronts was three times of that within the MEs, and it was much stronger in AEFs than in CEFs. The interannual variability in the number of ME fronts and EKE had no significant correlation with the El Niño-Southern Oscillation (ENSO) index. Possible mechanisms of ME fronts were discussed, but the contributions of mesoscale eddies to SST fronts need to be quantified in future studies.

**Key words:** detection method, mesoscale eddy SST front, northern South China Sea

**Citation:** Qiu Chunhua, Ouyang Juan, Yu Jiancheng, Mao Huabin, Qi Yongfeng, Wu Jiaxue, Su Danyi. 2020. Variations of mesoscale eddy SST fronts based on an automatic detection method in the northern South China Sea. Acta Oceanologica Sinica, 39(11): 82–90, doi: 10.1007/s13131-020-1669-y

## 1 Introduction

Oceanic fronts, or transition zones between water masses, play important roles in regulating oceanic heat, energy, and matter balances through associated vertical transport (Lévy et al., 2001; Ruiz et al., 2019). They also influence the atmospheric boundary layer (Xie, 2004). The observation and modeling of oceanic fronts are topics of interest in oceanography.

The South China Sea (SCS) is a large marginal sea in the tropical western Pacific Ocean. The complex topography and monsoon allow multiscale oceanic structures to prevail in the SCS; these include branches of the Kuroshio Current and the SCS Warm Current as well as western boundary currents, mesoscale eddies (MEs), river plumes, upwelling, and submesoscale structures (Hu et al., 2012; Yuan et al., 2006; Zhong et al., 2017; Feng et al., 2020). Fronts have been detected in the above structures, i.e., Kuroshio fronts (Liu et al., 2017), upwelling fronts (Jing et al., 2015), and river plume fronts (Qiu et al., 2017a). Seasonal variations of above thermal fronts were first statistically revealed by Wang et al. (2001), who found that thermal fronts were strong in winter to spring and weak in summer to autumn. In addition to the above fronts, which have lifetimes longer than one month, there are other fronts with temporal scales less than 30 d in the SCS (Hosoda et al., 2012), which might be induced by MEs, filaments and so on.

MEs are common in the SCS. The horizontal lengths/time scales of MEs are 50–300 km/1–10 months (Capet et al., 2008; McWilliams, 2016). Their horizontal scales of motion are characterized by baroclinic instability, at which the Rossby number $Ro=\frac{V}{fL}<1$, where $V$ and $L$ are horizontal velocity and length scales, respectively, and $f$ is the Coriolis frequency (Torres et al., 2018). Qiu et al. (2017a) found that the length scales depended on the local energy of MEs. One high eddy kinetic energy (EKE) band occurred in the northern SCS (NSCS), where both the number of MEs and the EKEs have no significant seasonal variations (Chen et al., 2009; Cheng and Qi, 2010). Interannual variations in EKE were suggested to be induced by the El Niño-Southern Oscillation (ENSO), which show a negative correlation between the SCS EKE and the ENSO index through conveying Kuroshio transport (Sun et al., 2016) or wind stress curl (Wang et al., 2008; Cheng and Qi, 2010). MEs deform with asymmetric shapes during propagation (Wang et al., 2018; Qiu et al., 2019b), resulting in strong vertical currents and turbulence at the ME boundary associated with thermal fronts (Yang et al., 2017, 2019; Qiu et al., 2019a).

The signals of strong coastal and Kuroshio fronts in winter and strong upwelling and river plume fronts in summer hide the high-frequency frontal signals in seasonal variation studies (Wang et al., 2001; Jing et al., 2015; Qiu et al., 2017a). The SST

Foundation item: The National Natural Science Foundation of China under contract No. 41976002.
*Corresponding author, E-mail: qiuchh3@mail.sysu.edu.cn; wujiaxue@mail.sysu.edu.cn

*Acta Oceanol. Sin.*, 2020, Vol. 39, No. 11, P. 91–102
https://doi.org/10.1007/s13131-020-1678-x
http://www.hyxb.org.cn
E-mail: hyxbe@263.net

# Statistical analysis of mesoscale eddy propagation velocity in the South China Sea deep basin

Runqi Huang[1], Lingling Xie[1, 2*], Quanan Zheng[3], Mingming Li[1, 2], Peng Bai[1, 2], Keyi Tan[1]

[1] Laboratory of Coastal Ocean Variation and Disaster Prediction, College of Ocean and Meteorology, Guangdong Ocean University, Zhanjiang 524088, China

[2] Marine Resources Big Data Center of South China Sea, Southern Marine Science and Engineering Guangdong Laboratory (Zhanjiang), Zhanjiang 524025, China

[3] Department of Atmospheric and Oceanic Science, University of Maryland, College Park, Maryland 20742, USA

Received 15 June 2020; accepted 10 August 2020



**Abstract**

Using mesoscale eddy trajectory product derived from satellite altimetry data from 1993 to 2017, this study analyzes the statistical characteristics of spatiotemporal distribution of mesoscale eddy propagation velocities ($\boldsymbol{C}$) in the South China Sea (SCS) deep basin with depths >1 000 m. Climatologically, the zonal propagation velocities ($c_x$) are westwards in the whole basin, and the meridional velocities ($c_y$) are southwards in the northwestern basin, and northwards in the southeastern basin. The variation of $c_y$ with longitude is consistent with that of the background meridional currents with correlation coefficient $R^2$ of 0.96, while the variation of $c_x$ is related both to the background zonal currents and $\beta$ effect. The propagation velocities characterize significant seasonality with the minimum magnitude occurring in summer and the maximum in winter for $c_x$ and $\boldsymbol{C}$. Interannually, larger values of $c_x$ and $c_y$ mostly occurred in La Niña years in the negative phase of the Pacific Decadal Oscillation (PDO). Mesoscale eddies move fast at the beginning and end of their life span, i.e., at their growth and dissipation periods, and slowly during their stable "midlife" period. This trend is negatively correlated with the rotating tangential velocity with $R^2$ of –0.93. Eddies with extreme propagation velocities are defined, which are slower (faster) than 1.5 cm/s (15.4 cm/s) and take 1.5% (1.9%) of the total eddies. The extremely slow-moving (fast-moving) eddies tend to appear in the middle (on the edge) of the basin, and mostly occur in summer (winter). The mechanism analysis reveals that the spatiotemporal distributions of the propagation velocities of mesoscale eddies in the SCS are modulated by the basin-scale background circulation.

**Key words:** South China Sea, mesoscale eddies, eddy propagation velocity, variation in life span, eddies with abnormal speeds

**Citation:** Huang Runqi, Xie Lingling, Zheng Quanan, Li Mingming, Bai Peng, Tan Keyi. 2020. Statistical analysis of mesoscale eddy propagation velocity in the South China Sea deep basin. Acta Oceanologica Sinica, 39(11): 91–102, doi: 10.1007/s13131-020-1678-x

## 1 Introduction

Mesoscale eddies broadly distributed in the global oceans are one of the primary processes responsible for marine material and energy transports (Chelton et al., 2011; Adams et al., 2011; Hausmann and Czaja, 2012; Zhang et al., 2014, 2016; Yang et al., 2015; He et al., 2018; Zhang and Guan, 2019). Therefore, they play important roles in global climate change, ocean circulation, marine ecological environment, and fishery distribution. Mesoscale eddies directly affect the three-dimensional distribution of deep-sea sediments and ecological-environmental factors such as concentrations/distributions of chlorophyll and nutrients (Lobel and Robinson, 1986; Salihoğlu et al., 1990; McGillicuddy et al., 1998; Johnson et al., 2005; Benitez-Nelson et al., 2007; Adams et al., 2011; Frenger et al., 2018). The propagation velocity of mesoscale eddy, i.e., $\boldsymbol{C}$ (bold indicates vector), directly determines the fluxes of material and energy transports. It is thus important to explore the temporal and spatial distribution characteristics and variations of the eddy propagation velocities (Morrow et al., 2004; Cheng and Qi, 2008; Yang et al., 2013; Pilo et al., 2015; Lü et al., 2017).

The South China Sea (SCS) is a large marginal sea in the Northwest Pacific, where mesoscale eddies are very active due to disturbances from the Pacific, seasonally reversed monsoons, and the complex bottom topography (Xie et al., 2016; Xie and Zheng, 2017; Zheng et al., 2017, 2019). Previous researchers have used satellite observations and numerical simulations to statistically characterize mesoscale eddies in the SCS in terms of scale, intensity, numbers, and structure (Wang et al., 2003, 2005; Lin, 2005; Zheng et al., 2007, 2011, 2014; Chen et al., 2011; Li et al., 2011; Lin et al., 2012a; Cui, 2015; Huang et al., 2016; He et al., 2018). Mesoscale eddies in the SCS are mainly distributed in areas where depths exceed 1 000 m and there is an approximately equal probability of occurrence of cyclonic (CE) and anticyclonic eddies (AE) (Zheng et al., 2017). As reviewed by Zheng et

Foundation item: The National Natural Science Foundation of China under contract Nos 41776034 and 41706025; the Fund of Southern Marine Science and Engineering Guangdong Laboratory (Zhanjiang) under contract No. ZJW-2019-08; the Special Project of Global Change and Air and Sea Interaction under contract No. GASI-02-SCS-YGST2-02; the Guangdong Province First-Class Discipline Plan under contract Nos CYL231419012 and 231389002; the Scientific Research Setup Fund of Guangdong Ocean University under contract No.101302/R18001.

*Corresponding author, E-mail: xiell@gdou.edu.cn

*Acta Oceanol. Sin.*, 2020, Vol. 39, No. 11, P. 103–114
https://doi.org/10.1007/s13131-020-1668-z
http://www.hyxb.org.cn
E-mail: hyxbe@263.net

# Physical structure and phytoplankton community off the eastern Hainan coast during summer 2015

Sumin Liu[1, 2, 3], Bo Hong[4*], Guifen Wang[5], Weiqiang Wang[1], Qiang Xie[2, 6], Zekai Ni[2], Liu Yu[2], Huichang Jiang[2], Tong Long[2], Hongzhou Xu[2*]

[1] State Key Laboratory of Tropical Oceanography, South China Sea Institute of Oceanology, Chinese Academy of Sciences, Guangzhou 510301, China

[2] Institute of Deep-sea Science and Engineering, Chinese Academy of Sciences, Sanya 572000, China

[3] Graduate School, University of Chinese Academy of Sciences, Beijing 100049, China

[4] South China University of Technology, Guangzhou 510641, China

[5] Hohai University, Nanjing 210098, China

[6] Center for Ocean Mega-Science, Chinese Academy of Sciences, Qingdao 266071, China

Received 9 May 2020; accepted 31 May 2020



**Abstract**

Based on satellite remote sensing dataset and survey data during upwelling season of 2015, the spatial structures of phytoplankton biomass and community for the first time in the eastern Hainan upwelling (EHU) and its adjacent area, the eastern Leizhou Peninsula upwelling (ELPU) were illustrated. It is found that a significant cold tongue with high salinity and low temperature along the eastern Hainan coast driven by upwelling-favorable summer monsoon. The ELPU was relative weaker than the EHU because of its wide and gentle continental slope. Due to mixing by tides and waves, DO concentration with high value (>6.0 mg/L) were almost homogenous from surface to 30 m depth at the EHU. Beneath that, low DO water (<6.0 mg/L, anoxia) were pumped upward from bottom by the upwelling. The ELPU has worse DO condition compared with the EHU where bottom DO were lower than 3.5 mg/L owing to abundant DO consumption. The phytoplankton biomass reached maximal value about 1.5 mg/m$^3$ at 30 m depth layer rather than surface layer at the EHU indicating the impact limit of upwelling on phytoplankton growth and DO distribution. Nourished by rich nutrient input, the phytoplankton biomass at the ELPU were much higher than the EHU where the maximal value can reach about 4.0 mg/m$^3$. The phytoplankton biomass were reduced to about 0.2–0.3 mg/m$^3$ at the offshore areas of the EHU and ELPU which were close to the value at open sea. At the inshore of the EHU, the phytoplankton community was dominated by diatom which accounted for about 50% of phytoplankton biomass. And prokaryotes (about 40%), green algae (about 20%) and prochlorococcus (about 20%) became main species at the offshore of the EHU. At the ELPU, diatom accounted for about 80% of phytoplankton biomass followed by green algae, indicating a different ecosystem at this region compared with the EHU.

**Key words:** eastern Hainan upwelling, cold tongue, dissolved oxygen, phytoplankton community

**Citation:** Liu Sumin, Hong Bo, Wang Guifen, Wang Weiqiang, Xie Qiang, Ni Zekai, Yu Liu, Jiang Huichang, Long Tong, Xu Hongzhou. 2020. Physical structure and phytoplankton community off the eastern Hainan coast during summer 2015. Acta Oceanologica Sinica, 39(11): 103–114, doi: 10.1007/s13131-020-1668-z

## 1 Introduction

Oceanic upwelling is a common phenomenon in coastal region which takes deep water with low temperature, high salinity, and rich nutrients to upper layer that impacts carbon cycling, blooms biotic community, and raises fishery production (Smith, 1995; Pauly and Christensen, 1995). It has been found in global coastal areas including the South China Sea (Xie et al., 2003; Gan et al., 2009; Wang et al., 2014; Shu et al., 2018), the Yellow Sea (Lü et al., 2010), the East China Sea (Yang et al., 2013), the California coast (Benson et al., 2002; Du and Peterson, 2018), the Chile coast (Sobarzo et al., 2007), the Baltic Sea (Lehmann and Myrberg, 2008), the Eastern Atlantic coast (Roy and Reason, 2001), and the North Benguela coast (Emeis et al., 2018).

The eastern Hainan upwelling (EHU) is one of the strongest upwelling systems in the northern South China Sea (NSCS) (Wu and Li, 2003). This upwelling occurs in summer driven by Asian summer monsoon (Hong and Li, 1991; Li, 1993; Gan et al., 2009). Its spatial structure and intensity have been identified by many studies. For instance, Han et al. (1990) defined a region below 30 m depth where sea surface temperature (SST) were less than 24.5°C and salinity were higher than 34.3 psu as the upwelling center off the eastern Hainan coast (EHC). Guo et al. (1998) extended the upwelling center to region within 40 km offshore and depth less than 100 m based on 2-D model results. Xu et al. (2013) found the EHU can merge with western Guangdong upwelling system in the subsurface layer based on survey data. More studies revealed

Foundation item: The National Key Research and Development Program of China under contract No. 2018YFC0309800; the National Natural Science Foundation of China under contract Nos 41666001, 41576006, 41976014, 41776045; the Chinese Academy of Sciences Frontier Basic Research Project under contract No. QYJC201910; the Sanya Governmental Academy-Locality S&T Cooperation Program under contract No. 2015YD28.

*Corresponding author, E-mail: bohong@scut.edu.cn; hzxu@idsse.ac.cn

*Acta Oceanol. Sin.*, 2021, Vol. 40, No. 2, P. 1–12
https://doi.org/10.1007/s13131-021-1754-x
http://www.hyxb.org.cn
E-mail: hyxbe@263.net

# The geological characteristics of the large- and medium-sized gas fields in the South China Sea

Gongcheng Zhang[1, 2], Dongdong Wang[1*], Lei Lan[2], Shixiang Liu[2], Long Su[3, 4], Long Wang[2], Wu Tang[2], Jia Guo[2], Rui Sun[2]

[1] College of Earth Science and Engineering, Shandong University of Science and Technology, Qingdao 266590, China

[2] CNOOC Research Institute Co., Ltd., Beijing 100028, China

[3] Northwest Institute of Eco-Environment and Resources, Chinese Academy of Sciences, Lanzhou 730000, China

[4] Key Laboratory of Petroleum Resources, Gansu Province, Lanzhou 730000, China

Received 23 March 2020; accepted 17 July 2020



**Abstract**

By the end of 2019, more than 220 gas fields had been discovered in the South China Sea. In order to accurately determine the geological characteristics of the large- and medium-sized gas fields in the South China Sea, this study conducted a comprehensive examination of the gas fields. Based on the abundant available geologic and geochemical data, the distribution and key controlling factors of the hydrocarbon accumulation in the South China Sea were analyzed. The geological and geochemical features of the gas fields were as follows: (1) the gas fields were distributed similar to beads in the shape of a "C" along the northern, western, and southern continental margins; (2) the natural gas in the region was determined to be composed of higher amounts of alkane gas and less $CO_2$; (3) the majority of the alkane gas was observed to be coal-type gas; (4) the gas reservoir types included structural reservoirs, lithologic reservoirs, and stratigraphic reservoirs, respectively; (5) the reservoir ages were mainly Oligocene, Miocene, and Pliocene, while the lithology was mainly organic reef, with some sandstone deposits; and (6) the main hydrocarbon accumulation period for the region was determined to be the late Pliocene-Quaternary Period. In addition, the main controlling factors of the gas reservoirs were confirmed to have been the development of coal measures, sufficient thermal evolution, and favorable migration and accumulation conditions.

**Key words:** coal-type gas, coal measures, thermal evolution, hydrocarbon traps, organic reefs, South China Sea

**Citation:** Zhang Gongcheng, Wang Dongdong, Lan Lei, Liu Shixiang, Su Long, Wang Long, Tang Wu, Guo Jia, Sun Rui. 2021. The geological characteristics of the large- and medium-sized gas fields in the South China Sea. Acta Oceanologica Sinica, 40(2): 1–12, doi: 10.1007/s13131-021-1754-x

## 1 Introduction

The South China Sea, the largest marginal sea in the northwestern part of the Pacific Ocean, has an overall area of approximately $350 \times 10^4$ km$^2$. It is surrounded by continents and islands. Its north is bordered by China's Guangdong, Guangxi, Hainan, and Taiwan Provinces. The south is bordered by Belitung, Kalimantan, and Palawan, with the east bordered by the Luzon, and west bordered by the Indo-China Peninsula. The South China Sea resembles a diamond shape, measuring approximately 3 000 km in length and 1 600 km in width. It extends NE to SW along the long axis. An abyssal plain with continental margins is located in the middle region, with an average water depth over 1 000 m. The continental shelf (or island shelf) is relatively flat and the continental slope (or island slope) is rugged.

There are 14 large basins in the South China Sea, which are mainly situated on the continental shelf and slope (Fig. 1). These include the Southwest Taiwan Basin, Zhujiang River Mouth Basin, Beibu Gulf Basin, and Qiongdongnan Basin on the northern continental margin (Zhang et al., 2013b); Yinggehai Basin, Zhongjiannan Basin, Wan'an Basin, and Mekong Basin on the western continental margin; and the Zengmu Basin, Brunei-Sabah Basin, Palawan Basin, Nanweixi Basin, Beikang Basin, and Liyue Basin on the southern continental margin. These basins are known to be filled with Cenozoic sediment and local residual Mesozoic sediment.

The history of the onshore oil and gas explorations around the South China Sea can be traced back 100 years, since the beginning of the 20th century. Large-scale exploration activities commenced during the mid-1960s in the shallow-water areas and expanded to the deep-water areas in the 1980s (Gong, 1997). The explorations for gas in the South China Sea began later than the oil exploration activities. By the end of 2019, more than 220 gas fields had been discovered in the region, and the cumulative proven gas in place was estimated at up to 6 000 billion m$^3$ (conventional hydrocarbon gas only) in the South China Sea. The gas fields in the South China Sea are distributed in groups, and

Foundation item: The National Petroleum Major Projects under contract Nos 2016ZX05026, 2011ZX05025 and 2008ZX05025; the National Natural Science Foundation Major Research Program of China under contract No. 91528303; the National Program on Key Basic Research Project of China (973 Program) under contract No. 2009CB219400; the Key Laboratory Project of Gansu Province under contract No. 1309RTSA041; the National Natural Science Foundation of China under contract No. 41872172; the SDUST Research Found under contract No. 2018TDJH101.
*Corresponding author, E-mail: wdd02_1@163.com

*Acta Oceanol. Sin.*, 2021, Vol. 40, No. 2, P. 13–28
https://doi.org/10.1007/s13131-021-1757-7
http://www.hyxb.org.cn
E-mail: hyxbe@263.net

# Reinterpretation of the northern South China Sea pre-Cenozoic basement and geodynamic implications of the South China continent: constraints from combined geological and geophysical records

Weilin Zhu[1], Yuchi Cui[1, 2]*, Lei Shao[1]*, Peijun Qiao[1], Peng Yu[1], Jianxiang Pei[3], Xinyu Liu[3], Hao Zhang[1]

[1] State Key Laboratory of Marine Geology, Tongji University, Shanghai 200092, China

[2] The Institute for Geoscience Research (TIGeR), School of Earth and Planetary Sciences, Curtin University, Perth 6845, Australia

[3] Hainan Energy Co., Ltd., CNOOC, Haikou 570145, China

Received 20 November 2019; accepted 3 June 2020



**Abstract**

The pre-Cenozoic northern South China Sea (SCS) Basin basement was supposed to exist as a complex of heterogeneous segments, divided by dozens of N–S faulting. Unfortunately, only the Hainan Island and the northeastern SCS region were modestly dated while the extensive basement remains roughly postulated by limited geophysical data. This study presents a systematic analysis including U-Pb geochronology, elemental geochemistry and petrographic identification on granite and meta-clastic borehole samples from several key areas. Constrained from gravity-magnetic joint inversion, this interpretation will be of great significance revealing the tectono-magmatic evolution along the southeastern margin of the Eurasian Plate. Beneath the thick Cenozoic sediments, the northern SCS is composed of a uniform Mesozoic basement while the Precambrian rocks are only constricted along the Red River Fault Zone. Further eastern part of the northern SCS below the Cenozoic succession was widely intruded by granites with Jurassic-to-early Cretaceous ages. Further western part, on the other hand, is represented by meta-sedimentary rocks with relatively sporadic granite complexes. To be noted, the western areas derived higher-degree and wider metamorphic zones, which is in contrast with the lower-degree and narrower metamorphic belt developed in the eastern region. Drastic collisions between the Indochina Block and South China continent took place since at least late Triassic, resulting in large-scale suturing and deformation zones. At the westernmost part of the northern SCS, the intracontinental amalgamation with closure of the Meso-Tethys has caused fairly stronger and broader metamorphism. One metamorphic biotite granite is located on the suturing belt and yields a Precambrian U-Pb age. It likely represents the relict from the ancient Gondwana supercontinent or its fringes. Arc-continental collision between the Paleo-Pacific and the southeast China Block, on the other hand, results in a relatively narrow NE–SW trending metamorphic belt during the late Mesozoic. Within the overall geological setting, the Cenozoic SCS oceanic basin was subsequently generated from a series of rifting and faulting processes along the collisional-accretionary continental margin.

**Key words:** South China Sea, pre-Cenozoic basement, U-Pb geochronology, Paleo-Pacific subduction, intracontinental collision, metamorphic belt

**Citation:** Zhu Weilin, Cui Yuchi, Shao Lei, Qiao Peijun, Yu Peng, Pei Jianxiang, Liu Xinyu, Zhang Hao. 2021. Reinterpretation of the northern South China Sea pre-Cenozoic basement and geodynamic implications of the South China continent: constraints from combined geological and geophysical records. Acta Oceanologica Sinica, 40(2): 13–28, doi: 10.1007/s13131-021-1757-7

## 1 Introduction

The South China Sea (SCS) is the largest marginal sea within the western Pacific. Extensive investigations have been conducted on the SCS, including scientific and industrial drilling, dredging, and multiple-channel seismic profiles. These surveys have significantly refined the understandings on the origin and subsequent opening of the SCS (Briais et al., 1993; Hsu et al., 2004; Franke et al., 2011; Barckhausen et al., 2014). In particular, recent International Ocean Drilling Program expeditions revealed that the northern SCS margin was neither completely "magma-rich" nor "magma-poor" identified in the other North Atlantic magmatism models (Larsen et al., 2018). Instead, the northern SCS is a representative of hyperextended margin, which is now considered as a missing link between "magma-rich" and "magma-poor" margins (Lei and Ren, 2016; Lei et al., 2019a). In order to precisely evaluate the Cenozoic tectonic evolution of the SCS, researches are also urged to be underpinned from the pre-Cenozoic framework and the geological processes which have greatly controlled the following Cenozoic evolutionary events. Beneath the Cenozoic sedimentary layer, the SCS Basin basement study is of crucial significance in structural geology and regional geodynamic reconstruction (Nissen et al., 1995a, 1995b;

Foundation item: The National Natural Science Foundation of China under contract Nos 42076066, 92055203 and 41874076; the National Science and Technology Major Project under contract Nos 2016ZX05026004-002 and 2017ZX05026005-005; the Fund of China Association for Science and Technology under contract No. 2018CASRQNJL18.
*Corresponding author, E-mail: cuiyuchi@tongji.edu.cn; lshao@tongji.edu.cn

*Acta Oceanol. Sin.*, 2021, Vol. 40, No. 2, P. 29–41
https://doi.org/10.1007/s13131-021-1751-0
http://www.hyxb.org.cn
E-mail: hyxbe@263.net

# A buried submarine canyon in the northwestern South China Sea: architecture, development processes and implications for hydrocarbon exploration

Bin Wang[1], Fuliang Lü[1], Shuang Li[2, 3, 4*], Jian Li[2, 3, 4], Zhili Yang[1], Li Li[1], Xuefeng Wang[1], Yintao Lu[1], Taotao Yang[1], Jingwu Wu[1], Guozhong Sun[1], Hongxia Ma[1], Xiaoyong Xu[1]

[1] Petrochina Hangzhou Research Institute of Geology, Hangzhou 310023, China

[2] University of Chinese Academy of Sciences, Beijing 100049, China

[3] Key Laboratory of Ocean and Marginal Sea Geology, Chinese Academy of Sciences, Guangzhou 510301, China

[4] Innovation Academy of South China Sea Ecology and Environmental Engineering, Chinese Academy of Sciences, Guangzhou 510301, China

Received 30 August 2019; accepted 19 March 2020



**Abstract**

High-resolution multichannel seismic data enables the discovery of a previous, undocumented submarine canyon (Huaguang Canyon) in the Qiongdongnan Basin, northwestern South China Sea. The Huaguang Canyon with a NW orientation is 140 km in length, and 2.5 km to 5 km in width in its upper reach and 4.6 km to 9.5 km in width in its lower reach. The head of the Huaguang Canyon is close to the Xisha carbonate platform and its tail is adjacent to the Central Canyon. This buried submarine canyon is formed by gravity flows from the Xisha carbonate platform when the sea level dropped in the early stage of the late Miocene (around 10.5 Ma). The internal architecture of the Huaguang Canyon is mainly characterized by high amplitude reflections, indicating that this ancient submarine canyon was filled with coarse-grained sediments. The sediment was principally scourced from the Xisha carbonate platform. In contrast to other buried large-scale submarine canyons (Central Canyon and Zhongjian Canyon) in the Qiongdongnan Basin, the Huaguang Canyon displays later formation time, smaller width and length, and single sediment supply. The coarse-grained deposits within the Huaguang Canyon provide a good environment for reserving oil and gas, and the muddy fillings in the Huaguang Canyon have been identified as regional caps. Therefore, the Huaguang Canyon is a potential area for future hydrocarbon exploration in the northwestern South China Sea. The result of this paper may contribute to a better understanding of the evolution of submarine canyons formed in carbonate environment.

**Key words:** South China Sea, Qiongdongnan Basin, submarine canyon, evolution

**Citation:** Wang Bin, Lü Fuliang, Li Shuang, Li Jian, Yang Zhili, Li Li, Wang Xuefeng, Lu Yintao, Yang Taotao, Wu Jingwu, Sun Guozhong, Ma Hongxia, Xu Xiaoyong. 2021. A buried submarine canyon in the northwestern South China Sea: architecture, development processes and implications for hydrocarbon exploration. Acta Oceanologica Sinica, 40(2): 29–41, doi: 10.1007/s13131-021-1751-0

## 1 Introduction

Submarine canyons are prominent topographic features on both passive and active continental margins, which can extend for thousands of kilometres across the seafloor (Harris and Whiteway, 2011). They are more common in distal slope regions and play an essential role in determining the sediment dispersal pattern, and the growth of the whole fan. They are with great research value and meaning in the hydrocarbon industry (Piper and Normark, 1983; Mayall et al., 2006; McHargue et al., 2011; Ortiz-Karpf et al., 2015). Submarine canyons are very important as they could transport large volumes of sediment from the continental shelf into deep-water and form the largest sedimentary deposits on earth (Wynn et al., 2007). These deposits are significant hosts for gas and oil reserves, and hold key information on past climate change and mountain building episodes. The initiation and evolution of submarine canyons result from a combination of factors, including basin tectonics, climate, sea-level changes, and Coriolis force (deviate to right in the northern hemisphere) that control the type, supply and deposition of sediment (Bouma, 2004; Kolla, 2007; Richards et al., 1998; Peakall et al., 2012; Cossu and Wells, 2013; De Leeuw et al., 2016). The research on submarine canyons is of great importance for characterizing ancient and buried turbidite units that may contain hydrocarbons (Li et al., 2013; Su et al., 2014).

Submarine canyons have been widely documented in the South China Sea where now is a promising area for hydrocarbon exploration. The Cental Canyon in Qiongdongnan Basin (QDNB) has been identified as a main hydrocarbon reservoir, which is

Foundation item: The National Scientific Foundation of China under contract No.41876054; the National Science and Technology Major Project "the evaluations of deepwater oil and gas geological conditions and targets in Zhongjian area of the South China Sea" under contract No.2017ZX05026006; the CNPC Science and Technology Major Projects under contract No. 2019A-1009&2019D-4309; the Strategic Priority Research Program of the Chinese Academy of Sciences under contract No. XDA13010101; the National Natural Science Foundation of China under contract No. 41706054.

*Corresponding author, E-mail: lishuang@scsio.ac.cn

*Acta Oceanol. Sin.*, 2021, Vol. 40, No. 2, P. 42–53
https://doi.org/10.1007/s13131-021-1753-y
http://www.hyxb.org.cn
E-mail: hyxbe@263.net

# Structural characteristics of central depression belt in deep-water area of the Qiongdongnan Basin and the hydrocarbon discovery of Songnan low bulge

Mo Ji[1], Qingbo Zeng[1], Haizhang Yang[1], Shuai Guo[1], Kai Zhong[2, 3*]

[1] CNOOC Research Institute Co., Ltd., Beijing 100028, China

[2] State Key Laboratory of Marine Geology, Tongji University, Shanghai 200092, China

[3] Marine Resource Research Center, Tongji University, Shanghai 200092, China

Received 6 September 2019; accepted 24 April 2020



**Abstract**

The Qiongdongnan Basin has the first proprietary high-yield gas field in deep-water areas of China and makes the significant breakthroughs in oil and gas exploration. The central depression belt of deep-water area in the Qiongdongnan Basin is constituted by five sags, i.e. Ledong Sag, Lingshui Sag, Songnan Sag, Baodao Sag and Changchang Sag. It is a Cenozoic extensional basin with the basement of pre-Paleogene as a whole. The structural research in central depression belt of deep-water area in the Qiongdongnan Basin has the important meaning in solving the basic geological problems, and improving the exploration of oil and gas of this basin. The seismic interpretation and structural analysis in this article was operated with the 3D seismic of about $1.5\times10^4$ km$^2$ and the 2D seismic of about $1\times10^4$ km. Eighteen sampling points were selected to calculate the fault activity rates of the No.2 Fault. The deposition rate was calculated by the ratio of residual formation thickness to deposition time scale. The paleo-geomorphic restoration was obtained by residual thickness method and impression method. The faults in the central depression belt of deep-water area of this basin were mainly developed during Paleogene, and chiefly trend in NE–SW, E–W and NW–SE directions. The architectures of these sags change regularly from east to west: the asymmetric grabens are developed in the Ledong Sag, western Lingshui Sag, eastern Baodao Sag, and western Changchang Sag; half-grabens are developed in the Songnan Sag, eastern Lingshui Sag, and eastern Changchang Sag. The tectonic evolution history in deep-water area of this basin can be divided into three stages, i.e. faulted-depression stage, thermal subsidence stage, and neotectonic stage. The Ledong-Lingshui sags, near the Red River Fault, developed large-scale sedimentary and subsidence by the uplift of Qinghai-Tibet Plateau during neotectonic stage. The Baodao-Changchang sags, near the northwest oceanic sub-basin, developed the large-scale magmatic activities and the transition of stress direction by the expansion of the South China Sea. The east sag belt and west sag belt of the deep-water area in the Qiongdongnan Basin, separated by the ancient Songnan bulge, present prominent differences in deposition filling, diaper genesis, and sag connectivity. The west sag belt has the advantages in high maturity, well-developed fluid diapirs and channel sand bodies, thus it has superior conditions for oil and gas migration and accumulation. The east sag belt is qualified by the abundant resources of oil and gas. The Paleogene of Songnan low bulge, located between the west sag belt and the east sag belt, is the exploration potential. The YL 8 area, located in the southwestern high part of the Songnan low bulge, is a favorable target for the future gas exploration. The Well 8-1-1 was drilled in August 2018 and obtained potential business discovery, and the Well YL8-3-1 was drilled in July 2019 and obtained the business discovery.

**Key words:** Qiongdongnan Basin, deep-water area, structural differentiation

**Citation:** Ji Mo, Zeng Qingbo, Yang Haizhang, Guo Shuai, Zhong Kai. 2021. Structural characteristics of central depression belt in deep-water area of the Qiongdongnan Basin and the hydrocarbon discovery of Songnan low bulge. Acta Oceanologica Sinica, 40(2): 42–53, doi: 10.1007/s13131-021-1753-y

## 1 Introduction

The Qiongdongnan Basin was extensively studied in its structural characteristics, as its special geotectonic location and abundant oil and gas resources. Li and Zhu (2005) considered that the fault activity in the Qiongdongnan Basin can be divided into four stages: Eocene–early Oligocene (Yacheng period), late Oligocene (Lingshui period), early–middle Miocene and late Miocene–Quaternary, the NE-trending and near EW-trending basement faults in the Paleogene are "faults controlling basin and belts", and the faults had strong vertical dredging capacity during the early–middle Miocene. Li et al. (2006) believed that the Qiongdongnan Basin experienced two stages of extension process (Eocene–early Oligocene and late Oligocene), forming two types of rift structural styles (half-graben and graben) and the architecture characteristics of "zoning in north-south, segmenting in east-west". Xie et al. (2007) suggested that NE- and NW-trending faults predominate the eastern part of the Qiongdongnan Basin, while near EW-trending faults predominate the west-

Foundation item: The National Natural Science Foundation of China under contract No. 91528303; the National Science and Technology Major Project under contract Nos 2016ZX05026, 2011ZX05025 and 2008ZX05025; the National Basic Research Program (973 Program) of China under contract No. 2009CB219400.

*Corresponding author, E-mail: zhongkai@tongji.edu.cn

*Acta Oceanol. Sin.*, 2021, Vol. 40, No. 2, P. 54–64
https://doi.org/10.1007/s13131-021-1749-7
http://www.hyxb.org.cn
E-mail: hyxbe@263.net

# Control effects of the synsedimentary faults on the basin-marginal fans in the central part of the deep-water area of early Oligocene Qiongdongnan Basin, South China Sea

Guangzeng Song[1, 2*], Zengxue Li[2], Haizhang Yang[3], Dongdong Wang[2], Ying Chen[3], Rui Sun[3]

[1] School of Water Conservancy and Environment, University of Jinan, Ji'nan 250022, China

[2] Key Laboratory of Sedimentary Mineralization and Sedimentary Minerals in Shandong Province, Shandong University of Science and Technology, Qingdao 266590, China

[3] Beijing Research Center, CNOOC (China) Co., Ltd., Beijing 100010, China

Received 26 August 2019; accepted 30 March 2020



**Abstract**

The synsedimentary faults and basin-marginal fans located in the central part of the deep-water area of the early Oligocene Qiongdongnan Basin have been investigated using seismic profiles, boreholes, and well-log data. Through the formations of the characterized paleogeomorphology, such as transverse anticlines, fault ditches, and step-fault belts, the synsedimentary faults are known to have controlled the development position, distribution direction, and extension scales of the basin-marginal fans. For example, at the pitching ends of two adjacent faults, transverse anticlines developed, which controlled the development positions and distributions of the fans. During the early Oligocene, the faults controlled the subsidence center, and fault ditches were formed at the roots of the faults. In the surrounding salient or low salient areas, which were exposed as provenance areas during early Oligocene, the fault ditches acted as the source channels and determined the flow paths of the clastics, where incised valley fills were obviously developed. The fault ditches which developed in the sedimentary basins were able to capture the drainage systems and influenced the distributions of the fans. The large boundary faults and the secondary faults generated two fault terraces and formed step-fault belts. The first fault terrace caused the clastics to be unloaded. As a result, fans were formed at the entrance to the basin. Then, the second fault terrace caused the fans to move forward, with the fans developing in a larger extension scale. The results obtained in this study will potentially be beneficial in the future prospecting activities for reservoirs and coal-measure source rocks in the basins located in the deep-water areas of the South China Sea.

**Key words:** deep-water area, synsedimentary fault, basin-marginal fan, transverse anticline, fault ditch, step-fault belt

**Citation:** Song Guangzeng, Li Zengxue, Yang Haizhang, Wang Dongdong, Chen Ying, Sun Rui. 2021. Control effects of the synsedimentary faults on the basin-marginal fans in the central part of the deep-water area of early Oligocene Qiongdongnan Basin, South China Sea. Acta Oceanologica Sinica, 40(2): 54–64, doi: 10.1007/s13131-021-1749-7

## 1 Introduction

In the past twenty years (1999–2019), research has been conducted regarding the control effects of synsedimentary structures (in particular, synsedimentary faults) on the sequence architecture or sedimentation in rift basins. These have become international hot topics for the petroleum basin analysis, and have drawn attention from the researchers both at home and abroad (Ravnås and Steel, 1998; Lin et al., 2004; Athmer and Luthi, 2011; Liu et al., 2015; Yang et al., 2017). Howell and Flint (1996) considered that the synsedimentary faults and fault conversion zones in rift basins were similar to the shelf slopes in passive continental margins. When researching marine rift basins, Ravnås and Steel (1998) concluded that the activations of synsedimentary faults could have control effects on the formations of accommodation spaces and transfer zones, and also further influence the source channels and unloading of source clastics in a basin. Lin et al. (2004) suggested that the synsedimentary faults in the Dongying Sag and Zhanhua Sag had potentially influenced the development and distributions of the sedimentary systems, and presented the concept of a slope break belt. In the studies conducted by Athmer and Luthi (2011), it was suggested that the synsedimentary faults and their combination patterns had led to the formation of relay ramps, and discussed the effects of relay ramps on the routes and deposition of sediment. Although Song et al. (2014) and Liao et al. (2016) have conducted similar research, the majority of the previous researchers seldom focused on the rift basins located in deep-water sea areas which lack borehole information data. In such cases, recognizing the control effects of synsedimentary faults on basin sedimentation could be very beneficial.

With the success of the explorations conducted in the Gulf of Mexico, Columbus Basin, and the coast of Africa, basin-marginal

Foundation item: The National Natural Science Foundation of China under contract Nos 41872172, 41672096 and 41702114; the Major National Science and Technology Projects under contract No. 2016ZX05026007-004; the Natural Science Foundation of Shandong Province under contract No. ZR2019QD008; the Natural Science Foundation of Guizhou Province under contract No. 20191148.
*Corresponding author, E-mail: songguangzeng2006@163.com

*Acta Oceanol. Sin.*, 2021, Vol. 40, No. 2, P. 65–80
https://doi.org/10.1007/s13131-021-1759-5
http://www.hyxb.org.cn
E-mail: hyxbe@263.net

# Characteristics and origins of middle Miocene mounds and channels in the northern South China Sea

Yufeng Li[1, 2, 3, 4], Gongcheng Zhang[5], Renhai Pu[2, 3*], Hongjun Qu[2, 3], Huailei Shen[5], Xueqin Zhao[1]

[1] School of Environment and Resource, Southwest University of Science and Technology, Mianyang 621010, China

[2] State Key Laboratory of Continental Dynamics, Xi'an 710069, China

[3] Department of Geology, Northwest University, Xi'an 710069, China

[4] Key Laboratory of Marine Mineral Resources, Ministry of Natural Resources, Guangzhou 510075, China

[5] CNOOC Research Institute Co., Ltd., Beijing 100028, China

Received 1 October 2019; accepted 25 May 2020



**Abstract**

Numerous elongated mounds and channels were found at the top of the middle Miocene strata using 2D/3D seismic data in the Liwan Sag of Zhujiang River Mouth Basin (ZRMB) and the Beijiao Sag of Qiongdongnan Basin (QDNB). They occur at intervals and are rarely revealed by drilling wells in the deepwater areas. Origins of the mounds and channels are controversial and poorly understood. Based on an integrated analysis of the seismic attribute, palaeotectonics and palaeogeography, and drilling well encountering a mound, research results show that these mounds are dominantly distributed on the depression centres and/or slopes of the Liwan and Beijiao sags and developed in a bathyal sedimentary environment. In the Liwan and Beijiao sags, the mounds between channels (sub) parallel to one another are 1.0–1.5 km and 1.5–2.0 km wide, 150–300 m and 150–200 m high, and extend straightly from west to east for 5–15 km and 8–20 km, respectively. Mounds and channels in the Liwan Sag are parallel with the regional slope. Mounds and channels in the Beijiao Sag, however, are at a small angle to the regional slope. According to internal geometry, texture and external morphology of mounds, the mounds in Beijiao Sag are divided into weak amplitude parallel reflections (mound type I), blank or chaotic reflections (mound type II), and internal mounded reflections (mound type III). The mounds in Liwan Sag, however, have the sole type, i.e., mound type I. Mound type I originates from the incision of bottom currents and/or gravity flows. Mound type II results from gravity-driven sediments such as turbidite. Mound type III is a result of deposition and incision of bottom currents simultaneously. The channels with high amplitude between mounds in the Beijiao and Liwan sags are a result of gravity-flow sediments and it is suggested they are filled by sandstone. Whereas channels with low-mediate amplitudes are filled by bottom-current sediments only in the Beijiao Sag, where they are dominantly composed of mudstone. This study provides new insights into the origins of the mounds and channels worldwide.

**Key words:** South China Sea, middle Miocene, channels and mounds, contour currents

**Citation:** Li Yufeng, Zhang Gongcheng, Pu Renhai, Qu Hongjun, Shen Huailei, Zhao Xueqin. 2021. Characteristics and origins of middle Miocene mounds and channels in the northern South China Sea. Acta Oceanologica Sinica, 40(2): 65–80, doi: 10.1007/s13131-021-1759-5

## 1 Introduction

The Zhujiang River Mouth Basin (ZRMB) and Qiongdongnan Basin (QDNB) (together abbreviated as ZRMB-QDNB) are located in the northern South China Sea (SCS). There are a wide variety of geological phenomena in the northern SCS, some of which are various similarly mounded seismic reflection bodies, such as sand intrusion mounds (Yang et al., 2014), mud diapirs or mud volcanoes (Meng et al., 2012), volcanoes dome (Pu et al., 2013; Zhang et al., 2013), carbonate reefs (Chen et al., 2011; Zhang et al., 2011; Wang et al., 2015), sediment waves related to bottom currents (Zhao et al., 2013), contourite drifts (Chen et al., 2016; Sun et al., 2017), lime-mud mounds (Andresen et al., 2009), and remnant mounds originated from the bottom current incision (Sun et al., 2016). In recent years, the modern channels formed by contour (bottom) currents are documented in previous studies (Chen et al., 2014, 2016; Gong et al., 2016; Sun et al., 2017), some of which can be traced back to the early late Miocene in the northern SCS.

In recent years, pervasive mounds are found in the middle Miocene in the ZRMB-QDNB, which attracts much attention from geologists. In the academic circle, most geologists widely accept a viewpoint that it is an important period of reef development in the middle Miocene in the northern SCS (Wu et al., 2014; Shao et al., 2017). Furthermore, the middle Miocene Liuhua field reefs containing oil and gas are found in the Dongsha Uplift in the ZRMB (Ma et al., 2010). In the Liwan and Beijiao sags, mounds and channels are pervasively identified using both the 2D and 3D seismic surveys in the middle Miocene. Based on the shape, property, and locations of mounded seismic reflections, Wu et al. (2009), Zhang et al. (2011), Huang et al. (2012), and Yi

Foundation item: The National Science and Technology Major Project of China under contract Nos 2011ZX05025-006-02 and 2016ZX05026-007; the National Natural Science Foundation of China under contract Nos 41390451 and 41672206; the Doctoral Fund of Southwest University of science and technology under contract No. 18zx711901; the Fund of Key Laboratory of Marine Mineral Resources of Ministry of Natural Resources under contract No. KLMMR-2018-B-07.
*Corresponding author, E-mail: purenhai@126.com

*Acta Oceanol. Sin.*, 2021, Vol. 40, No. 2, P. 81–94
https://doi.org/10.1007/s13131-021-1750-1
http://www.hyxb.org.cn
E-mail: hyxbe@263.net

# Migrated hybrid turbidite-contourite channel-lobe complex of the late Eocene Rovuma Basin, East Africa

Yintao Lu[1, 2], Xiwu Luan[2, 3*], Boqing Shi[4], Weimin Ran[2, 3], Fuliang Lü[1], Xiujuan Wang[5], Quanbin Cao[1], Xiaoyong Xu[1], Hui Sun[1], Genshun Yao[1]

[1] PetroChina Hangzhou Research Institute of Geology, Hangzhou 310023, China

[2] Qingdao Institute of Marine Geology, China Geological Survey, Qingdao 266071, China

[3] Laboratory of Marine Mineral Resources, Pilot National Laboratory for Marine Science and Technology (Qingdao), Qingdao 266237, China

[4] China National Oil and Gas Exploration and Development Corporation, Beijing 100034, China

[5] Institute of Oceanology, Chinese Academy of Sciences, Qingdao 266071, China

Received 27 August 2019; accepted 25 May 2020



**Abstract**

Analysis of 3D seismic data and well log data from the Rovuma Basin in East Africa reveals the presence of a late Eocene channel-lobe complex on its slope. The first two channels, denoted as channel-1 and channel-2, are initiated within a topographic low on the slope but come to a premature end when they are blocked by a topographic high in the northwest region of the basin. New channels migrate southeastward from channel-1 to channel-6 due to the region's sufficient sediment supply and stripping caused by bottom currents. The primary factors controlling the development of the channel complex include its initial paleo-topographic of seafloor, the property of gravity flows, the direction of the bottom current, and the stacking and expansion of its levees. The transition zone from channel to lobe can also be clearly identified from seismic sections by its pond-shaped structure. At a certain point, thest systems record a transiton from erosive features to sedimentary features, and record a transition from a confined environment to an open environment. Channels and lobes can be differentiated by their morphologies: thick slump-debris flows are partly developed under channel sand sheets, whereas these slump-debris flows are not very well developed in lobes. Well log responses also record different characteristics between channels and lobes. The interpreted shale volume throughout the main channel records a box-shaped curve, thereby implying that confined channel complexes record high energy currents and abundant sand supply, whereas the interpreted shale volume throughout the lobe records an upward-fining shape curve, thereby indicating the presence of a reduced-energy current in a relatively open environment. Within the Rovuma Basin of East Africa, the average width of the Rovuma shelf is less than 10 km, the width of the slope is only approximately 40 km, and the slope gradient is 2°–4°. Due to this steep slope gradient, the sand-rich top sheet within the channel also likely contributes to the straight feature of the channel system. It is currently unclear whether the bottom current has any effect on its sinuosity.

**Key words:** East Africa, Rovuma Basin, deep-water sediment, channel-lobe complex

**Citation:** Lu Yintao, Luan Xiwu, Shi Boqing, Ran Weimin, Lü Fuliang, Wang Xiujuan, Cao Quanbin, Xu Xiaoyong, Sun Hui, Yao Genshun. 2021. Migrated hybrid turbidite-contourite channel-lobe complex of the late Eocene Rovuma Basin, East Africa. Acta Oceanologica Sinica, 40(2): 81–94, doi: 10.1007/s13131-021-1750-1

## 1 Introduction

Deep-water environment represents one of the most important depositional settings on the earth (Callow et al., 2014). Submarine canyons and channels on the continental slope facilitate the transportation of sediment from the continental shelf through the slope, and the sediment might be finally deposited in submarine fan lobes on the lower slope and basin floor (Normark, 1970; Shepard, 1981; Normark and Carlson, 2003; Paull et al., 2011; Peakall and Sumner, 2015). A typical submarine lobe developed at the mouth of its feeding channel, which is commonly aligned parallel to the axis of the feeder channel (Normark, 1970). Submarine channel-lobe systems vary widely in size and shape, of which deposits represent one of the most important sedimentary units as common targets for the petroleum industry (Lewis and Pantin, 2002; Migeon et al., 2004), and have attracted much attention and have been studied in great detail (Normark et al., 1979, 1998; Bowen et al., 1984; Bouma et al., 1985; Weimer and Link, 1991; Pickering et al., 1995; Zaragosi et al., 2000).

Some submarine channels are straight, whereas others are sinuous (Clark et al., 1992; Peakall et al., 2007, 2013; Sylvester et al., 2013; Peakall and Sumner, 2015). Submarine fans could be formed by turbidity currents (Vail et al., 1991) and mass transport deposits (MTDs), which are mainly sandy slumps and sandy debris flows (Shanmugam et al., 1995), during periods of global sea-level lowstands (Shanmugam and Moiola, 1982, 1985).

Foundation item: The China-ASEAN Maritime Cooperation Fund Project under contract No. 12120100500017001; the National Natural Science Foundation of China under contract Nos 42076219, 92055211 and 42006067.
*Corresponding author, E-mail: xluan@qnlm.ac

*Acta Oceanol. Sin.*, 2021, Vol. 40, No. 2, P. 95–106
https://doi.org/10.1007/s13131-021-1748-8
http://www.hyxb.org.cn
E-mail: hyxbe@263.net

# Peat formation and accumulation mechanism in northern marginal basin of South China Sea

Zengxue Li[1]*, Qingbo Zeng[2], Meng Xu[3], Dongdong Wang[1], Guangzeng Song[4], Pingli Wang[1], Xiaojing Li[1], Xue Zheng[1]

[1] Key Laboratory of Sedimentary Mineralization and Sedimentary Minerals in Shandong Province, Shandong University of Science and Technology, Qingdao 266590, China

[2] Beijing Research Center, CNOOC (China) Co., Ltd., Beijing 100010, China

[3] No. 1 Institute of Geology and Mineral Resources of Shandong Province, Ji'nan 250014, China

[4] School of Water Conservancy and Environment, University of Jinan, Ji'nan 250022, China

Received 24 August 2019; accepted 21 June 2020



**Abstract**

In the present study, the coal-rock organic facies of Oligocene Yacheng Formation of the marginal basin in the South China Sea were classified and divided. In addition, through the correlations of the large-scale coal-bearing basins between the epicontinental sea and the South China Sea, it was concluded that the coal forming activities in the South China Sea presented particularity and complexity. Furthermore, the coal forming mechanisms also presented distinctiveness. The marginal basins in the South China Sea consist of several large and complex rift or depression basins, which are distributed at different tectonic positions in the South China Sea. Therefore, the marginal basins in the South China Sea are not simple traditional units with onshore continental slopes extending toward the deep sea. The marginal basins are known to consist of multi-level structures and distinctive types of basins which differ from the continental regions to the sea. During the Oligocene, the existing luxuriant plants and beneficial conditions assisted in the development of peat. Therefore, the Oligocene was the significant period for the formation and aggregation of the peat. However, the peat did not form in unified sedimentary dynamic fields, but instead displayed multi-level geographical units, multiple provenance areas, instability, and nonevent characteristics. As a result, the marginal basins in the South China Sea are characterized by non-uniform peat aggregation stages. In another words, the majority of the peat had entered the marine system in a dispersive manner and acted as part of the marine deposits, rather than during one or several suitable coal-forming stages. These peat deposits then became the main material source for hydrocarbon generation in all of the marginal basins of the South China Sea. The study will be of much significance for the hydrocarbon exploration in the marginal basins of the South China Sea.

**Key words:** South China Sea, marginal basins, land-sea interactions, peat dispersion, Oligocene

**Citation:** Li Zengxue, Zeng Qingbo, Xu Meng, Wang Dongdong, Song Guangzeng, Wang Pingli, Li Xiaojing, Zheng Xue. 2021. Peat formation and accumulation mechanism in northern marginal basin of South China Sea. Acta Oceanologica Sinica, 40(2): 95–106, doi: 10.1007/s13131-021-1748-8

## 1 Introduction

The Oligocene coastal marsh facies source rock, Miocene marine mudstone, and carbonaceous mudstone are known to be well developed in the sedimentary basins of the South China Sea. It has been determined in previous studies that the main mudstone and carbonaceous mudstone in the Oligocene coastal marsh facies coal series are Type II2 kerogen and Type III kerogen (Liu, 2005, 2010; Feng et al., 2010; Zhu, 2010; Mi et al., 2010; Li et al., 2011b).

The initial substances which form coal are plant material. Peat is formed by a series of biophysical and biochemical processes which occur in plants. Such materials are generally not produced by the denudation process, but rather are grown from and refer to as "authigenic" organic materials. The processes (which do not include the eventual formation of coal) are complex and characteristic of peat deposits. The formations of coal deposits and seams, as a special sedimentary mineral in nature, obviously also follow the basic laws of material formation, processing, and finally aggregation (Li et al., 2011c, 2018). For example, the coal mines in East Asia are formed under the control of geodynamics. However, the formation processes are essentially different from that of the majority of sedimentary rock. Therefore, as special organic sedimentary bodies, the formation processes of coal do not completely follow the sedimentary genetic mechanisms of other types of sedimentary rock.

Peat formation and aggregation are known to have been highly sensitive to environmental conditions. In other words, peat is easily affected and controlled by external conditions. The basic conditions for coal formation in geological history are the results of the interactions and mutual restrictions of the paleo-

Foundation item: The National Natural Science Foundation of China under contract Nos 41872172 and 41672096; the Major National Science and Technology Projects under contract No. 2016ZX05026007-004; the Science Foundation of Shandong Province under contract No. ZR2019QD008.

*Corresponding author, E-mail: lizengxue@126.com

*Acta Oceanol. Sin.*, 2021, Vol. 40, No. 2, P. 107–113
https://doi.org/10.1007/s13131-021-1755-9
http://www.hyxb.org.cn
E-mail: hyxbe@263.net

# Study on fault-controlled hydrocarbon migration and accumulation process and models in Zhu I Depression

Wenqi Zhu[1]*, Keqiang Wu[1], Ling Ke[1], Kai Chen[1], Zhifeng Liu[1]

[1] CNOOC Research Institute Co., Ltd., Beijing 100028, China

Received 19 September 2019; accepted 29 June 2020



**Abstract**

Through the analysis of the faults and their internal structure in Zhu I Depression, it is found that the internal structure of the late fault is obviously segmented vertically. It develops unitary structure (simple fault plane) in shallow layers, binary structure (induced fracture zone in hanging wall and sliding fracture zone in footwall) in middle, layers and ternary structure (induced fracture zone in hanging wall and sliding fracture zone in middle, and induced fracture zone in footwall) in deep layers. Because the induced fracture zone is a high porosity and permeability zone, and the sliding fracture zone is a low porosity and ultra-low permeability zone, the late fault in middle layers has the character of "transporting while sealing". The late fault can transport hydrocarbon by its induced fracture zone in the side of the hanging wall and seal hydrocarbon by its sliding fracture zone in the side of the footwall. In deep layers, the late fault has the character of "dual-transportation", induced fracture zones in both sides of hanging wall and footwall can transport hydrocarbon. The early fault that only developed in the deep layers is presumed to be unitary structure, which plays a completely sealing role in the process of hydrocarbon migration and accumulation due to inactivity during the hydrocarbon filling period. Controlled by hydrocarbon source, early/late faults, sand bodies and traps, two reservoir-forming models of "inverted L" and "stereo-spiral" can be proposed in middle layers, while two reservoir-forming models of "cross fault" and "lateral fault sealing" are developed in the deep layers of Zhu I Depression.

**Key words:** fault structure, transport/sealing, migration and accumulation process, reservoir-forming model, Zhu I Depression

**Citation:** Zhu Wenqi, Wu Keqiang, Ke Ling, Chen Kai, Liu Zhifeng. 2021. Study on fault-controlled hydrocarbon migration and accumulation process and models in Zhu I Depression. Acta Oceanologica Sinica, 40(2): 107–113, doi: 10.1007/s13131-021-1755-9

## 1 Introduction

Many theories and experiences have been formed in the study of hydrocarbon migration and accumulation in China, for example, source-control theory (Hu, 2005), multiple hydrocarbon accumulation belt (Hu et al., 1986), structural ridge accumulating oil (Zou et al., 1991), source-cap co-control theory (Zhou and Wang, 2000), compound transduction and meshwork-carpet reservoir (Zhang et al., 2003), full-concave oil-bearing (Zhao et al., 2004), multiple oil-control and phase potential-control accumulation (Li, 2003). Hydrocarbon migration and accumulation process is the key of hydrocarbon accumulation research, which mainly describe the migration period, migration path (Li, 1988; Zhou et al., 2008) and migration direction (Chen et al., 2003b) of hydrocarbon with the help of geochemical and basin model methods at present. Applying the theories and methods above, a lot of works have been carried out in the study of hydrocarbon reservoir formation in Zhu I Depression (Gong et al., 2012; He et al., 2012; Shi, 2013, 2015). However, through the analysis of the reasons for the failure of more than 140 exploratory wells in Zhu I Depression, there are 72 of them failed due to migration. Hence the unclear process of hydrocarbon migration and accumulation is still the biggest problem restricting petroleum exploration in Zhu I Depression.

Faults, especially late faults (Tian et al., 2008), are the keys to control hydrocarbon migration and accumulation in Zhu I Depression. Fault-sand transport system is the most important hydrocarbon transport combination in Zhu I Depression, especially when faults contact with source rocks (Wu et al., 2001). The fault activity, internal structure and spatial association of fault-sand all have a vital impact on the migration-accumulation process of hydrocarbon. This study classified the faults according to the differences of fault formation stages. On this basis, the internal structure of fault zone and its role in the process of hydrocarbon migration and accumulation are emphatically analyzed. The process of hydrocarbon migration and accumulation under the control of faults is basically clarified, and a variety of reservoir-forming modes is established. These models can be used for guiding the exploration of Zhu I Depression and even the whole Zhujiang River Mouth Basin.

## 2 Geological setting

The Zhu I Depression with an area of about $4\times10^4$ km$^2$ is located in the northern depression zone of Zhujiang River Mouth Basin in the north of South China Sea (Fig. 1). It is a Cenozoic faulted lake basin developed on the basement of Mesozoic continental shelf. The Enping (EP) Sag, Xijiang (XJ) Sag, Huizhou (HZ) Sag, Lufeng (LF) Sag and Hanjiang (HJ) Sag successively developed from west to east. From deep to shallow, the depositional environment is lacustrine in Wenchang (WC) formation, fluvial in Enping (EP) formation, marine delta in Zhuhai (ZH) forma-

Foundation item: The National Science and Technology Major Project of the Ministry of Science and Technology of China under contract No. 2016ZX05024-002.

*Corresponding author, E-mail: zhuwq3@cnooc.com.cn

*Acta Oceanol. Sin.*, 2021, Vol. 40, No. 2, P. 114–122
https://doi.org/10.1007/s13131-021-1756-8
http://www.hyxb.org.cn
E-mail: hyxbe@263.net

# Sediment source and environment evolution in Taiwan Island during the Eocene–Miocene

Yuanli Hou[1], Weilin Zhu[1]*, Peijun Qiao[1], Chi-Yue Huang[1], Yuchi Cui[1], Xianbo Meng[1]

[1] State Key Laboratory of Marine Geology, Tongji University, Shanghai 200092, China

Received 29 September 2019; accepted 16 June 2020



**Abstract**

Taiwan Island's outcropping strata can provide important insights into the sedimentary environment and source development of the southeast China margin. This research is based on the Eocene–Miocene strata of the Tsukeng area in the central Western Foothills, northeast shoreline of Taiwan Island and two sites of the East China Sea Shelf Basin (ECSSB), using petrology and detrital zircon U-Pb age for the analysis. Results show that central and northeast Taiwan Island experienced a transformation from continental to marine facies during the Eocene–Miocene, and the sandstone maturity changed with time. Source analysis shows that sediments from the Eocene–early Oligocene strata mainly originated from near-source Mesozoic rocks, whose zircon age is consistent with the igneous rock in the surrounding area and coastal Cathaysia, showing 120 Ma and 230 Ma peaks in the age spectrum diagram. Since the late Oligocene, peaks of 900 Ma and 1 800 Ma are seen, indicating that deposition of matter from the old block began. The sediments could be a mixture of the surrounding Mesozoic volcanic and fewer pre-Cambrian rocks sourced from the coastal river and sporadic old basement in the ECSSB instead of long-distance transportation.

**Key words:** Taiwan Island, sedimentary source, sandstone, zircon, sedimentary environment

**Citation:** Hou Yuanli, Zhu Weilin, Qiao Peijun, Huang Chi-Yue, Cui Yuchi, Meng Xianbo. 2021. Sediment source and environment evolution in Taiwan Island during the Eocene–Miocene. Acta Oceanologica Sinica, 40(2): 114–122, doi: 10.1007/s13131-021-1756-8

## 1 Introduction

East Asia has experienced a series of tectonic movements since the Cenozoic, including the turnover and subduction of the Pacific Plate (Sharp and Clague, 2006), collision of the Philippine Plate and Eurasia (Hall, 1996), and collision of the India Plate and Eurasia, which resulted in the uplift of the Tibetan Plateau (Wang et al., 2002; Hu et al., 2015). These events greatly influenced the tectonics, geological evolution and climate of East Asia. Specifically, the reversal of the west-tilting topography in East Asia, resulting from the uplift of the Tibetan Plateau (Wang, 2004; Cao et al., 2018), led to a dramatic shift in the sediment transportation and deposition in East China (Clark et al., 2004; Shao et al., 2007; Zheng et al., 2013). Thus, studying the sedimentary materials in East China is a useful method to understand the tectonic and geological development of East Asia during the Cenozoic.

Taiwan Island is an important area in East Asia, whose sediments formed from the erosion and deposition of terrigenous material from the East Asian continental margins (Huang et al., 2012). When the Philippine Plate drifted northwestward and collided with Eurasia during the middle Miocene, the Cenozoic sedimentary sequence of the East Asian continental margins underwent distortion and uplift, eventually formed the Taiwan Island (Suppe, 1984; Huang et al., 2000). Hence, the exposed strata of Taiwan Island sediments can be viewed as the Cenozoic sedimentary record of the East Asian continental margins.

There have been numerous studies regarding the Cenozoic sedimentary environment of Taiwan (Huang et al., 1997, 2000); however, there is controversy regarding the sediment sources. One of these controversies concerned the shifting of the Eocene-Miocene sediment source recorded in the Taiwan Island sediments (Deng et al., 2017a, 2017b; Lan et al., 2016; Zhang et al., 2014, 2017; Wang et al., 2018; Chen et al., 2019). Recently, a strengthened theory claimed that the Changjiang River could have influenced the Eocene-Miocene source shifting by transporting its sediments after entering the East China Sea, southward through the East China Sea Shelf Basin (ECSSB) (Deng et al., 2017b; Zhang et al., 2014, 2017; Wang et al., 2018). However, integrated and comprehensive studies on the mechanism of southward transportation are scarce. Meanwhile, as the present studies mainly focused on zircon U-Pb age regarding the sediment source development (Deng et al., 2017b; Zhang et al., 2017; Wang et al., 2018; Chen et al., 2019), multiple solutions cannot be ignored. Hence, more information regarding the detrital zircon U-Pb age and petrological features from widely distributed locations is required to understand the sediment source development.

In this study, the petrology and sediment source features of Eocene-Miocene samples from middle and north Taiwan Island were investigated. This was combined with sedimentary data from two sites of the ECSSB (Xihu Sag and Changjiang Depression) and some published data of East Asian areas. This investigation aimed to reveal the sedimentary environment and source development of Taiwan Island, and the connection of the source development between Taiwan Island and the ECSSB. Furthermore, the feasibility of the present source development model and new understanding are discussed (Fig. 1).

Foundation item: The National Natural Science Foundation of China under contract Nos 42076066, 41874076 and 92055203; the National Key Research and Development Program of China under contract No. 2018YFE0202400; the National Science and Technology Major Project under contract No. 2016ZX05026004-002.
*Corresponding author, E-mail: zhuwl@tongji.edu.cn

*Acta Oceanol. Sin.*, 2021, Vol. 40, No. 2, P. 123–135
https://doi.org/10.1007/s13131-020-1628-7
http://www.hyxb.org.cn
E-mail: hyxbe@263.net

# Geochemistry and zircon U-Pb ages of the Oligocene sediments in the Baiyun Sag, Zhujiang River Mouth Basin

Rui Sun[1, 4, 5, 6], Ming Ma[2, 3], Kai Zhong[7], Xiayang Wang[8], Zhao Zhao[6], Shuai Guo[6], Xingzong Yao[9], Gongcheng Zhang[6]*

[1] State Key Laboratory of Lithospheric Evolution, Institute of Geology and Geophysics, Chinese Academy of Sciences, Beijing 100029, China

[2] Northwest Institute of Eco-Environment and Resources, Chinese Academy of Sciences, Lanzhou 730000, China

[3] Key Laboratory of Petroleum Resources, Gansu Province, Lanzhou 730000, China

[4] Innovation Academy for Earth Science, Chinese Academy of Sciences, Beijing 100029, China

[5] University of Chinese Academy of Sciences, Beijing 100049, China

[6] CNOOC Research Institute Co., Ltd., Beijing 100028, China

[7] State Key Laboratory of Marine Geology, Tongji University, Shanghai 200092, China

[8] Research Institute of Petroleum Exploration & Development, PetroChina, Beijing 100083, China

[9] Department of Geology, Northwest University, Xi'an 710069, China

Received 5 September 2019; accepted 29 June 2020



**Abstract**

In this study, element geochemistry and zircon chronology are used to analyze the Oligocene sediments in the Baiyun Sag, Zhujiang River Mouth Basin. The experimental results are discussed with respect to weathering conditions, parent rock lithologies, and provenances. The chemical index of alteration and the chemical index of weathering values of mudstone samples from the lower Oligocene Enping Formation indicate that clastic particles in the study area underwent moderate weathering. Mudstone samples exhibit relatively enriched light rare earth elements and depleted heavy rare earth elements, "V"-shaped negative Eu anomalies, and negligible Ce anomalies. The rare earth element distribution curves are obviously right-inclined, with shapes and contents similar to those of post-Archean Australian shale and upper continental crust, indicating that the samples originated from acid rocks in the upper crust. The Hf-La/Th and La/Sc-Co/Th diagrams show this same origin for the sediments in the study area. For the samples from the upper Enping deltas, the overall age spectrum shows four major age peaks ca. 59–68 Ma, 98–136 Ma, 153–168 Ma and 239–260 Ma. For the Zhuhai Formation samples, the overall age spectrum shows three major age peaks ca. 149 Ma, 252 Ma and 380 Ma. The detrital zircon shapes and U-Pb ages reveal that during Oligocene sedimentation, the sediments on the northwestern margin of the Baiyun Sag were supplied jointly from two provenances: Precambrian-Paleozoic metamorphic rocks in the extrabasinal South China fold zone and Mesozoic volcanic rocks in the intrabasinal Panyu Low Uplift, and the former supply became stronger through time. Thus, the provenance of the Oligocene deltas experienced a transition from an early proximal intrabasinal source to a late distal extrabasinal source.

**Key words:** weathering degree, lithology of parent rock, provenance, element geochemistry, zircon U-Pb ages, Baiyun Sag

**Citation:** Sun Rui, Ma Ming, Zhong Kai, Wang Xiayang, Zhao Zhao, Guo Shuai, Yao Xingzong, Zhang Gongcheng. 2021. Geochemistry and zircon U-Pb ages of the Oligocene sediments in the Baiyun Sag, Zhujiang River Mouth Basin. Acta Oceanologica Sinica, 40(2): 123–135, doi: 10.1007/s13131-020-1628-7

## 1 Introduction

Previous studies on provenance in the South China Sea (SCS) area mainly focused on the Neogene (postrift units), whereas provenance evolution in the Paleogene (synrift units) was rarely investigated (Cao et al., 2015, 2018; Wang et al., 2019; Zeng et al., 2019). The SCS has sparse borehole coverage of the Paleogene strata because of high drilling costs together with a complex geological setting and deeply buried units (Shao et al., 2016a). For provenance analysis in the Zhujiang River Mouth Basin (ZRMB) of the northern SCS, the intrabasinal uplifts of the ZRMB also formed a series of important source regions during the Paleogene synrift stage (Wang et al., 2017, 2019; Liu et al., 2017; Cao et al., 2018; Zeng et al., 2019), but their ability to provide debris is still unclear. An important issue is determining the roles of the intrabasinal source system from the uplifts and the potential extrabasinal provenance from the South China Block.

Element geochemistry analysis is an efficient method to identify the weathering conditions, parent rock lithology and provenance of sedimentary rocks (Castillo et al., 2015; Amendola et al., 2016; Shu et al., 2016; Ma et al., 2019). The trace element

Foundation item: The National Natural Science Foundation of China under contract No. 91528303; the National Science and Technology Major Project under contract Nos 2016ZX05026, 2011ZX05025 and 2008ZX05025; the National Basic Research Program (973 Program) of China under contract No. 2009CB219400; the Foundation for Excellent Youth Scholars of NIEER, CAS.
*Corresponding author, E-mail: zhanggch@cnooc.com.cn

*Acta Oceanol. Sin.*, 2021, Vol. 40, No. 2, P. 136–146
https://doi.org/10.1007/s13131-021-1758-6
http://www.hyxb.org.cn
E-mail: hyxbe@263.net

# An insight into shallow gas hydrates in the Dongsha area, South China Sea

Bin Liu[1], Jiangxin Chen[2, 3]*, Luis M. Pinheiro[4], Li Yang[1], Shengxuan Liu[1], Yongxian Guan[1], Haibin Song[5], Nengyou Wu[2, 3], Huaning Xu[2, 3], Rui Yang[2, 3]

[1] Key Laboratory of Marine Mineral Resources, Ministry of Natural Resources, Guangzhou Marine Geological Survey, Guangzhou 510075, China

[2] Key Laboratory of Gas Hydrate, Ministry of Natural Resources, Qingdao Institute of Marine Geology, Qingdao 266071, China

[3] Laboratory for Marine Mineral Resources, Pilot National Laboratory for Marine Science and Technology (Qingdao), Qingdao 266237, China

[4] Departamento de Geociências and Centre for Environmental and Marine Studies, Universidade de Aveiro, Aveiro 3800, Portugal

[5] State Key laboratory of Marine Geology, Tongji University, Shanghai 200092, China

Received 16 January 2020; accepted 16 June 2020



**Abstract**

Previous studies of gas hydrate in the Dongsha area mainly focused on the deep-seated gas hydrates that have a high energy potential, but cared little about the shallow gas hydrates occurrences. Shallow gas hydrates have been confirmed by drill cores at three sites (GMGS2 08, GMGS2 09 and GMGS2 16) during the GMGS2 cruise, which occur as veins, blocky nodules or massive layers, at 8–30 m below the seafloor. Gas chimneys and faults observed on the seismic sections are the two main fluid migration pathways. The deep-seated gas hydrate and the shallow hydrate-bearing sediments are two main seals for the migrating gas. The occurrences of shallow gas hydrates are mainly controlled by the migration of fluid along shallow faults and the presence of deep-seated gas hydrates. Active gas leakage is taking place at a relatively high-flux state through the vent structures identified on the geophysical data at the seafloor, although without resulting in gas plumes easily detectable by acoustic methods. The presence of strong reflections on the high-resolution seismic profiles and dim or chaotic layers in the sub-bottom profiles are most likely good indicators of shallow gas hydrates in the Dongsha area. Active cold seeps, indicated by either gas plume or seepage vent, can also be used as indicators for neighboring shallow gas hydrates and the gas hydrate system that is highly dynamic in the Dongsha area.

**Key words:** shallow gas hydrate, Dongsha, cold seep, fluid flow, methane-derived authigenic carbonate, South China Sea

**Citation:** Liu Bin, Chen Jiangxin, Pinheiro Luis M., Yang Li, Liu Shengxuan, Guan Yongxian, Song Haibin, Wu Nengyou, Xu Huaning, Yang Rui. 2021. An insight into shallow gas hydrates in the Dongsha area, South China Sea. Acta Oceanologica Sinica, 40(2): 136–146, doi: 10.1007/s13131-021-1758-6

## 1 Introduction

Gas hydrates are ice-like compound of water and methane (or higher hydrocarbons). Gas hydrates are formed under low temperature and high pressure conditions. They represent a potential important energy source and they contain a large amount of carbon (Boswell and Collett, 2011). They may have greatly contributed to the past climate changes, considering their facility to decompose in response to changes of temperature or pressure and their potential to release massive amounts of methane, a potential greenhouse gas, into the upper hydrosphere and atmosphere (Kvenvolden, 1993; Etiope et al., 2008; Reagan and Moridis, 2007; Ruppel and Kessler, 2017). Gas hydrates are also highly significant as concerns seafloor stability, given their potential to fluidize sediments by dissociation and produce submarine landslides (Vanneste et al., 2014). Although gas hydrates can be found onshore at high latitudes, most gas hydrates occur in marine settings. They occur as large-scale gas hydrates distributed near the lower boundary of the gas hydrate stability zone (GHSZ), and as localized gas hydrates concentrated near the seafloor (Riedel et al., 2006; Bahk et al., 2009). Near-seafloor gas hydrates form a small amount of the total gas hydrates, but they play a significant role in helping to better understand how gas hydrate respond to environmental changes (Suess et al., 2001). Moreover, shallow gas hydrates (SGH) provide new insights into the migration of hydrocarbon-rich fluids to the seabed and their role in sustaining deep sea communities and ecosystems (Foucher et al., 2009; Wenau et al., 2015).

SGH have been documented in many oceans around the world, such as the Ulleung Basin in Korea (Bahk et al., 2009), the Cascadia margin (Riedel et al., 2006), the Gulf of Mexico (Mac-

Foundation item: The Laboratory for Marine Mineral Resources, Qingdao National Laboratory for Marine Science and Technology under contract No. MMRKF201810; the National Key Research & Development Program of China under contract Nos 2018YFC0310000 and 2017YFC0307406; the Shandong Province "Taishan Scholar" Construction Project.
*Corresponding author, E-mail: jiangxin_chen@sina.com

*Acta Oceanol. Sin.*, 2021, Vol. 40, No. 1, P. 135–146
https://doi.org/10.1007/s13131-021-1701-x
http://www.hyxb.org.cn
E-mail: hyxbe@263.net

# Study and application of an improved four-dimensional variational assimilation system based on the physical-space statistical analysis for the South China Sea

Yumin Chen[1, 2], Jie Xiang[1], Huadong Du[1*], Sixun Huang[1, 3], Qingtao Song[4]

[1] College of Meteorology and Oceanology, National University of Defense Technology, Nanjing 211101, China

[2] The 93056 Army of People's Liberation Army, Anshan 114000, China

[3] State Key Laboratory of Satellite Ocean Environment Dynamics, Second Institute of Oceanography, Ministry of Natural Resources, Hangzhou 310012, China

[4] National Satellite Ocean Application Service, Beijing 100081, China

Received 11 February 2020; accepted 11 March 2020



**Abstract**

The four-dimensional variational assimilation (4D-Var) has been widely used in meteorological and oceanographic data assimilation. This method is usually implemented in the model space, known as primal approach (P4D-Var). Alternatively, physical space analysis system (4D-PSAS) is proposed to reduce the computation cost, in which the 4D-Var problem is solved in physical space (i.e., observation space). In this study, the conjugate gradient (CG) algorithm, implemented in the 4D-PSAS system is evaluated and it is found that the non-monotonic change of the gradient norm of 4D-PSAS cost function causes artificial oscillations of cost function in the iteration process. The reason of non-monotonic variation of gradient norm in 4D-PSAS is then analyzed. In order to overcome the non-monotonic variation of gradient norm, a new algorithm, Minimum Residual (MINRES) algorithm, is implemented in the process of assimilation iteration in this study. Our experimental results show that the improved 4D-PSAS with the MINRES algorithm guarantees the monotonic reduction of gradient norm of cost function, greatly improves the convergence properties of 4D-PSAS as well, and significantly restrains the numerical noises associated with the traditional 4D-PSAS system.

**Key words:** four-dimensional variational data assimilation (4D-Var), physical space analysis system (PSAS), conjugate gradient algorithm (CG), minimal residual algorithm (MINRES), South China Sea

**Citation:** Chen Yumin, Xiang Jie, Du Huadong, Huang Sixun, Song Qingtao. 2021. Study and application of an improved four-dimensional variational assimilation system based on the physical-space statistical analysis for the South China Sea. Acta Oceanologica Sinica, 40(1): 135–146, doi: 10.1007/s13131-021-1701-x

## 1 Introduction

In meteorology and oceanography, variational data assimilation (VDA) uses all valuable observational information to achieve the most accurate description of atmospheric and oceanic states by minimizing the difference between model solutions and observations. The VDA includes three-dimensional VDA (3D-Var) and four-dimensional VDA (4D-Var) (Courtier, 1997; Wang et al., 2019b). Both 3D-Var and 4D-Var play an important role in numerical prediction, reanalysis data construction, parameter inversion and sensitivity analysis (Huang et al., 2005; Moore et al., 2011a, b; Zhang et al., 2017; Zhou et al., 2018; Shi et al., 2018; Wang et al., 2019a).

According to the difference in solution spaces, the 4D-Var can be divided into two kinds. One is solved in the model space, denoted $\mathbb{R}^n$, with the dimension $n$ up to $10^7$–$10^9$, which is usually known as the primal 4D-Var (P4D-Var) (Parrish and Derber, 1992) or the primal formulation of incremental strong constraint 4D-Var (I4D-Var) (Moore et al., 2011c), and the other in the physical space, i.e., the observation space, denoted $\mathbb{R}^m$, with the dimension $m$ only to $10^5$, which is usually known as the physical space analysis system (4D-PSAS) (Cohn et al., 1998). Since there is generally $m \ll n$ in atmosphere and ocean, 4D-PSAS is in fact solved in the lower dimensional space, which makes 4D-PSAS have the following two benefits: less memory requirement and lower computational burden; being suitable for application to the weakly constrained 4D-Var with model errors (Trémolet, 2007; Zhong et al., 2012).

Despite the benefits mentioned above, 4D-PSAS is seldom adopted in the atmospheric and oceanic numerical models. While, P4D-Var is now widely used in the 4D-Var system of the European Centre for Medium-Range Weather Forecasts (ECMWF) (Rabier et al., 2000), National Centers for Environmental Prediction (NECP) (Parrish and Derber, 1992), Met Office (Rawlins et al., 2007), China Meteorological Administration (CMA), National Climate Center (NCC) (Liu et al., 2005) and other institutions, and its utility has been widely tested.

Recently, Moore et al. (2011a) develop the Regional Ocean Modeling System (ROMS). The ROMS contains its own 4D-Var system, which includes three modules: a primal formulation of incremental strong constraint 4D-Var (I4D-Var), a dual formula-

Foundation item: The National Key Research and Development Program of China under contract Nos 2017YFC1501803 and 2018YFC1506903; the National Natural Science Foundation of China under contract Nos 91730304, 41475021 and 41575026.
*Corresponding author, E-mail: huadong.du@gmail.com

*Acta Oceanol. Sin.*, 2021, Vol. 40, No. 3, P. 58–69
https://doi.org/10.1007/s13131-021-1746-x
http://www.hyxb.org.cn
E-mail: hyxbe@263.net

# Evaluation of reanalysis surface wind products with quality-assured buoy wind measurements along the north coast of the South China Sea

Jing Cha[1*], Xinyu Lin[1], Xiaogang Guo[1], Xiaofang Wan[1], Dawei You[2]

[1] Third Institute of Oceanography, Ministry of Natural Resources, Xiamen 361005, China

[2] South China Sea Branch, Ministry of Natural Resources, Guangzhou 510000, China

Received 22 October 2020; accepted 2 November 2020



**Abstract**

Three archived reanalysis wind vectors at 10 m height in the wind speed range of 2–15 m/s, namely, the second version of the National Centres for Environmental Prediction (NCEP) Climate Forecast System Reanalysis (CFSv2), European Centre for Medium-Range Weather Forecasting Interim Reanalysis (ERA-I) and NCEP-Department of Energy (DOE) Reanalysis 2 (NCEP-2) products, are evaluated by a comparison with the winds measured by moored buoys in coastal regions of the South China Sea (SCS). The buoy data are first quality controlled by extensive techniques that help eliminate degraded measurements. The evaluation results reveal that the CFSv2 wind vectors are most consistent with the buoy winds (with average biases of 0.01 m/s and 1.76°). The ERA-I winds significantly underestimate the buoy wind speed (with an average bias of –1.57 m/s), while the statistical errors in the NCEP-2 wind direction have the largest magnitude. The diagnosis of the reanalysis wind errors shows the residuals of all three reanalysis wind speeds (reanalysis-buoy) decrease with increasing buoy wind speed, suggesting a narrower wind speed range than that of the observations. Moreover, wind direction errors are examined to depend on the magnitude of the wind speed and the wind speed biases. In general, the evaluation of three reanalysis wind products demonstrates that CFSv2 wind vectors are the closest to the winds along the north coast of the SCS and are sufficiently accurate to be used in numerical models.

**Key words:** evaluation, quality control, buoy wind, coastal regions of the South China Sea

**Citation:** Cha Jing, Lin Xinyu, Guo Xiaogang, Wan Xiaofang, You Dawei. 2021. Evaluation of reanalysis surface wind products with quality-assured buoy wind measurements along the north coast of the South China Sea. Acta Oceanologica Sinica, 40(3): 58–69, doi: 10.1007/s13131-021-1746-x

## 1 Introduction

Surface wind is one of the major factors in the generation and movement of ocean currents and waves, constituting a forcing role in ocean and coupled models. Accurate global high-resolution surface winds are critical for improving numerical weather prediction and climate model forecasting (Large et al., 1991; Josse et al., 1999; Bourassa et al., 2010). Surface ocean winds are commonly measured by in situ techniques or remote sensing instruments. Buoys are moored with the primary goal of sustained marine observations. China has arranged an intensive offshore buoy observation network, especially in the East China Sea and South China Sea (SCS). This network offers real-time meteorological and marine monitoring, which is quite valuable for fishery industries and other marine activities. However, due to the uniformity of moored buoys, buoy winds are not the appropriate input parameters in climate models. Instead, the most available forcing of ocean movement in models is remote sensing winds or reanalysis wind products. But these wind products have limited spatial resolutions which are not sufficient to resolve small-scale processes, especially in coastal regions. Spatial resolution problems would bring increase in errors to the gridded wind products. Scatterometer wind data are found to degrade near shore (Tang et al., 2004) due to the inadequacy of the geophysical model function in addressing coastal conditions and light winds situations. Moreover, reanalysis wind products are the result of assimilation by multiple observations, the accuracy of which is heavily dependent on the accuracy of original data and the skills of assimilation. It is suggested that reanalysis wind products have limited ability in depicting surface winds in coastal waters (Schmidt et al., 2017). Therefore, it is necessary to perform the evaluation of reanalysis wind products to investigate how these datasets represent real wind fields at the air-sea interface in coastal regions.

In evaluation studies, *in situ* winds observed by buoys are considered true winds (Ebuchi et al., 2002; Tang et al., 2004; Yang and Zhang, 2018). However, without normal functioning or effective calibration of buoy sensors, automatic measurements by buoys would be invalid which cause large biases. Moreover, those erroneous but seeming like reasonable observations may lead to an incorrect analysis of the weather or climate change. These remaining problems result in unreliable and meaningless evaluations. As a result, it is important to detect and reduce the degraded measurements of moored buoys prior to evaluating the

Foundation item: The Scientific Research Foundation of the Third Institute of Oceanography, Ministry of Natural Resources under contract Nos 2014028, 2017011 and 2017012; the State Oceanic Administration Program on Global Change and Air-Sea Interactions under contract Nos GASI-IPOVAI-02 and GASI-IPOVAI-03.

*Corresponding author, E-mail: chajing@tio.org.cn

*Acta Oceanol. Sin.*, 2021, Vol. 40, No. 3, P. 94–111
https://doi.org/10.1007/s13131-021-1713-6
http://www.hyxb.org.cn
E-mail: hyxbe@263.net

# Facies character and geochemical signature in the late Quaternary meteoric diagenetic carbonate succession at the Xisha Islands, South China Sea

Wanli Chen[1, 3], Xiaoxia Huang[1, 4*], Shiguo Wu[1, 2, 3*], Gang Liu[5, 6], Haotian Wei[7], Jiaqing Wu[7]

[1] Laboratory of Marine Geophysics and Georesources, Institute of Deep-sea Science and Engineering, Sanya 572000, China

[2] Laboratory for Marine Geology, Pilot National Laboratory for Marine Science and Technology (Qingdao), Qingdao 266034, China

[3] University of China Academy of Sciences, Beijing 100049, China

[4] Institute of Earth and Environmental Science, University of Potsdam, Potsdam 14476, Germany

[5] Institute of Marine Geology Survey, Bureau of Hainan Marine Geology Survey, Haikou 570206, China

[6] Key Laboratory of Marine Geological Resources and Environment of Hainan Province, Marine Geological Survey Institute of Hainan Province, Haikou 570206, China

[7] College of Marine Geosciences, Ocean University of China, Qingdao 266100, China

Received 30 March 2020; accepted 7 May 2020



**Abstract**

The late Quaternary shallow-water carbonates have been altered by a variety of diagenetic processes, and further influenced by high-amplitude global and regional sea level changes. This study utilizes a new borehole drilled on the Yongxing Island, Xisha Islands to investigate meteoric diagenetic alteration in the late Quaternary shallow-water carbonates. Petrographic, mineralogical, stable isotopic and elemental data provide new insights into the meteoric diagenetic processes of the reef limestone. The results show the variation in the distribution of aragonite, high-Mg calcite (HMC) and low-Mg calcite (LMC) divides the shallow-water carbonates in Core SSZK1 into three intervals, which are Unit I (31.20–55.92 m, LMC), Unit II (18.39–31.20 m, aragonite and LMC) and Unit III (upper 18.39 m of core, aragonite, LMC and HMC). Various degrees of meteoric diagenesis exist in the identified three units. The lowermost Unit I has suffered almost complete freshwater diagenesis, whereas the overlying Units II and III have undergone incompletely meteoric diagenesis. The amount of time that limestone has been in the freshwater diagenetic environment has the largest impact on the degree of meteoric diagenesis. Approximately four intact facies/water depth cycles are recognized. The cumulative depletion of elements such as strontium (Sr), sodium (Na) and sulphur (S) caused by duplicated meteoric diagenesis in the older reef sequences are distinguished from the younger reef sequences. This study provides a new record of meteoric diagenesis, which is well reflected by whole-rock mineralogy and geochemistry.

**Key words:** shallow-water carbonates, meteoric diagenesis, elemental concentration, facies cycles, Xisha Islands, late Quaternary

**Citation:** Chen Wanli, Huang Xiaoxia, Wu Shiguo, Liu Gang, Wei Haotian, Wu Jiaqing. 2021. Facies character and geochemical signature in the late Quaternary meteoric diagenetic carbonate succession at the Xisha Islands, South China Sea. Acta Oceanologica Sinica, 40(3): 94–111, doi: 10.1007/s13131-021-1713-6

## 1 Introduction

The studies of the Quaternary shallow-water carbonates in meteoric diagenetic environments, generally with karstic features, have provided insights into sequence stratigraphy, paleoenvironmental interpretation and the prediction of hydrocarbon reservoirs (Allan and Matthews, 1982; Hajikazemi et al., 2010; Holail, 1999; Jian et al., 1997; Melim et al., 2002; Quinn, 1991; Sherman et al., 1999). A meteoric diagenetic model of Pleistocene shallow-water carbonates, called as the "Barbados model", has been established to describe the isotope patterns associated with thorough meteoric diagenesis of carbonates in which aragonite was completely converted to low-Mg calcite (Allan and Matthews, 1982). The isotope patterns summarized by the Barbados model are useful for identifying different diagenetic environments. The coexistence of unstable aragonite and high-Mg calcite (HMC), as well as stable low-Mg calcite (LMC), occurs in the Barbados boreholes, showing the signature of incomplete meteoric diagenesis and mineralogical stabilization. Research on stable carbon and oxygen isotopes, together with mineralogy of suites of rocks, has been considered as the most effective way to

Foundation item: The National Natural Science Foundation of China-Guangdong Joint Foundation under contract No. U1701245; the Hainan Provincial Natural Science Foundation of China under contract No. 418QN306; the Land and Georesource Bureau of Hainan Province under contract No. SQ2016KJHZ0027; the Pioneer Hundred Talents Program under contract No. Y910091001; the Guangzhou Marine Geological Survey Project under contract No. GZH201400210.
*Corresponding author, E-mail: huangxx@idsse.ac.cn; swu@idsse.ac.cn

*Acta Oceanol. Sin.*, 2021, Vol. 40, No. 5, P. 20–29
https://doi.org/10.1007/s13131-021-1808-0
http://www.hyxb.org.cn
E-mail: ocean2@hyxb.org.cn

# Effects of westward shoaling pycnocline on characteristics and energetics of internal solitary wave in the Luzon Strait by numerical simulations

Haibin Lü[1, 2, 3, 4], Yujun Liu[1], Xiaokang Chen[1], Guozhen Zha[1], Shuqun Cai[2, 3, 5, 6*]

[1] Jiangsu Key Laboratory of Marine Bioresources and Environment/Jiangsu Key Laboratory of Marine Biotechnology, Jiangsu Ocean University, Lianyungang 222005, China

[2] State Key Laboratory of Tropical Oceanography, South China Sea Institute of Oceanology, Chinese Academy of Sciences, Guangzhou 510301, China

[3] Southern Marine Science and Engineering Guangdong Laboratory (Guangzhou), Guangzhou 511458, China

[4] Jiangsu Institute of Marine Resources Development, Lianyungang 222005, China

[5] University of Chinese Academy of Sciences, Beijing 100049, China

[6] Innovation Academy of South China Sea Ecology and Environmental Engineering, Chinese Academy of Sciences, Guangzhou 510301, China

Received 29 March 2020; accepted 29 December 2020



**Abstract**

An internal gravity wave model was employed to simulate the generation of internal solitary waves (ISWs) over a sill by tidal flows. A westward shoaling pycnocline parameterization scheme derived from a three-parameter model was adopted, and then 14 numerical experiments were designed to investigate the influence of the pycnocline thickness, density difference across the pycnocline, westward shoaling isopycnal slope angle and pycnocline depth on the ISWs. When the pycnocline thickness on both sides of the sill increases, the total barotropic kinetic energy, total baroclinic energy and ratio of baroclinic kinetic energy (KE) to available potential energy (APE) decrease, whilst the depth of isopycnal undergoing maximum displacement and ratio of baroclinic energy to barotropic energy increase. When the density difference on both sides of the sill decreases synchronously, the total barotropic kinetic energy, ratio of baroclinic energy to barotropic energy and total baroclinic energy decrease, whilst the depth of isopycnal undergoing maximum displacement increases. When the westward shoaling isopycnal slope angle increases, the total baroclinic energy increases whilst the depth of turning point almost remains unchanged. When the depth of westward shoaling pycnocline on both sides of the sill reduces, the ratio of baroclinic energy to barotropic energy and total baroclinic energy decrease, whilst the total barotropic kinetic energy and ratio of KE to APE increase. When one of the above four different influencing factors was increased by 10% while the other factors keep unchanged, the amplitude of the leading soliton in ISW Packet A was decreased by 2.80%, 7.47%, 3.21% and 6.42% respectively. The density difference across the pycnocline and the pycnocline depth are the two most important factors in affecting the characteristics and energetics of ISWs.

**Key words:** internal solitary waves, baroclinic energy, South China Sea, pycnocline

**Citation:** Lü Haibin, Liu Yujun, Chen Xiaokang, Zha Guozhen, Cai Shuqun. 2021. Effects of westward shoaling pycnocline on characteristics and energetics of internal solitary wave in the Luzon Strait by numerical simulations. Acta Oceanologica Sinica, 40(5): 20–29, doi: 10.1007/s13131-021-1808-0

## 1 Introduction

Internal solitary waves (ISWs) are important dynamic phenomena, usually generated by a tidally driven flow over submerged variable topography in a stratified ocean. It is expected that internal wave activity would increase in the northeastern South China Sea (SCS) through the 21st century because of the warming in the upper 100 m of the ocean since 1900 (DeCarlo et al., 2015). ISWs in the northeastern SCS evolve out of the internal tide generated in the Luzon Strait (Li et al., 2013; Zhao, 2014), where two underwater sea ridges, namely Lan-Yu Ridge to the east and Heng-Chun Ridge to the west, are located (Zheng et al., 2007; Du et al., 2008; Wang et al., 2012; Cao et al., 2017; Bai et al.,

Foundation item: The Key Research Program of Frontier Sciences, Chinese Academy of Sciences (CAS) under contract No. QYZDJ-SSW-DQC034; the Talent Project from Southern Marine Science and Engineering Guangdong Laboratory (Guangzhou) under contract No. GML2019ZD0304; the National Natural Science Foundation of China (NSFC) under contract Nos 41521005 and 62071207; the Priority Academic Program Development of Jiangsu Higher Education Institutions (PAPD); the Natural Science Foundation of Huai Hai Institute of Technology under contract No. Z2017006; the Project from Department of Natural Resources of Guangdong Province under contract No. (2020)017; the Open Project of State Key Laboratory of Tropical Oceanography, South China Sea Institute of Oceanology, CAS under contract No. LTO1702; Postgraduate Research & Practice Innovation Program of Jiangsu Province under contract No. SJCX19_0963.

*Corresponding author, E-mail: caisq@scsio.ac.cn

*Acta Oceanol. Sin.*, 2021, Vol. 40, No. 7, P. 1–14
https://doi.org/10.1007/s13131-021-1815-1
http://www.aosocean.com
E-mail: ocean2@hyxb.org.cn

# Three-dimensional circulation in northern South China Sea during early summer of 2015

Huiqun Wang[1], Yaochu Yuan[1], Weibing Guan[1, 2, 3, 4*], Chenghao Yang[1], Dongfeng Xu[1]

[1] State Key Laboratory of Satellite Ocean Environment Dynamics, Second Institute of Oceanography, Ministry of Natural Resources, Hangzhou 310012, China

[2] Southern Marine Science and Engineering Guangdong Laboratory (Zhuhai), Zhuhai 519080, China

[3] School of Oceanography, Shanghai Jiao Tong University, Shanghai 200030, China

[4] Ocean College, Zhejiang University, Zhoushan 316021, China

Received 28 November 2020; accepted 17 January 2021



**Abstract**

Using the hydrographic data obtained during two nearly simultaneous surveys in June 2015, we carried out semi-diagnostic calculations with the help of a finite element model and a modified inverse method, to study the circulation in the northern South China Sea (NSCS) during the early summer of 2015. A number of new circulation features were found. (1) In most of the observation region, a large, basin-scale anticyclonic gyre appeared south of the 50-m isobath, which contained anticyclonic eddies. One anticyclonic eddy existed from the sea surface to 50-m depth, whose center showed no tilt, while the center of another eddy tilted eastward from the sea surface to 500-m depth. In the eastern part of the observation region, which is west of the Dongsha Islands, there was a sub-basin-scale cyclonic gyre containing a cyclonic eddy whose center tilted southward from the sea surface to 200-m depth. (2) There was a cross-continental slope current (CCSC) in the area southwest of the Dongsha Islands. Its volume transport was about $2.0\times10^6$ m$^3$/s. (3) From the estimated order of magnitude of the stream function equation, the joint effect term of the baroclinity and relief (JEBAR) and $\beta$-effect term are two important dynamic mechanisms affecting the variation of the circulation in the NSCS. (4) The JEBAR, as a transport-generating term, resulted in the dynamic mechanism determining the pattern of the depth-averaged flow across the contours of potential vorticity $fH^{-1}$. Furthermore, we show that the negative values of the JEBAR were the most dominant dynamic mechanism, causing the CCSC southwest of the Dongsha Islands to deflect from the isobaths and veer toward the deep water. The CCSC around the Dongsha Islands was located further southwest during the early summer of 2015 than during the fall of 2005 (revealed by a published study), which suggests that the location of the CCSC around the Dongsha Islands may vary with season.

**Key words:** South China Sea, circulation, numerical model, cross-continental slope current, seasonality of cross-continental slope current

**Citation:** Wang Huiqun, Yuan Yaochu, Guan Weibing, Yang Chenghao, Xu Dongfeng. 2021. Three-dimensional circulation in northern South China Sea during early summer of 2015. Acta Oceanologica Sinica, 40(7): 1–14, doi: 10.1007/s13131-021-1815-1

## 1 Introduction

The South China Sea (SCS) is the world's largest tropical marginal sea, with an average depth over 1 000 m. The SCS is under the influence of the East Asia monsoon, with northeasterly winds in winter, southwesterly winds in summer, and transitional periods in April–May and September–October. The northern SCS (NSCS, Fig. 1) contains a relatively narrow, steep slope and a broad continental shelf. It connects to the East China Sea through the Taiwan Strait and to the Pacific Ocean through the Luzon Strait. A branch of the Kuroshio passes through the Luzon Strait and makes a westward intrusion (Qu et al., 2004; Yuan et al., 2008, 2014, 2015; Fang et al., 2009; Tseng et al., 2012). Yuan et al. (2015) confirmed the influence of the Kuroshio on the currents in the Luzon Strait and on the circulations in the NSCS from July 2010 to May 2015. The Zhujiang River (Pearl River), the 13th largest river in the world in terms of discharge, flows into the shelf of the NSCS and delivers about $3.5\times10^{11}$ m$^3$/a of fresh water, with 80% of its total discharge occurring in the wet season (April–September) (Zhao, 1990). The East Asian monsoon and large water flows, including the Kuroshio intrusion, Zhujiang River plume, and the water exchange between the SCS and Taiwan Strait (Cai et al., 2005; Fang et al., 2003, 2009) result in a complicated variation of circulations in the NSCS, which, combined with a complex bottom topography, results in a complicated energy cycle. Based on three-year observations using an acoustic Doppler current profiler (ADCP), the three-year-mean

Foundation item: The Joint Project of Guangxi-Provincial and China-National Natural Science Foundations under contract No. U20A20104; the National Basic Research Program of China under contract No. 2014CB441501; the National Natural Science Foundation of China under contract Nos 41830540 and 42076216; the Innovation Group Project of Southern Marine Science and Engineering Guangdong Laboratory (Zhuhai) under contract No. 311020003; the Project of State Key Laboratory of Satellite Ocean Environment Dynamics, Second Institute of Oceanography, Ministry of Natural Resources, under contract Nos SOEDZZ2101 and SOEDZZ2003.

*Corresponding author, E-mail: gwb@sio.org.cn

*Acta Oceanol. Sin.*, 2021, Vol. 40, No. 7, P. 15–30
https://doi.org/10.1007/s13131-021-1766-6
http://www.aosocean.com
E-mail: ocean2@hyxb.org.cn

# A Lagrangian study of the near-surface intrusion of Pacific water into the South China Sea

Gaolong Huang[1, 3], Haigang Zhan[1, 2*], Qingyou He[1, 2], Xing Wei[1, 2], Bo Li[1, 2]

[1] State Key Laboratory of Tropical Oceanography, South China Sea Institute of Oceanology, Chinese Academy of Sciences, Guangzhou 510301, China

[2] Southern Marine Science and Engineering Guangdong Laboratory (Guangzhou), Guangzhou 511458, China

[3] University of Chinese Academy of Sciences, Beijing 100049, China

Received 15 May 2020; accepted 24 November 2020



**Abstract**

Satellite-tracked Lagrangian drifters are used to investigate the transport pathways of near-surface water around the Luzon Strait. Particular attention is paid to the intrusion of Pacific water into the South China Sea (SCS). Results from drifter observations suggest that except for the Kuroshio water, other Pacific water that carried by zonal jets, Ekman currents or eddies, can also intrude into the SCS. Motivated by this origin problem of the intrusion water, numerous simulated trajectories are constructed by altimeter-based velocities. Quantitative estimates from simulated trajectories suggest that the contribution of other Pacific water to the total intrusion flux in the Luzon Strait is approximately 13% on average, much smaller than that of Kuroshio water. Even so, over multiple years and many individual intrusion events, the contribution from other Pacific water is quite considerable. The interannual signal in the intrusion flux of these Pacific water might be closely related to variations in a wintertime westward current and eddy activities east of the Luzon Strait. We also found that Ekman drift could significantly contribute to the intrusion of Pacific water and could affect the spreading of intrusion water in the SCS. A case study of an eddy-related intrusion is presented to show the detailed processes of the intrusion of Pacific water and the eddy-Kuroshio interaction.

**Key words:** Kuroshio intrusion, Lagrangian transport, Luzon Strait, South China Sea

**Citation:** Huang Gaolong, Zhan Haigang, He Qingyou, Wei Xing, Li Bo. 2021. A Lagrangian study of the near-surface intrusion of Pacific water into the South China Sea. Acta Oceanologica Sinica, 40(7): 15–30, doi: 10.1007/s13131-021-1766-6

## 1 Introduction

The Luzon Strait, located between the Taiwan Island and Luzon Island, is a wide (approximately 360 km) meridional gap of the western Pacific boundary and the only deep (>2 000 m) channel connecting the South China Sea (SCS) and the Pacific Ocean. Leading considerable material and dynamical fluxes through the Luzon Strait, the intrusion of Pacific water significantly influences the hydrological characteristics, circulation patterns, eddy activities, and biological production of the Northern South China Sea (Qu et al., 2004; Cai et al., 2005; Nan et al., 2011b; He et al., 2016; Zhang et al., 2017).

The intrusion of Pacific water is closely related to the behavior of Kuroshio in the Luzon Strait. As the primary western boundary current (WBC) of the North Pacific subtropical gyre, the Kuroshio originates from the North Equatorial Current (NEC) bifurcation at approximately 10°N to 15°N (Nitani, 1972; Qiu and Chen, 2010). During its course northward, the Kuroshio usually bends clockwise into the Luzon Strait, with inflow and outflow through the Balintang and Bashi Channel, respectively. In the mean state, the Kuroshio axis is mainly confined within the Luzon Strait, indicating a gap-leaping path of the Kuroshio (Caruso et al., 2006; Liang et al., 2008; Lu and Liu, 2013). Lu and Liu (2013) suggested that the gap-leaping Kuroshio with a strong potential vorticity front can act as a dynamic barrier, blocking the westward propagation of Rossby waves and eddies from the Pacific. However, the Kuroshio occasionally meanders into the northeastern SCS in the form of a loop current, which is no longer restricted to the Luzon Strait (Li and Wu, 1989; Farris and Wimbush, 1996; Jia and Liu, 2004; Yuan et al., 2006; Liu et al., 2016; Zhang et al., 2017). Associated with the westward extension, part of the Kuroshio water can intrude deep into the SCS, primarily in winter. For example, early hydrographic studies by Shaw (1991) and Qu et al. (2000) observed the North Pacific high-salinity water on the continental slope of the northern SCS in winter. Centurioni et al. (2004) found that surface drifters deployed in the Pacific crossed the Luzon Strait and reached the inner SCS between October and January.

The Kuroshio is highly variable in the Luzon Strait. Previous satellite and *in situ* observations suggest that inflows and outflows in the upper layer of the Luzon Strait often appear altern-

Foundation item: The Strategic Priority Program on Space Science, the Chinese Academy of Sciences under contract No. XDA15020901; the National Natural Science Foundation of China under contract Nos 41876205 and 41906026; the Key Special Project for Introduced Talents Team of Southern Marine Science and Engineering Guangdong Laboratory (Guangzhou) under contract Nos GML2019ZD0305 and GML2019ZD0302; the Natural Science Foundation of Guangdong under contract No. 2018A0303100002; the Project of State Key Laboratory of Tropical Oceanography under contract No. LTOZZ2002; the Open Fund of the Key Laboratory of Ocean Circulation and Waves, Chinese Academy of Sciences under contract No. KLOCW1905.
*Corresponding author, E-mail: hgzhan@scsio.ac.cn

*Acta Oceanol. Sin.*, 2021, Vol. 40, No. 7, P. 68–76
https://doi.org/10.1007/s13131-021-1735-0
http://www.aosocean.com
E-mail: ocean2@hyxb.org.cn

# Application of deep learning technique to the sea surface height prediction in the South China Sea

Tao Song[1, 6], Ningsheng Han[1], Yuhang Zhu[2, 3, 5], Zhongwei Li[1], Yineng Li[2, 3, 4], Shaotian Li[2, 3], Shiqiu Peng[2, 3, 4, 5*]

[1] College of Computer and Communication Engineering, China University of Petroleum (East China), Qingdao 266580, China

[2] State Key Laboratory of Tropical Oceanography, South China Sea Institute of Oceanology, Chinese Academy of Sciences, Guangzhou 510301, China

[3] Southern Marine Science and Engineering Guangdong Laboratory (Guangzhou), Guangzhou 511458, China

[4] Key Laboratory of Science and Technology on Operational Oceanography, Chinese Academy of Sciences, Guangzhou 511458, China

[5] Guangxi Key Laboratory of Marine Disaster in the Beibu Gulf, Bubei Gulf University, Qinzhou 535011, China

[6] Department of Artificial Intelligence, Faculty of Computer Science, Polytechnical University of Madrid, Boadilla del Monte 28660, Madrid, Spain

Received 26 August 2020; accepted 16 September 2020



**Abstract**

A deep-learning-based method, called ConvLSTMP3, is developed to predict the sea surface heights (SSHs). ConvLSTMP3 is data-driven by treating the SSH prediction problem as the one of extracting the spatial-temporal features of SSHs, in which the spatial features are "learned" by convolutional operations while the temporal features are tracked by long short term memory (LSTM). Trained by a reanalysis dataset of the South China Sea (SCS), ConvLSTMP3 is applied to the SSH prediction in a region of the SCS east off Vietnam coast featured with eddied and offshore currents in summer. Experimental results show that ConvLSTMP3 achieves a good prediction skill with a mean RMSE of 0.057 m and accuracy of 93.4% averaged over a 15-d prediction period. In particular, ConvLSTMP3 shows a better performance in predicting the temporal evolution of mesoscale eddies in the region than a full-dynamics ocean model. Given the much less computation in the prediction required by ConvLSTMP3, our study suggests that the deep learning technique is very useful and effective in the SSH prediction, and could be an alternative way in the operational prediction for ocean environments in the future.

**Key words:** deep learning, sea surface height prediction, convolutional operation, long short term memory

**Citation:** Song Tao, Han Ningsheng, Zhu Yuhang, Li Zhongwei, Li Yineng, Li Shaotian, Peng Shiqiu. 2021. Application of deep learning technique to the sea surface height prediction in the South China Sea. Acta Oceanologica Sinica, 40(7): 68–76, doi: 10.1007/s13131-021-1735-0

## 1 Introduction

Sea surface heights (SSHs) are one of the key factors affecting algae growth, fish distribution and coastal city flooding. It is also vital to marine engineering such as offshore oil production and offshore aquaculture. The change of SSHs is associated with various dynamical processes in the ocean, including mesoscale eddies, waves, currents, tides, etc. As such, the prediction of SSHs has always been a challenge for the oceanographers. Currently, numerical models based on physical equations are usually used to predict SSHs; although the prediction skills are acceptable, considerable uncertainties still exist. On the other hand, the prediction using numerical models requires large computational resources and thus it time consuming, which may not satisfy the need of some emergency situations.

In the last several decades, oceanic data (including *in situ* observations and reanalysis data) are rapidly accumulated, which makes it feasible to use artificial intelligence (AI) for marine environmental prediction. As a boosting technique, it has been found that deep learning can both track spatial features and temporal changing of the marine environment factors from large amount of data through convolutional operations (e.g., convolutional neural network, CNN; Ji et al., 2013; Shin et al., 2016; Zhang et al., 2016; Huang et al., 2017) and recurrent patterns (e.g., recurrent neural network, RNN; Cho et al., 2014), respectively. For

Foundation item: The National Key Research and Development Program under contract Nos 2018YFC1406204 and 2018YFC1406201; the Guangdong Special Support Program under contract No. 2019BT2H594; the Taishan Scholar Foundation under contract No. tsqn201812029; the National Natural Science Foundation of China under contract Nos U1811464, 61572522, 61572523, 61672033, 61672248, 61873280, 41676016 and 41776028; the Natural Science Foundation of Shandong Province under contract Nos ZR2019MF012 and 2019GGX101067; the Fundamental Research Funds of Central Universities under contract Nos 18CX02152A and 19CX05003A-6; the fund of the Shandong Province Innovation Researching Group under contract No. 2019KJN014; the Key Special Project for Introduced Talents Team of the Southern Marine Science and Engineering Guangdong Laboratory (Guangzhou) under contract No. GML2019ZD0303.

*Corresponding author, E-mail: speng@scsio.ac.cn

*Acta Oceanol. Sin.*, 2021, Vol. 40, No. 7, P. 88–99
https://doi.org/10.1007/s13131-021-1739-9
http://www.aosocean.com
E-mail: ocean2@hyxb.org.cn

# Seasonal variation in the three-dimensional structures of coastal thermal front off western Guangdong

Yan Zhang[1, 3], Lili Zeng[2], Qiang Wang[2], Bingxu Geng[2], Changjian Liu[1, 3], Rui Shi[2], Na Liu[2], Weiping Wang[1, 3*], Dongxiao Wang[2]

[1] South China Sea Marine Survey and Technology Center, Ministry of Natural Resources, Guangzhou 510300, China

[2] State Key Laboratory of Tropical Oceanography (LTO), South China Sea Institute of Oceanology, Chinese Academy of Sciences, Guangzhou 510301, China

[3] Key Laboratory of Marine Environmental Survey Technology and Application, Ministry of Natural Resources, Guangzhou 510300, China

Received 17 July 2020; accepted 17 September 2020



**Abstract**

The seasonal structure and dynamic mechanism of oceanic surface thermal fronts (STFs) along the western Guangdong coast over the northern South China Sea shelf were analyzed using *in situ* observational data, remote sensing data, and numerical simulations. Both *in situ* and satellite observations show that the coastal thermal front exhibits substantial seasonal variability, being strongest in winter when it has the greatest extent and strongest sea surface temperature gradient. The winter coastal thermal front begins to appear in November and disappears after the following April. Although runoff water is more plentiful in summer, the front is weak in the western part of Guangdong. The frontal intensity has a significant positive correlation with the coastal wind speed, while the change of temperature gradient after September lags somewhat relative to the alongshore wind. The numerical simulation results accurately reflect the seasonal variation and annual cycle characteristics of the frontal structure in the simulated area. Based on vertical cross-section data, the different frontal lifecycles of the two sides of the Zhujiang (Pearl) River Estuary are analyzed.

**Key words:** oceanic thermal fronts, South China Sea, seasonal dynamics

**Citation:** Zhang Yan, Zeng Lili, Wang Qiang, Geng Bingxu, Liu Changjian, Shi Rui, Liu Na, Wang Weiping, Wang Dongxiao. 2021. Seasonal variation in the three-dimensional structures of coastal thermal front off western Guangdong. Acta Oceanologica Sinica, 40(7): 88–99, doi: 10.1007/s13131-021-1739-9

## 1 Introduction

An oceanic front is a typical mesoscale oceanic phenomenon identified by a discontinuity in, for example, temperature, salinity, or nutrient and chlorophyll *a* contents (Belkin et al., 2009). According to Yanagi and Koike (1987), oceanic fronts are classified into coastal water fronts, shelf fronts, and open ocean fronts. Numerous studies on the relationship between sea surface temperature (SST) and sea surface wind have been conducted on continental shelf and open ocean fronts in the equatorial and mid-latitude oceans. However, studies on the modification of the effect of sea surface wind on coastal water fronts have rarely been reported.

As an important physical process in the continental shelf, oceanic fronts play a vital role in the regional climate, carbon cycle, primary production, fisheries, coral bleaching, marine birds and mammals, and regional ecosystem (Simpson et al., 1978; D'Croz and Maté, 2004; Pauly and Christensen, 1995; Bost et al., 2009; Cabrera et al., 2011; Omand et al., 2015). The vigorous thermal fronts accompanied by high chlorophyll concentrations stretch several hundreds of kilometers along the shelf (Wang et al., 2001; Hu et al., 2003; Liu et al., 2010). Intense horizontal thermohaline gradients, enhanced turbulence, current shear, and surface convergence are closely linked with persistent fronts (Qiu et al., 2019). These dynamic processes contribute significantly to the high biological productivity in frontal zones (Johannessen et al., 2005; Holt and Umlauf, 2008; D'Asaro et al., 2011; Johnston et al., 2011; Long et al., 2012; Mahadevan et al., 2012; Omand et al., 2015).

The South China Sea (SCS) is an epi-continental marginal sea of the western Pacific Ocean, with a maximum depth of over 3 000 m (Liu et al., 2004). A main feature of its topography is a broad continental shelf shallower than 200 m (Fig. 1), linked to the deep basin by a steep shelf slope in the northern SCS (NSCS), where the isobaths are approximately parallel to the coastline. The climate and upper ocean circulation in the NSCS are dominated by the Asian monsoon, which blows northeasterly from October to April and southwesterly from May to September; spring and autumn are the monsoon transition periods (Xie et al., 2003). In response to monsoon forcing, the basin-scale circulation in the NSCS experiences an energetic seasonal cycle, which is generally cyclonic in winter and anticyclonic in summer (Hu et al., 2000; Liu et al., 2001; Su, 2004). Eddies with a range of hori-

Foundation item: The National Natural Science Foundation of China under contract Nos 41776025, 41576003, 41776026, 41676018 and 41806035; the Pearl River S&T Nova Program of Guangzhou under contract No. 201906010051; the Rising Star Foundation of the South China Sea Institute of Oceanology under contract No. NHXX2019WL0101; the Science and Technology Program of Guangzhou under contract No. 202002030490.

*Corresponding author, E-mail: wangweiping@smst.gz.cn

*Acta Oceanol. Sin.*, 2021, Vol. 40, No. 8, P. 14–31
https://doi.org/10.1007/s13131-021-1794-2
http://www.aosocean.com
E-mail: ocean2@hyxb.org.cn

# Analysis of the spatial and temporal distributions of ecological variables and the nutrient budget in the Beibu Gulf

Huanglei Pan[1, 2], Dishi Liu[1, 3], Dalin Shi[1, 2], Shengyun Yang[1, 3], Weiran Pan[1, 3*]

[1] State Key Laboratory of Marine Environmental Science (Xiamen University), Xiamen 361102, China

[2] College of the Environment and Ecology, Xiamen University, Xiamen 361102, China

[3] College of Ocean and Earth Sciences, Xiamen University, Xiamen 361102, China

Received 31 May 2020; accepted 25 September 2020



**Abstract**

Based on a hydrodynamic-ecological model, the temperature, salinity, current, phytoplankton (Chl *a*), zooplankton, and nutrient (dissolved inorganic nitrogen, DIN, and dissolved inorganic phosphorous, DIP) distributions in the Beibu Gulf were simulated and the nutrient budget of 2015 was quantitatively analyzed. The simulated results show that interface processes and monsoons significantly influence the ecological processes in the gulf. The concentrations of DIN, DIP, phytoplankton and zooplankton are generally higher in the eastern and northern gulf than that in the western and southern gulf. The key regions affected by ecological processes are the Qiongzhou Strait in winter and autumn and the estuaries along the Guangxi coast and the Red River in summer. In most of the studied domains, biochemical processes contribute more to the nutrient budget than do physical processes, and the DIN and DIP increase over the year. Phytoplankton plays an important role in the nutrient budget; phytoplankton photosynthetic uptake is the nutrient sink, phytoplankton dead cellular release is the largest source of DIN, and phytoplankton respiration is the largest source of DIP. The nutrient flux in the connected sections of the Beibu Gulf and open South China Sea (SCS) inflows from the east and outflows to the south. There are 113 709 t of DIN and 5 277 t of DIP imported from the open SCS to the gulf year-around.

**Key words:** Beibu Gulf, hydrodynamic-ecological model, marine ecosystem, nutrient budget

**Citation:** Pan Huanglei, Liu Dishi, Shi Dalin, Yang Shengyun, Pan Weiran. 2021. Analysis of the spatial and temporal distributions of ecological variables and the nutrient budget in the Beibu Gulf. Acta Oceanologica Sinica, 40(8): 14–31, doi: 10.1007/s13131-021-1794-2

## 1 Introduction

The Beibu Gulf (16°00′–21°30′N, 105°40′–111°00′E) is an important semienclosed gulf located in the northwestern South China Sea (SCS) and is rich in natural resources (e.g., fish, oil, and tourist destinations); thus, it has considerable ecological and economical value (Han, 2013; Lin et al., 2008). The Beibu Gulf connects to the open SCS by the Qiongzhou Strait in the northeastern part and the open sea in the southern part (Fig. 1). It has a shallow depth of less than 100 m and has an area of approximately $12.8\times10^4$ km$^2$ (Chen et al., 2009a; Gao et al., 2013, 2017; Huang et al., 2008). The Red River in Vietnam and the Fangcheng River, Nanliu River, Qin River, Dafeng River, Beilun River, and Changhua River in China provide the major river discharges into the gulf, along with some smaller rivers along the coast (Chen et al., 2009a; Tang et al., 2003). The hydrological features and the general circulation in the gulf have strong seasonality, which are mainly driven by prevailing northeasterly monsoons from September to April and southwesterly monsoons during May to August; thus, the dynamic and biological processes are active (Chen et al., 2011; Gao et al., 2017; Huang et al., 2008; Tang et al., 2003).

Although the general environmental conditions in the Beibu Gulf are good, the fast development along the Beibu Gulf Economical Rim has placed the environment in the Beibu Gulf under pressure. According to marine environmental reports (Department of Ocean and Fisheries of Guangxi Zhuang Autonomous Region of China, 2013, 2016, 2017), some local areas along bays, such as the Qinzhou Bay, Dafeng River Estuary, and Fangcheng Bay, have severe environmental conditions (under level IV), and the most out-of-limit pollutants are dissolved inorganic nitrogen (DIN), active phosphate and oil, which are causing increasing detriment to the Beibu Gulf environment. The conditions of these items may affect the ecosystem in the gulf through transportation and biochemical processes. Studying the nutrient distributions, budget and flux is of great importance in providing a scientific perspective on the Beibu Gulf.

One way to study the subjects above is field investigations. Some field investigations concerning the water quality, biological processes, and distributions of ecological factors, such as nutrients, phytoplankton, zooplankton, benthic animals, and fish, have involved special periods and stations, showing that these factors have their own distribution characteristics and that the water mass exchange across the gulf and human activity along the estuaries may be critical (Cai et al., 2012; Chen et al., 2011; Fu et al., 2012; Liu et al., 1998; Tang et al., 2003; Wang et al., 2015; Zheng et al., 2014; Zhou et al., 2011). However, compared to those in the open SCS, field investigation data in the Beibu Gulf are relatively sparse (Bauer and Waniek, 2013). Moreover, outside the areas and periods of field investigations, many details have remained unknown, which makes some analyses difficult, especially quantitative analyses of the nutrient budget and flux.

Foundation item: The National Key Research and Development Program of China under contract No. 2017YFC1404801; the Program of Xiamen Southern Oceanographic Center under contract No. 15PZB009NF05.
*Corresponding author, E-mail: panwr@xmu.edu.cn

*Acta Oceanol. Sin.*, 2021, Vol. 40, No. 10, P. 17–29
https://doi.org/10.1007/s13131-021-1770-x
http://www.aosocean.com
E-mail: ocean2@hyxb.org.cn

# Three-dimensional properties of mesoscale cyclonic warm-core and anticyclonic cold-core eddies in the South China Sea

Wenjin Sun[1, 2], Yu Liu[2, 3], Gengxin Chen[4], Wei Tan[5], Xiayan Lin[3], Yuping Guan[4, 6], Changming Dong[1, 2*]

[1] School of Marine Sciences, Nanjing University of Information Science and Technology, Nanjing 210044, China

[2] Southern Marine Science and Engineering Guangdong Laboratory (Zhuhai), Zhuhai 519080, China

[3] Marine Science and Technology College, Zhejiang Ocean University, Zhoushan 316022, China

[4] State Key Laboratory of Tropical Oceanography, South China Sea Institute of Oceanology, Chinese Academy of Sciences, Guangzhou 510301, China

[5] College of Ocean Science and Engineering, Shandong University of Science and Technology, Qingdao 266590, China

[6] College of Earth and Planetary Sciences, University of Chinese Academy of Sciences, Beijing 100049, China

Received 31 October 2020; accepted 28 December 2020



**Abstract**

In general, a mesoscale cyclonic (anticyclonic) eddy has a colder (warmer) core, and it is considered as a cold (warm) eddy. However, recently research found that there are a number of "abnormal" mesoscale cyclonic (anticyclonic) eddies associated with warm (cold) cores in the South China Sea (SCS). These "abnormal" eddies pose a challenge to previous works on eddy detection, characteristic analysis, eddy-induced heat and salt transports, and even on mesoscale eddy dynamics. Based on a 9-year (2000–2008) numerical modelling data, the cyclonic warm-core eddies (CWEs) and anticyclonic cold-core eddies (ACEs) in the SCS are analyzed. This study found that the highest incidence area of the "abnormal" eddies is the northwest of Luzon Strait. In terms of the eddy snapshot counting method, 8 620 CWEs and 9 879 ACEs are detected, accounting for 14.6% and 15.8% of the total eddy number, respectively. The size of the "abnormal" eddies is usually smaller than that of the "normal" eddies, with the radius only around 50 km. In the generation time aspect, they usually appear within the 0.1–0.3 interval in the normalized eddy lifespan. The survival time of CWEs (ACEs) occupies 16.3% (17.1%) of the total eddy lifespan. Based on two case studies, the intrusion of Kuroshio warm water is considered as a key mechanism for the generation of these "abnormal" eddies near the northeastern SCS.

**Key words:** mesoscale eddy, cyclonic warm-core eddy, anticyclonic cold-core eddy, Kuroshio intrusion, South China Sea, abnormal mesoscale eddy

**Citation:** Sun Wenjin, Liu Yu, Chen Gengxin, Tan Wei, Lin Xiayan, Guan Yuping, Dong Changming. 2021. Three-dimensional properties of mesoscale cyclonic warm-core and anticyclonic cold-core eddies in the South China Sea. Acta Oceanologica Sinica, 40(10): 17–29, doi: 10.1007/s13131-021-1770-x

## 1 Introduction

The South China Sea (SCS) is the deepest and largest semi-closed marginal sea in the northwestern Pacific Ocean (Fig. 1). Its northern, western and southern boundaries are land, and it is separated from the Pacific Ocean by the Philippine Islands and Taiwan Island in the east. The SCS is connected to the Sulu Sea, the Indian Ocean and the Pacific Ocean through the Mindoro Strait, Malacca Strait and Luzon Strait, respectively. Several previous literature points out that the SCS is a hotspot for energetic mesoscale eddy activities. Their research refers to eddy statistical characteristic (Wang et al., 2003, 2015a, 2019a; Zhang et al., 2018; He et al., 2018), eddy case study (Nan et al., 2011; Chu et al., 2014; Wang et al., 2015b; Qiu et al., 2019a, 2019b), eddy–mean flow interaction (Zhong et al., 2016; Su et al., 2020), eddy-induced variations of oceanic and atmospheric physical parameters (Xian et al., 2012; Zhang et al., 2015; Liu et al., 2017b; Yang et al., 2017; Li et al., 2018), eddy formation mechanisms (Yang et al., 2013; Qiu et al., 2020), among others (Wang et al., 2020).

There are 32.9±2.4 eddies identified from numerical modelling data in terms of the surface characteristic aspect, and

Foundation item: The National Natural Science Foundation of China under contract Nos 41906008, 41806039, 41806030, 42076021, 41676010 and 41706205; the State Key Laboratory of Tropical Oceanography, South China Sea Institute of Oceanology, Chinese Academy of Sciences under contract Nos LTO1902 and LTO1807; the Strategic Priority Research Program of Chinese Academy of Sciences under contract No. XDB42000000; the Youth Innovation Promotion Association CAS under contract No. 2017397; the Pearl River S&T Nova Program of Guangzhou under contract No. 201806010105; the Open Fund of State Key Laboratory of Satellite Ocean Environment Dynamics, Second Institute of Oceanography, MNR under contract No. QNHX2022; the Startup Foundation for Introducing Talent of Nanjing University of Information Science & Technology under contract No. 2019r049; the Startup Foundation for Introducing Talent of Zhejiang Ocean University; the National Key Research Programs of China under contract Nos 2016YFC1401407 and 2017YFA0604100; the National Programme on Global Change and Air-Sea Interaction under contract Nos GASI-IPOVAI-03 and GASI-IPOVAI-05; the Innovation Group Project of Southern Marine Science and Engineering Guangdong Laboratory (Zhuhai) under contract No. 311020004.

*Corresponding author, E-mail: cmdong@nuist.edu.cn

*Acta Oceanol. Sin.*, 2021, Vol. 40, No. 10, P. 49–64
https://doi.org/10.1007/s13131-021-1831-1
http://www.aosocean.com
E-mail: ocean2@hyxb.org.cn

# Impacts of human interventions on the seasonal and nodal dynamics of the $M_2$ and $K_1$ tidal constituents in Lingdingyang Bay of the Zhujiang River Delta, China

Ping Zhang[1, 2, 3], Qingshu Yang[1, 2, 3], Haidong Pan[4], Heng Wang[1, 2, 3], Meifang Xie[1, 2, 3], Huayang Cai[1, 2, 3]*, Nanyang Chu[5], Liangwen Jia[1, 2, 3]

[1] Institute of Estuarine and Coastal Research, School of Marine Engineering and Technology, Sun Yat-sen University, Zhuhai 519082, China

[2] Guangdong Provincial Engineering Research Center of Coasts, Islands and Reefs, Zhuhai 519082, China

[3] Southern Marine Science and Engineering Guangdong Laboratory (Zhuhai), Zhuhai 519080, China

[4] Key Laboratory of Physical Oceanography, Ministry of Education, Qingdao 266100, China

[5] School of Marine Science, Sun Yat-sen University, Zhuhai 519082, China

Received 3 November 2020; accepted 28 February 2021



**Abstract**

Natural and human-induced changes may exert considerable impacts on the seasonal and nodal dynamics of $M_2$ and $K_1$ tidal constituents. Therefore, quantifying the influences of these factors on tidal regime changes is essential for sustainable water resources management in coastal environments. In this study, the enhanced harmonic analysis was applied to extract the seasonal variability of the $M_2$ and $K_1$ tidal amplitudes and phases at three gauging stations along Lingdingyang Bay of the Zhujiang River Delta. The seasonal dynamics in terms of tidal wave celerity and amplification/damping rate were used to quantify the impacts of human-induced estuarine morphological alterations on $M_2$ and $K_1$ tidal hydrodynamics in inner and outer Lingdingyang Bay. The results show that both tidal amplification/damping rate and wave celerity were considerably increased from the pre-anthropogenic activity period (Pre-AAP) to the post-anthropogenic activity period (Post-AAP) excepting the tidal amplification/damping rate in outer Lingdingyang Bay, and the variations in outer Lingdingyang Bay was larger than those in inner Lingdingyang Bay. The alterations in these two parameters were more significant in flood season than in dry season in both inner and outer Lingdingyang Bay. The seasonal variability of $M_2$ and $K_1$ tidal amplitudes were further quantified using a regression model accounting for the 18.61-year lunar nodal modulation, where this study observes a considerable alteration in $M_2$ constituent owing to human interventions. During the Post-AAP, the $M_2$ amplitudes at the downstream station were larger than those that would have occurred in the absence of strong human interventions, whereas the opposite was true for the upstream station, leading to a substantial decrease in tidal amplification in outer Lingdingyang Bay. However, it is opposite in inner Lingdingyang Bay. The underlying mechanism can be primarily attributed to channel deepening and narrowing caused by human interventions, that resulted in substantial enlargement of the bay volume and reduced the effective bottom friction, leading to faster wave celerity and stronger amplified waves.

**Key words:** tidal dynamics, S_TIDE model, nodal modulation, channel deepening, tidal wave celerity

**Citation:** Zhang Ping, Yang Qingshu, Pan Haidong, Wang Heng, Xie Meifang, Cai Huayang, Chu Nanyang, Jia Liangwen. 2021. Impacts of human interventions on the seasonal and nodal dynamics of the $M_2$ and $K_1$ tidal constituents in Lingdingyang Bay of the Zhujiang River Delta, China. Acta Oceanologica Sinica, 40(10): 49–64, doi: 10.1007/s13131-021-1831-1

## 1 Introduction

It is essential to understand tidal variability in coastal areas because it directly impacts channel navigation, coastal flooding, and ecology. Previous studies examining tidal dynamics have shown that tidal fluctuations occur over a wide range of time scales (including sub-daily, daily, fortnightly, seasonal, yearly, and decadal) owing to the changes in predictable astronomical variations and the physical properties of the ocean and coastal morphology (Devlin et al., 2014, 2017, 2018). This study mainly focuses on the seasonal variability of tides, which is significant in the Zhujiang River Delta (ZRD) located in the southern part of China. Of particular interest are the impacts of large-scale human interventions on the seasonal variability of tides.

Seasonal variability of the main tidal constituents has been documented for a long time (Corkan, 1934; Kang et al., 1995; Gräwe et al., 2014; Müller et al., 2014). In the coastal ocean, it is usually observed that tidal amplitudes are larger during summer than during winter (Huess and Andersen, 2001; Tazkia et al., 2017; Wang et al., 2020a). This can be primarily attributed to the seasonal variation in frictional effects exerted on tides when they propagate from the deep ocean to the open area of the coastal ocean. In contrast, in the inner parts of the delta, amplitudes of

Foundation item: The National Key R&D Program of China under contract No. 2016YFC0402600; the National Natural Science Foundation of China under contract No. 51979296; the Guangzhou Science and Technology Program of China under contract No. 202002030452.

*Corresponding author, E-mail: caihy7@mail.sysu.edu.cn

*Acta Oceanol. Sin.*, 2021, Vol. 40, No. 11, P. 70–78
https://doi.org/10.1007/s13131-021-1870-7
http://www.aosocean.com
E-mail: ocean2@hyxb.org.cn

# Interannual variability in the sea surface cooling induced by tropical cyclones in the South China Sea

Juan Ouyang[1], Chunhua Qiu[1, 2, 3]*, Zhenhui Yi[1], Dongxiao Wang[1, 2, 3, 4], Danyi Su[5], Hong Liang[1], Zihao Yang[1]

[1] School of Marine Sciences, Sun Yat-sen University, Guangzhou 510275, China

[2] Southern Marine Science and Engineering Guangdong Laboratory (Zhuhai), Zhuhai 519020, China

[3] Pearl River Estuary Marine Ecosystem Research Station, Ministry of Education, Zhuhai 519020, China

[4] Guangdong Provincial Key Laboratory of Marine Resources and Coastal Engineering, Zhuhai 519020, China

[5] Hydrate Engineering Technology Center, China Geological Survey, Guangzhou 510760, China

Received 15 April 2021; accepted 21 June 2021



**Abstract**

Sea surface cooling induced by tropical cyclones (TCs) is an important component of air-sea interactions. Using coordinate transformation and composite analysis methods, we examined the interannual variability in TC-induced sea surface cooling (TCSSC) in the South China Sea (SCS). The frequency of surface cooling cases was over 86% and that of surface warming cases was less than 14%. The magnitude of TCSSC was defined as the absolute value of TCSSC. The maximum magnitude of TCSSC occurred on the right side of the TC track, and the mean magnitude of TCSSC decreased by 0.04°C/a from 2006 to 2018. The interannual variability in TCSSC was highly correlated with the TC translation speed and pre-TC mixed layer depth. Notably, TCSSC got enhanced in El Niño years of 2007, 2010, and 2015. The El Niño types were suggested to determine the occurring periods of strong TCSSC via controlling the positions of SCS anticyclones, which brought pre-TC shallow mixed layer and caused strong TCSSC via vertical mixing process during El Niño events. To quantify how the anticyclone influences TCSSC, we need to use mixed layer heat balances model in the next study.

**Key words:** sea surface cooling, tropical cyclone, El Niño-Southern Oscillation (ENSO), South China Sea, anticyclone

**Citation:** Ouyang Juan, Qiu Chunhua, Yi Zhenhui, Wang Dongxiao, Su Danyi, Liang Hong, Yang Zihao. 2021. Interannual variability in the sea surface cooling induced by tropical cyclones in the South China Sea. Acta Oceanologica Sinica, 40(11): 70–78, doi: 10.1007/s13131-021-1870-7

## 1 Introduction

Tropical cyclones (TCs) occur frequently in the western North Pacific (WNP) (D'Asaro et al., 2011), and are one of the most destructive natural disasters, causing tremendous economic damages and loss of lives. TCs can trigger strong surface cooling by enhancing air-sea heat fluxes and oceanic vertical mixing, with the former accounting for 15% of sea surface cooling and the latter for 85% (Price, 1981). The TC-induced sea surface cooling (TCSSC), in turn, can reduce TC's intensity, because TCs tend to weaken (strengthen) when passing cold (warm) water (Brand, 1971; Cione and Uhlhorn, 2003; Lin et al., 2005). In a coupled model, the negative sea surface temperature (SST) feedback produced by a TC could reduce the TC intensity by more than 50% (Schade and Emanuel, 1999). In addition, TCSSC can affect local atmospheric conditions (Lin et al., 2003b) as well as global climate changes (Sriver and Huber, 2010). Therefore, the study of TCSSC is of great significance.

TCSSC usually ranges in 0–5°C (Leipper, 1967; Cione and Uhlhorn, 2003; D'Asaro et al., 2007; Wang et al., 2016) and mostly exhibits a rightward bias in the Northern Hemisphere (Leipper, 1967; Price, 1981; Shay et al., 1992; Price et al., 1994), although a few researchers have argued that maximal TCSSC is not only found on the right side but also on the left side of the TC track (Leipper, 1967; Ko et al., 2014). TCSSC has a recovery time of 7 d to 1 month (Hazelworth, 1968; Price et al., 2008; Dare and McBride, 2011).

Statistical analyses show that TCSSC might be related to TCs' properties (i.e., intensity, translation speed, and size) and the pre-TC oceanic states. Generally, the more intense and slower the TC is, the larger magnitude the TCSSC reaches (Mei and Pasquero, 2013). Pre-TC oceanic conditions can also impact the magnitude of TCSSC. For example, a warm eddy can suppress the vertical mixing process, thus weakening TCSSC. Lin (2012) found that the most intense tropical cyclone of 2003 Maemi could not induce obvious TCSSC due to pre-storm warm eddies. Wang et al. (2016) used Argo profiles to construct the three-dimensional structure of upper-layer responses to TCs over the WNP, which suggested that the deeper (shallower) the mixed layer extended, the weaker (stronger) the TCSSC was. Mei et al. (2015) compared TCSSC in the South China Sea (SCS) and the WNP and found that the mixed layer is shallower in the SCS than in the WNP, resulting in larger magnitude of TCSSC in the SCS.

The SCS is the largest marginal sea of the WNP and has a high concentration of TCs (10.3 per year), some of which form in the

Foundation item: The National Natural Science Foundation of China under contract No. 41976002.
*Corresponding author, E-mail: qiuchh3@mail.sysu.edu.cn

*Acta Oceanol. Sin.*, 2022, Vol. 41, No. 2, P. 41–50
https://doi.org/10.1007/s13131-021-1880-5
http://www.aosocean.com
E-mail: ocean2@hyxb.org.cn

# Bias correction of sea surface temperature retrospective forecasts in the South China Sea

Guijun Han[1], Jianfeng Zhou[1], Qi Shao[1, 2], Wei Li[1, 2*], Chaoliang Li[1*], Xiaobo Wu[1], Lige Cao[1], Haowen Wu[1], Yundong Li[1], Gongfu Zhou[1]

[1] School of Marine Science and Technology, Tianjin University, Tianjin 300072, China

[2] Tianjin Key Laboratory for Oceanic Meteorology, Tianjin 300074, China

Received 21 May 2021; accepted 12 June 2021



**Abstract**

Offline bias correction of numerical marine forecast products is an effective post-processing means to improve forecast accuracy. Two offline bias correction methods for sea surface temperature (SST) forecasts have been developed in this study: a backpropagation neural network (BPNN) algorithm, and a hybrid algorithm of empirical orthogonal function (EOF) analysis and BPNN (named EOF-BPNN). The performances of these two methods are validated using bias correction experiments implemented in the South China Sea (SCS), in which the target dataset is a six-year (2003–2008) daily mean time series of SST retrospective forecasts for one-day in advance, obtained from a regional ocean forecast and analysis system called the China Ocean Reanalysis (CORA), and the reference time series is the gridded satellite-based SST. The bias-correction results show that the two methods have similar good skills; however, the EOF-BPNN method is more than five times faster than the BPNN method. Before applying the bias correction, the basin-wide climatological error of the daily mean CORA SST retrospective forecasts in the SCS is up to −3°C; now, it is minimized substantially, falling within the error range (±0.5°C) of the satellite SST data.

**Key words:** sea surface temperature retrospective forecasts, bias correction, backpropagation neural network, empirical orthogonal function analysis, South China Sea

**Citation:** Han Guijun, Zhou Jianfeng, Shao Qi, Li Wei, Li Chaoliang, Wu Xiaobo, Cao Lige, Wu Haowen, Li Yundong, Zhou Gongfu. 2022. Bias correction of sea surface temperature retrospective forecasts in the South China Sea. Acta Oceanologica Sinica, 41(2): 41–50, doi: 10.1007/s13131-021-1880-5

## 1 Introduction

Like numerical weather forecasts, numerical ocean forecasts are becoming more and more common. This is in part due to significant advances in the development of real-time ocean observing system, the ability of modeling the ocean and assimilating ocean data, and availability of high performance computing resources. A common problem, exactly as facing weather forecasters today, is the presence of systematic model errors, referred to as the biases (Dalcher and Kalnay, 1987), resulted from deficiencies of ocean models themselves. As a result, two kinds of bias correction techniques used to deal with the numerical weather forecasting errors are considered by marine forecasters: one is offline bias correction, and the other is online bias correction (Danforth et al., 2007). Offline bias correction is a typical postprocedure for the output of an operational numerical weather prediction model by accounting for the model bias derived from the statistics of short-term forecast errors with respect to a reference time series. This technique can trace its roots all the way back to the approaches of "perfect prog" (PP) (Klein et al., 1959; Klein, 1971) and model output statistics (MOS) (Glahn and Lowry, 1972; Carter et al., 1989). Note that such offline bias correction is empirical, and has no dynamic effect on the forecasts; in contrast, online bias correction is more robust for being state-dependent and made along with model integration. For instance, data assimilation in the presence of forecast bias (Dee and Da Silva, 1998) belongs to the category of online bias correction. However, online bias correction algorithms are usually computationally complicated and expensive. Offline bias correction is particularly valuable for being independent of the model and easy to implement so that up to now it is still of great interest in both research and practice ( Bhargava et al., 2018; Chang et al., 2019).

Sea surface temperature (SST) is not only used as the main index describing the thermal condition of the ocean surface but also an important indicator of ocean primary productivity, and plays a key role in the interaction between the ocean and the atmosphere. Therefore, it is of great scientific significance and practical application prospect to correct SST forecast bias in numerical weather prediction, ocean forecasting, and climate research (Kug et al., 2008; Ashfaq et al., 2011; LaRow, 2013; Abhilash et al., 2014; Narapusetty et al., 2014; Vitart and Balmaseda, 2018; Hernández-Díaz et al., 2019; Voldoire et al., 2019). This study is motivated by recent extensive applications of various types of artificial neural networks in areas where more reliable reference data from meteorologic and oceanographic observations and reanalyses are available. Two methods employing artificial neural network trained by the traditional backpropagation (BP) algorithm are proposed as post-processing solutions for

Foundation item: The National Key Research and Development Program of China under contract No. 2018YFC1406206; the National Natural Science Foundation of China under contract No. 41876014.
*Corresponding author, E-mail: liwei1978@tju.edu.cn; chaoliang_li0608@163.com

*Acta Oceanol. Sin.*, 2022, Vol. 41, No. 2, P. 139–146
https://doi.org/10.1007/s13131-021-1837-8
http://www.aosocean.com
E-mail: ocean2@hyxb.org.cn

# Turning depths of internal tides in the South China Sea inferred from profile data

Kun Liu[1], Lianglong Da[1, 2*], Wuhong Guo[1, 2], Chenglong Liu[1], Junchuan Sun[1, 3]

[1] Pilot National Laboratory for Marine Science and Technology (Qingdao), Qingdao 266237, China

[2] PLA Navy Submarine Academy, Qingdao 266041, China

[3] Key Laboratory of Marine Science and Numerical Modeling, First Institute of Oceanography, Ministry of Natural Resources, Qingdao 266061, China

Received 28 October 2020; accepted 29 March 2021



**Abstract**

Theoretically, propagating internal tides in the ocean may reflect at turning depths, where buoyancy frequencies equal tidal frequencies, before colliding with the air-sea interface or rugged bottom topography. Globally, the internal tide lower turning depths (ITLTDs) in the open ocean have been mapped; however, knowledge of the presence of ITLTDs in the South China Sea (SCS) is lacking. In this study, 2 125 high-quality temperature-salinity profiles (including 58 deep-sea hydrographic measurements with observational depths exceeding 3 000 m) are collected and analyzed to investigate the existence of ITLTDs in the SCS. Furthermore, the concept of the upper turning depth is first introduced in the context of internal tides, and internal tide upper turning depths (ITUTDs) are also investigated. ITLTDs are found to exist at several abyssal stations; these stations are distributed mostly in the southern part of the SCS basin, possibly due to the greater water depths there. Fewer locations show the presence of ITLTDs for $K_1$ versus $M_2$ tidal frequencies because of the lower tidal frequency. The distance between ITLTDs and the seafloor ranged from 270 m to more than 1 200 m, implying the possible existence of multiple internal wave evanescent regions in the abyssal bottom. ITUTDs of tens of meters are ubiquitous in the SCS; stations with the presence of ITUTDs are located mainly in the northeastern SCS due to the intensive observations there. However, the calculated ITUTDs have large uncertainties; they are sensitive to the selected bin values. The horizontal propagation directions of internal tides in the SCS change dramatically, and as a result, the estimated turning depths under the full Coriolis force definition are different compared to that under the traditional approximation.

**Key words:** turning depth, internal tide, buoyancy frequency, South China Sea

**Citation:** Liu Kun, Da Lianglong, Guo Wuhong, Liu Chenglong, Sun Junchuan. 2022. Turning depths of internal tides in the South China Sea inferred from profile data. Acta Oceanologica Sinica, 41(2): 139–146, doi: 10.1007/s13131-021-1837-8

## 1 Introduction

Internal tides are ubiquitous in the ocean and have dual impacts on human maritime activities. First, the breaking of internal tides is regarded as one of the major catalysts of ocean mixing, which is crucial for large-scale ocean circulation (Munk and Wunsch, 1998). Internal tidal-induced upwelling can pump nutrients upward to the euphotic layer; this surface nutrient enrichment can in turn increase fishing yields (Jan and Chen, 2009). Second, the steepening of internal tides can induce large-amplitude internal solitary waves, which are key environmental factors in the design of offshore oil and gas engineering projects. Internal waves are considered to be second only to typhoons in terms of disaster potential due to the enormous threat they pose to undersea equipment (Fang and Duan, 2014).

The propagation of internal tides in the ocean is significantly affected by the inhomogeneous hydrological environment (Gerkema et al., 2004). In linear theory, freely propagating internal waves have a lower frequency limit of the local inertial frequency and a higher frequency limit of the buoyancy frequency ($f < \omega < N$). In view of this theoretical basis and the fact that buoyancy frequencies are generally exponentially dampened with depth in the abyssal sea, Munk (1981) first proposed the possible existence of internal tide turning depths, where the local buoyancy frequency matches the tidal frequency. The presence of turning depths can impact the pathways and energy losses of internal tides during propagation by reflecting or refracting internal tidal beams at the turning interface and preventing internal tides from colliding with rugged bottom topographies. Numerical and experimental studies have suggested that internal tidal beams behave remarkably differently according to the presence or absence of turning depths (Paoletti and Swinney, 2012). Moreover, the existence of turning depths may affect the generation of internal tides beneath them (Paoletti et al., 2014).

The identification of internal tide turning depths requires hydrographic observations of the abyssal ocean. Based on World Ocean Circulation Experiment data, King et al. (2012) mapped

Foundation item: The National Natural Science Foundation of China under contract Nos 41906005, 41149907 and 41706033; the National Basic Research Program of China under contract No. 2019-JCJQ-ZD-149-00; the Open Fund of the Laboratory for Regional Oceanography and Numerical Modeling, Pilot National Laboratory for Marine Science and Technology (Qingdao) under contract No. 2019A05.

*Corresponding author, E-mail: da_lianglong@126.com

*Acta Oceanol. Sin.*, 2022, Vol. 41, No. 5, P. 1–11
https://doi.org/10.1007/s13131-021-1879-y
http://www.aosocean.com
E-mail: ocean2@hyxb.org.cn

# Numerical investigation of the South China Sea deep circulation

Shengquan Tang[1], Xueen Chen[1]*, Zhi Zeng[1, 3], Xin Liu[2]

[1] College of Oceanic and Atmospheric Sciences, Ocean University of China, Qingdao 266100, China

[2] Shandong Computer Science Center (National Supercomputer Center in Jinan), Qilu University of Technology (Shandong Academy of Sciences), Jinan 250014, China

[3] College of Meteorology and Oceanography, National University of Defense Technology, Changsha 410073, China

Received 15 April 2021; accepted 29 June 2021



**Abstract**

Based on a two-level nested model from the global ocean to the western Pacific and then to the South China Sea (SCS), the high-resolution SCS deep circulation is numerically investigated. The SCS deep circulation shows a basin-scale cyclonic structure with a strong southward western boundary current in summer (July), a northeast-southwest through-flow pattern across the deep basin without a western boundary current in winter (January), and a transitional pattern in spring and autumn. The sensitivity model experiments illustrate that the Luzon Strait deep overflow is the main factor controlling the seasonal variation in the SCS deep circulation. The SCS surface wind can significantly influence the SCS deep circulation in winter. The Luzon Strait deep overflow transport from the Pacific into the SCS ranges from $0.68\times10^6$ m$^3$/s to $1.83\times10^6$ m$^3$/s, reaching its maximum in summer (July, up to $1.83\times10^6$ m$^3$/s), less in autumn and winter, and the minimum in spring (May, $0.68\times10^6$ m$^3$/s). In summer, the strong Luzon Strait deep overflow dominates the SCS deep circulation when the role of the SCS surface wind is small. In winter, the weaker Luzon Strait deep overflow and SCS surface wind jointly drive the SCS deep circulation into a northeast-southwest through-flow pattern. The potential vorticity (PV) dissipation in the SCS deep basin reaches its maximum (–0.122 m$^2$/s$^2$) in May and its minimum (–0.380 m$^2$/s$^2$) in July.

**Key words:** South China Sea, deep sea circulation, deep overflow, surface wind, potential vorticity

**Citation:** Tang Shengquan, Chen Xueen, Zeng Zhi, Liu Xin. 2022. Numerical investigation of the South China Sea deep circulation. Acta Oceanologica Sinica, 41(5): 1–11, doi: 10.1007/s13131-021-1879-y

## 1 Introduction

The South China Sea (SCS) is the largest marginal sea of the North Pacific (Chao et al., 1996; Wang et al., 2011). In the SCS deep basin, the Luzon Strait deep channel is the only channel connecting the SCS and the Pacific Ocean (Qu et al., 2006; Sun et al., 2017; Wang et al., 2011).

Influenced by the water exchange through the Luzon Strait and the East Asian monsoon, the climatological annual mean SCS circulation presents a "sandwich" structure in the vertical direction (Yuan, 2002). The climatological annual mean upper water and deep water of the SCS are cyclonic circulations, and the climatological annual mean intermediate water is an anticyclonic circulation (Gan et al., 2006, 2016; Li and Qu, 2006; Liu and Gan, 2017; Tian et al., 2006; Shu et al., 2014; Wang et al., 2012, 2016; Yuan, 2002; Zhu et al., 2016). The SCS deep circulation results from interactions among multiscale dynamic processes and complex topography and refers to the circulation system at more than 2 000 m depth in the SCS basin (Tian and Qu, 2012). There is a persistent density difference between the SCS water and the Pacific water below 1 500 m depth (the density is higher in the Pacific than in the SCS below 1 500 m), which is identified as a baroclinic pressure gradient driving flow from the Pacific into the SCS (Qu et al., 2006). After entering the SCS deep basin, the Luzon Strait deep overflow turns northwestward, forming an annual mean basin-scale cyclonic circulation (Yuan, 2002; Qu et al., 2006; Wang et al., 2011). Lan et al. (2013) also suggested that the most obvious features of the climatological annual mean SCS deep circulation are basin-scale cyclonic gyre and western intensification.

The mechanisms of the SCS deep circulation are complex. The water transported into the SCS deep basin through the Luzon Strait deep channel tends to follow potential vorticity (PV) contours, which are approximately parallel to the local isobaths (Pedlosky, 1982, 1996; Qu et al., 2006). Therefore, the pattern of the annual mean potential density and PV distribution in the SCS deep basin are consistent with the cyclonic circulation (Li and Qu, 2006; Qu et al., 2006; Wang et al., 2011). Lan et al. (2013) first used the PV-integral constraint to discuss the dynamic mechanisms of the SCS deep circulation. However, the spatial and temporal pattern of PV dissipation in the SCS deep basin remains unclear. As we discussed above, previous studies of SCS deep circulation have mainly focused on its annual mean characteristics, while its seasonal variation has received little attention. Using a model resolution of 0.5°×0.5°, Lan et al. (2015) first compared the SCS deep circulation in summer with that in winter and found that the SCS deep circulation is cyclonic in summer and weakly cyclonic in winter. Lan et al. (2015) also considered the effect of the whole Luzon Strait exchange on the SCS deep circulation by clos-

Foundation item: The National Key Research and Development Program of China under contract No. 2021YFF0704002; the Aoshan Science and Technology Innovation Program of Pilot National Laboratory for Marine Science and Technology (Qingdao) under contract No. 2018ASKJ01-04.

*Corresponding author, E-mail: xchen@ouc.edu.cn

*Acta Oceanol. Sin.*, 2022, Vol. 41, No. 10, P. 14–21
https://doi.org/10.1007/s13131-022-2005-5
http://www.aosocean.com
E-mail: ocean2@hyxb.org.cn

# Vertical multiple-layer structure of temperature and turbulent diffusivity in the South China Sea

Xin He[1, 2], Changrong Liang[1, 3, 4], Yang Yang[5], Guiying Chen[1, 3, 4], Xiaodong Shang[1, 3, 4*], Xiaozhou He[6*], Penger Tong[7]

[1] State Key Laboratory of Tropical Oceanography, South China Sea Institute of Oceanology, Chinese Academy of Sciences, Guangzhou 510301, China

[2] University of Chinese Academy of Sciences, Beijing 100049, China

[3] Southern Marine Science and Engineering Guangdong Laboratory (Guangzhou), Guangzhou 511458, China

[4] Institution of South China Sea Ecology and Environmental Engineering, Chinese Academy of Sciences, Guangzhou 510301, China

[5] Institute of Deep-Sea Science and Engineering, Chinese Academy of Sciences, Sanya 572000, China

[6] School of Mechanical Engineering and Automation, Harbin Institute of Technology, Shenzhen 518055, China

[7] Department of Physics, Hong Kong University of Science and Technology, Hong Kong 999077, China

Received 6 September 2021; accepted 7 January 2022



**Abstract**

We report field measurements of vertical profiles of the turbulent diffusivity and temperature at different stations in the South China Sea (SCS). Our study shows that the measured turbulent diffusivity follows a power-law distribution with a varying exponent in water layers. Similar multiple-layer scaling regimes were also observed from the temperature fluctuations. Combining turbulent diffusivity and temperature fluctuations, the vertical structure of temperature was revealed. Furthermore, we discussed the temperature profiles in each layer. A constant function of a dimensionless temperature profile was found in water layers that have identical turbulence conditions. Our results reveal the multiple-layer structure of temperature in the SCS. This study contributes to the understanding of the vertical structure of multiple layers in the SCS and provides clues for exploring the physical mechanism for maintaining the temperature structure.

**Key words:** temperature profile, turbulent diffusivity, South China Sea, multiple layers

**Citation:** He Xin, Liang Changrong, Yang Yang, Chen Guiying, Shang Xiaodong, He Xiaozhou, Tong Penger. 2022. Vertical multiple-layer structure of temperature and turbulent diffusivity in the South China Sea. Acta Oceanologica Sinica, 41(10): 14–21, doi: 10.1007/s13131-022-2005-5

## 1 Introduction

The South China Sea (SCS) covers a region from the equator to 23°N and from 99°E to 121°E with an average depth about 1 212 m. It is one of the largest tropical marginal seas on earth. It has a deep basin surrounded by a steep continental slope and connects to the East China Sea via the Taiwan Strait, to the western Pacific Ocean via the Luzon Strait, to the Sulu Sea via the Mindoro Strait, and to the Java Sea via the Karimata Strait.

A widely accepted notion is that the SCS has a unique, three-layer cyclonic-anticyclonic-cyclonic (CAC) circulation pattern. Upper-layer circulation in the SCS has been widely studied since the first report by Wyrtki (1961). The results of the Princeton Ocean Model suggests that seasonal upper-layer circulation patterns and upwelling phenomena are determined and forced by the wind, while the lateral boundary forcing plays a secondary role in determining the magnitude of circulation velocities (Chu et al., 1999). Principal component analysis of altimeter data shows that sea-level variation consists mainly of two modes, corresponding well to the first two modes of the wind stress curl. Mode 1 represents oscillation in the southern basin and shows little inter-annual variation, and Mode 2 represents weak oscillation in the southern basin and strong oscillation off the coast of central Vietnam (Shaw et al., 1999). It is thus concluded that, as a result of the seasonally reversed monsoon, upper circulation exhibits distinct seasonal variability with cyclonic circulation over the whole SCS basin in winter, cyclonic circulation in the northern half of the basin, and anticyclonic circulation in the southern half of the basin in summer (Hu et al., 2000; Liu et al., 2001; Su,

Foundation item: The National Key R&D Program of China under contract No. 2021YFC3101301; the Innovative Academy of Marine Information Technology, Chinese Academy of Sciences under contract No. CXBS202101; the Key Special Project for Introduced Talents Team of Southern Marine Science and Engineering Guangdong Laboratory (Guangzhou) under contract No. GML2019ZD0304; the National Natural Science Foundation of China under contract Nos 41876022, 41876023, 11772111 and 91952101; the Guangdong Natural Science Foundation of China under contract Nos 1914050004866 and 2020A1515011094; the Hong Kong Research Grants Council under contract Nos 16301719 and N-HKUST604/19; the Science, Technology and Innovation Commission of Shenzhen Municipality under contract No. KQJSCX20180328165817522; the Science and Technology Program of Guangzhou under contract No. 202102020707.
*Corresponding author, E-mail: xdshang@scsio.ac.cn; hexiaozhou@hit.edu.cn

*Acta Oceanol. Sin.*, 2022, Vol. 41, No. 10, P. 41–53
https://doi.org/10.1007/s13131-022-2012-6
http://www.aosocean.com
E-mail: ocean2@hyxb.org.cn

# Modified parameterization for near-inertial waves

Weiqi Hong[1], Lei Zhou[1, 2*], Xiaohui Xie[1, 2, 3], Han Zhang[2, 3, 4], Changrong Liang[5]

[1] School of Oceanography, Shanghai Jiao Tong University, Shanghai 200030, China

[2] Southern Marine Science and Engineering Guangdong Laboratory (Zhuhai), Zhuhai 519082, China

[3] State Key Laboratory of Satellite Ocean Environment Dynamics, Second Institute of Oceanography, Ministry of Natural Resources, Hangzhou 310012, China

[4] Fujian Provincial Key Laboratory for Coastal Ecology and Environmental Studies, Xiamen University, Xiamen 361102, China

[5] State Key Laboratory of Tropical Oceanography, South China Sea Institute of Oceanology, Chinese Academy of Sciences, Guangzhou 510301, China

Received 24 January 2022; accepted 27 January 2022



**Abstract**

The near-inertial waves (NIWs) are important for energy cascade in the ocean. They are usually significantly reinforced by strong winds, such as typhoon. Due to relatively coarse resolutions in contemporary climate models, NIWs and associated ocean mixing need to be parameterized. In this study, a parameterization for NIWs proposed by Jochum in 2013 (J13 scheme), which has been widely used, is compared with the observations in the South China Sea, and the observations are treated as model outputs. Under normal conditions, the J13 scheme performs well. However, there are noticeable discrepancies between the J13 scheme and observations during typhoon. During Typhoon Kalmaegi in 2014, the inferred value of the boundary layer is deeper in the J13 scheme due to the weak near-inertial velocity shear in the vertical. After typhoon, the spreading of NIWs beneath the upper boundary layer is much faster than the theoretical prediction of inertial gravity waves, and this fast process is not rendered well by the J13 scheme. In addition, below the boundary layer, NIWs and associated diapycnal mixing last longer than the direct impacts of typhoon on the sea surface. Since the energy dissipation and diapycnal mixing below the boundary layer are bounded to the surface winds in the J13 scheme, the prolonged influences of typhoon via NIWs in the ocean interior are missing in this scheme. Based on current examination, modifications to the J13 scheme are proposed, and the modified version can reduce the discrepancies in the temporal and vertical structures of diapycnal mixing.

**Key words:** near-inertial waves, parameterization, ocean mixing, upper ocean boundary layer, typhoon

**Citation:** Hong Weiqi, Zhou Lei, Xie Xiaohui, Zhang Han, Liang Changrong. 2022. Modified parameterization for near-inertial waves. Acta Oceanologica Sinica, 41(10): 41–53, doi: 10.1007/s13131-022-2012-6

## 1 Introduction

Near-inertial waves (NIWs) are the internal gravity waves with a frequency around the inertial frequency ($f = 2\Omega\sin\phi$; where $\phi$ is the latitude, $\Omega$=7.29×10$^{-5}$ rad/s), which are ubiquitous in the ocean interior (Alford et al., 2016; Webster, 1968). NIW is a major funnel for wind energy that goes into the ocean and about 2/3 of near-inertial energy is generated due to surface wind forcing (Fu, 1981). It is estimated that the wind energy of 0.3–0.7 TW (1 TW=10$^{12}$ W) enters the upper ocean via NIWs every year (Alford, 2020; Watanabe and Hibiya, 2002) which is approximately 1/6 of the total energy flux (~3 TW) from winds into the Ekman layer (Wang and Huang, 2004) and a significant amount of the total energy of 2 TW needed for maintaining the global ocean stratification (Munk and Wunsch, 1998; Wunsch and Ferrari, 2004). The energy of NIWs also penetrates the ocean interior, reinforcing the vertical shear and nourishing the ocean mixing (Alford and Gregg, 2001; Kunze et al., 1990; Munk and Wunsch, 1998; Sloyan and Rintoul, 2001). During extreme meteorological conditions such as tropical cyclones, the NIWs are significantly enhanced, and a series of ocean dynamic and thermodynamic responses can be triggered (Price, 1981), such as the enhancement of near-inertial currents characterized by opposite phases in the mixed layer and the thermocline (Zhang et al., 2016). Therefore, the NIWs are one of the most important forms of energy transport from the atmosphere to the ocean, an important component of the energy cascade in the ocean interior, and an important energy source for diapycnal mixing.

The NIWs have been captured in many *in-situ* observations. These waves and their interactions with the subtropical front were documented during FRONTS'80 (Kunze and Sanford, 1984).

Foundation item: The National Natural Science Foundation of China under contract Nos 42125601 and 42076001; the Scientific Research Fund of the Second Institute of Oceanography, Ministry of Natural Resources, under contract Nos HYGG2003 and QNYC2002; the project supported by the Southern Marine Science and Engineering Guangdong Laboratory (Zhuhai) under contract No. SML2021SP207; the Oceanic Interdisciplinary Program of Shanghai Jiao Tong University under contract No. SL2020MS032; the CEES Visiting Fellowship Program under contract No. CEESRS202001; the Innovation Group Project of Southern Marine Science and Engineering Guangdong Laboratory (Zhuhai) under contract No. 311021001.
*Corresponding author, E-mail: zhoulei1588@sjtu.edu.cn

*Acta Oceanol. Sin.*, 2022, Vol. 41, No. 12, P. 18–26
https://doi.org/10.1007/s13131-022-2066-5
http://www.aosocean.com
E-mail: ocean2@hyxb.org.cn

# Sea level rise along China coast in the last 60 years

Hui Wang[1], Wenshan Li[1], Wenxi Xiang[1]*

[1] National Marine Data and Information Service, Tianjin 300171, China

Received 20 April 2022; accepted 1 May 2022



**Abstract**

Based on long-term tide gauge observations in the last 60 years, the temporal and spatial variation characteristics of sea level change along the coast of China are analyzed. The results indicate that the sea level along the coast of China has been rising at an increasing rate, with an estimated acceleration of 0.07 mm/a$^2$. The rise rates were 2.4 mm/a, 3.4 mm/a and 3.9 mm/a during 1960–2020, 1980–2020 and 1993–2020, respectively. In the last 40 years, the coastal sea level has risen fastest in the South China Sea and slowest in the Yellow Sea. Seasonal sea levels all show an upward trend but rise faster in winter and spring and slower in autumn. Sea level change along the coast of China has significant periodic oscillations of quasi-2 a, 4 a, 7 a, 11 a, quasi-19 a and 30–50 a, among which the 2–3 a, 11 a, and 30–50 a signals are most remarkable, and the amplitude is approximately 1–2 cm. The coastal sea level in the most recent decade reached its highest value in the last 60 years. The decadal sea level from 2010 to 2019 was approximately 133 mm higher than the average of 1960–1969. Empirical orthogonal function analysis indicates that China's coastal sea level has been changing in a north-south anti-phase pattern, with Pingtan and Fujian as the demarcation areas. This difference was especially obvious during 1980–1983, 1995–1997 and 2011–2013. The coastal sea level was the highest in 2016, and this extreme sea level event was analyzed to be related mainly to the anomalous wind field and ENSO.

**Key words:** sea level, long-term change, tide gauge records, spatial and temporal variability

**Citation:** Wang Hui, Li Wenshan, Xiang Wenxi. 2022. Sea level rise along China coast in the last 60 years. Acta Oceanologica Sinica, 41(12): 18–26, doi: 10.1007/s13131-022-2066-5

## 1 Introduction

Affected by anthropogenic activities and natural factors, the world is experiencing changes characterized by warming over the past 100 years (WMO, 2019; Cook et al., 2016; IPCC, 2014). Ocean warming and thermal expansion, mass loss from ice sheets and glaciers, and terrestrial water storage fluxes have led to continuous global sea level rise (IPCC, 2014, 2019). Proxy and instrumental sea level data indicate a transition in the late 19th century to the early 20th century from a relatively slow rise over the previous two millennia to a faster rise rate. The rise rate of the global mean sea level (GMSL) was 1.7 mm/a during 1901–2010, 2.0 mm/a during 1971–2010, and 3.2 mm/a during 1993–2010 (IPCC, 2014). From 1993 to 2019, the rise rate of the GMSL was (3.24±0.3) mm/a. In 2019, the GMSL continued to rise, reaching its highest since the beginning of the high-precision altimetry record (WMO, 2020).

In step with the GMSL, China's coastal sea level has continued to be high in recent years. During 1993–2019, the sea level rise rate along the coast of China was 3.9 mm/a, higher than the global mean (MNR, 2020; WMO, 2020). Moreover, the frequency of seasonal to annual sea level anomalies and the extreme sea level have all increased significantly. Sea level rise along the coast of China is mainly contributed by global sea level rise, regional hydrogeological and meteorological changes (Cai, 2010; Gao et al., 2016; Gregory et al., 2001; Ablain et al., 2017; Willis et al., 2008), and vertical land movement in coastal areas (Liu et al., 2015). Many previous studies have focused on determining global mean geocentric rates of change (also referred to as "absolute" changes), and to date, most coastal risk assessments have been undertaken using global-average projections of geocentric sea level rise (SLR). However, from a coastal management and planning perspective, regional or local relative sea level changes (i.e., changes relative to the level of the land) are important (Wahl et al., 2013; Nicholls et al., 2011; Nicholls and Cazenave, 2010). Additionally, the occurrence of ENSO will affect the activities of the East Asian monsoon through processes such as atmospheric teleconnection (Cai and Su, 2018), thus affecting sea level changes along the coast of China. China has a continental coastline of over 18 000 km with a dense economy and population (Zhang and Ouyang, 2019) as well as spatially diverse marine climate change features (Fan and Li, 2006). The accelerated rise in coastal sea level and extreme sea level events may have major impacts on the social and natural ecological environment in Chinese coastal areas, resulting in tidal flat loss, lowland inundation and ecological environment damage, as well as disasters such as storm surges and floods in coastal cities (Gregory et al., 2001; Hamilton, 2005; Fan and Li, 2006; McGranahan et al., 2007; Cai et al., 2009; Arnell and Lloyd-Hughes, 2014; Le Cozannet et al., 2014; Gao et al., 2014; Zhao et al., 2014; Fang et al., 2017; Liu et al., 2019; Li et al., 2019). Coastal communities are increasingly aware of the threats and serious challenges of sea level rise and the importance and urgency of taking common measures to reduce and prevent climate risks (Addo, 2013; Barbier, 2015; Cui et al., 2015; Hereher, 2015; Gutiérrez et al., 2016).

In recent years, several studies have been conducted focusing on coastal sea level changes in the China seas (Qu et al., 2019; Chen et al., 2018; Cheng et al., 2016). However, due to the limited tide gauge data and the discontinuous, limited up-to-date and

*Corresponding author, E-mail: xwx@nmdis.org.cn

*Acta Oceanol. Sin.*, 2021, Vol. 40, No. 6, P. 1–15
https://doi.org/10.1007/s13131-021-1846-7
http://www.aosocean.com
E-mail: ocean2@hyxb.org.cn

# Using triple oxygen isotopes and oxygen-argon ratio to quantify ecosystem production in the mixed layer of northern South China Sea slope region

Zhuoyi Zhu[1, 2*], Jun Wang[3], Guiling Zhang[4, 5], Sumei Liu[4, 5], Shan Zheng[6], Xiaoxia Sun[6], Dongfeng Xu[3], Meng Zhou[1]

[1] School of Oceanography, Shanghai Jiao Tong University, Shanghai 200030, China

[2] State Key Laboratory of Estuarine and Coastal Research, East China Normal University, Shanghai 200241, China

[3] State Key Laboratory of Satellite Ocean Environment Dynamics, Second Institute of Oceanography, Ministry of Natural Resources, Hangzhou 310012, China

[4] Key Laboratory of Marine Chemistry Theory and Technology of Ministry of Education, Ocean University of China, Qingdao 266100, China

[5] Laboratory for Marine Ecology and Environmental Science, Pilot National Laboratory for Marine Science and Technology (Qingdao), Qingdao 266237, China

[6] Jiaozhou Bay National Marine Ecosystem Research Station, Institute of Oceanology, Chinese Academy of Sciences, Qingdao 266071, China

Received 4 November 2020; accepted 19 February 2021



**Abstract**

Quantifying the gross and net production is an essential component of carbon cycling and marine ecosystem studies. Triple oxygen isotope measurements and the $O_2$/Ar ratio are powerful indices in quantifying the gross primary production and net community production of the mixed layer zone, respectively. Although there is a substantial advantage in refining the gas exchange term and water column vertical mixing calibration, application of mixed layer depth history to the gas exchange term and its contribution to reducing indices error are unclear. Therefore, two cruises were conducted in the slope regions of the northern South China Sea in October 2014 (autumn) and June 2015 (spring). Discrete water samples at Station L07 in the upper 150 m depth were collected for the determination of $\delta^{17}O$, $\delta^{18}O$, and the $O_2$/Ar ratio of dissolved gases. Gross oxygen production (GOP) was estimated using the triple oxygen isotopes of the dissolved $O_2$, and net oxygen production (NOP) was calculated using $O_2$/Ar ratio and $O_2$ concentration. The vertical mixing effect in NOP was calibrated via a $N_2O$ based approach. GOP for autumn and spring was (169±23) mmol/(m$^2$·d) (by $O_2$) and (189±26) mmol/(m$^2$·d) (by $O_2$), respectively. While NOP was 1.5 mmol/(m$^2$·d) (by $O_2$) in autumn and 8.2 mmol/(m$^2$·d) (by $O_2$) in spring. Application of mixed layer depth history in the gas flux parametrization reduced up to 9.5% error in the GOP and NOP estimations. A comparison with an independent $O_2$ budget calculation in the diel observation indicated a 26% overestimation in the current GOP, likely due to the vertical mixing effect. Both GOP and NOP in June were higher than those in October. Potential explanations for this include the occurrence of an eddy process in June, which may have exerted a submesoscale upwelling at the sampling station, and also the markedly higher terrestrial impact in June.

**Key words:** gross primary production, net community production, triple oxygen isotopes, $O_2$/Ar, air-sea gas flux, piston velocity

**Citation:** Zhu Zhuoyi, Wang Jun, Zhang Guiling, Liu Sumei, Zheng Shan, Sun Xiaoxia, Xu Dongfeng, Zhou Meng. 2021. Using triple oxygen isotopes and oxygen-argon ratio to quantify ecosystem production in the mixed layer of northern South China Sea slope region. Acta Oceanologica Sinica, 40(6): 1–15, doi: 10.1007/s13131-021-1846-7

## 1 Introduction

Production and respiration are fundamental processes in marine ecology and carbon cycling. Marginal seas occupy less than one fifth of the surface area of the world's ocean, but they play a role equally important to that of the deep sea in terms of both production and carbon cycles (Walsh, 1991). Therefore, production and respiration in marginal seas are key research priorities in both marine ecology and carbon cycling studies.

In addition to widely used $^{14}C$ incubations, $O_2$ based methods provide parallel indices for quantifying marine production (Bender et al., 1987). This is because $O_2$ gas, together with organic C, is produced during photosynthesis, hence determination of $O_2$ gas in principle quantifies the production rates and such rates can be converted into C currency via the carbon-oxygen quotient

Foundation item: The National Key Research and Development Programs of China of the Ministry of Science and Technology under contract Nos 2020YFA0608301 and 2014CB441503; the National Natural Science Foundation of China under contract Nos 41976042 and 41776122; the Fundamental Research Funds for the Central Universities; the Taishan Scholars Program of Shandong Province, China.

*Corresponding author, E-mail: zhu.zhuoyi@sjtu.edu.cn

*Acta Oceanol. Sin.*, 2021, Vol. 40, No. 8, P. 1–13
https://doi.org/10.1007/s13131-021-1804-4
http://www.aosocean.com
E-mail: ocean2@hyxb.org.cn

# Spatial distribution and behavior of dissolved selenium speciation in the South China Sea and Malacca Straits during spring inter-monsoon period

Wanwan Cao[1]*, Yan Chang[1], Shan Jiang[1], Jian Li[2], Zhenqiu Zhang[2], Jie Jin[1], Jianguo Qu[1], Guosen Zhang[1], Jing Zhang[1, 3]

[1] State Key Laboratory of Estuarine and Coastal Research (East China Normal University), Shanghai 200241, China

[2] State Key Laboratory of Tropical Oceanography, South China Sea Institute of Oceanology, Chinese Academy of Sciences, Guangzhou 510301, China

[3] School of Oceanography, Shanghai Jiao Tong University, Shanghai 200030, China

Received 11 August 2020; accepted 25 November 2020



**Abstract**

Selenium (Se) has been recognized as a key trace element that is associated with growth of primary producers in oceans. During March and May 2018, surface water (67 samples) was collected and measured by HG-ICP-MS to investigate the distribution and behavior of selenite [Se(IV)], selenate [Se(VI)] and dissolved organic selenides (DOSe) concentrations in the Zhujiang River Estuary (ZRE), South China Sea (SCS) and Malacca Straits (MS). It showed that Se(IV) (0.14–3.44 nmol/L) was the dominant chemical species in the ZRE, related to intensive manufacture in the watershed; while the major species shifted to DOSe (0.05–0.79 nmol/L) in the MS, associated with the wide coverage of peatland and intensive agriculture activities in the Malaysian Peninsula. The SCS was identified as the northern and southern sections (NSCS and SSCS) based on the variations of surface circulation. The insignificant variation of Se(IV) in the NSCS and SSCS was obtained in March, potentially resulting from the high chemical activity and related preferential assimilation by phytoplankton communities. Contrastively, the lower DOSe concentrations in the SSCS likely resulted from higher primary production and utilization during March. During May, the concentration of Se(IV) remained low in the NSCS and SSCS, while DOSe concentrations increased notably in the SSCS, likely due to the impact of terrestrial inputs from surface current reversal and subsequent accumulation. On a global scale, DOSe is the dominant Se species in tropical oceans, while Se(IV) and Se(VI) are major fractions in high-latitude oceans, resulting from changes in predominated phytoplankton and related biological assimilation.

**Key words:** Selenium, speciation, spatial variability, monsoon, South China Sea, Malacca Straits

**Citation:** Cao Wanwan, Chang Yan, Jiang Shan, Li Jian, Zhang Zhenqiu, Jin Jie, Qu Jianguo, Zhang Guosen, Zhang Jing. 2021. Spatial distribution and behavior of dissolved selenium speciation in the South China Sea and Malacca Straits during spring inter-monsoon period. Acta Oceanologica Sinica, 40(8): 1–13, doi: 10.1007/s13131-021-1804-4

## 1 Introduction

Selenium (Se) is a vital trace nutrient for the growth of many marine biota, especially primary producers (Araie and Shiraiwa, 2016) due to biological requirement in synthetize of seleno-proteins (Böck et al., 1991; Baines and Fisher, 2001) and cell division (Araie and Shiraiwa, 2016). Selenium limitation can frequently decrease phytoplankton biomass and subsequently constrain the carbon sequestration capability (Wake et al., 2012). Thus, the investigation of Se species is essential for primary production estimation and global carbon cycle (Cutter, 2005; Wake et al., 2012).

Dissolved Se in oceans is defined as dissolved organic selenides (DOSe) and dissolved inorganic Se (DISe, including Se(VI) and Se(IV)) (Fig. 1). Se(IV) and Se(VI) perform a nutrient-like profile from surface ocean to seabed, while DOSe preforms an enrichment in surface and decreases in concentration with depth (Cutter and Cutter, 2001, 1998; Measures et al., 1983; Wambaugh, 2017). Such distribution are the results of intense biological process in euphotic surface layer and multiple regeneration in the deep water (Cutter and Bruland, 1984). Upwelling can introduce Se(IV) and Se(VI) from deep water to surface water (Cutter and Cutter, 1995, 2001; Cutter and Bruland, 1984; Measures et al., 1983; Wambaugh, 2017). Atmosphere deposition and surface loading are frequently assumed to be the major pathway for the transport of terrestrial Se into oceans (Chang et al., 2016; Ibrahim and Al-Farawati, 2017). Se concentrations in surface water are also related with environmental factors in watersheds, e.g. soil composition, temperature and erosion rate (Chang et al., 2020). In addition, anthropogenic activities, such as domestic sewage discharge and petrochemical industry, also deeply influence the land-ocean Se transport process (Duan et al., 2010). Both Se(VI) and Se(IV) can be assimilated by many primary producers, especially with a preference of Se(IV). DOSe inventory in marine systems is under a dynamic balance. On the one hand, decomposition of phytoplankton releases DOSe into the ambient water

Foundation item: The National Natural Science Foundation of China under contract Nos 41876071, 41476065 and 41806096; the Biogeochemical Cycle and Biodiversity Regulation Function of Biogenic Elements in the Indo-Pacific Confluence Area under contract No. 42090043.

*Corresponding author, E-mail: wwcaostu@163.com

*Acta Oceanol. Sin.*, 2021, Vol. 40, No. 9, P. 13–22
https://doi.org/10.1007/s13131-021-1862-7
http://www.aosocean.com
E-mail: ocean2@hyxb.org.cn

# Estimating submarine groundwater discharge at a subtropical river estuary along the Beibu Gulf, China

Xilong Wang[1, 3], Kaijun Su[2], Juan Du[4, 5], Linwei Li[4], Yanling Lao[1, 6*], Guizhen Ning[1], Li Bin[1]

[1] Guangxi Key Laboratory of Marine Disaster in the Beibu Gulf, Beibu Gulf University, Qinzhou 535011, China

[2] Institute of Radiation Medicine, Chinese Academy of Medical Sciences and Peking Union Medical College, Tianjin 300192, China

[3] Key Laboratory of Coastal Science and Engineering, Beibu Gulf University, Qinzhou 535011, China

[4] State Key Laboratory of Estuarine and Coastal Research, East China Normal University, Shanghai 200241, China

[5] Research Centre for Eco-Environmental Engineering, Dongguan University of Technology, Dongguan 523808, China

[6] Qinzhou Key Laboratory of Land Resources Use and Monitor, Beibu Gulf University, Qinzhou 535011, China

Received 31 March 2021; accepted 2 June 2021



**Abstract**

In certain regions, submarine groundwater discharge (SGD) into the ocean plays a significant role in coastal material fluxes and their biogeochemical cycle; therefore, the impact of SGD on the ecosystem cannot be ignored. In this study, SGD was estimated using naturally occurring radium isotopes ($^{223}$Ra and $^{224}$Ra) in a subtropical estuary along the Beibu Gulf, China. The results showed that the Ra activities of submarine groundwater were approximately 10 times higher than those of surface water. By assuming a steady state and using an Ra mass balance model, the SGD flux in May 2018 was estimated to be $5.98\times10^6$ m$^3$/d and $3.60\times10^6$ m$^3$/d based on $^{224}$Ra and $^{223}$Ra, respectively. At the same time, the activities of Ra isotopes fluctuated within a tidal cycle; that is, a lower activity was observed at high tide and a higher activity was seen at low tide. Based on these variations, the average tidal pumping fluxes of SGD were $1.15\times10^6$ m$^3$/d and $2.44\times10^6$ m$^3$/d with $^{224}$Ra and $^{223}$Ra, respectively. Tidal-driven SGD accounts for 24%–51% of the total SGD. Therefore, tidal pumping is an important driving force of the SGD in the Dafengjiang River (DFJR) Estuary. Furthermore, the SGD of the DFJR Estuary in the coastal zone contributes significantly to the seawater composition of the Beibu Gulf and the material exchange between land and sea.

**Key words:** radium isotopes, submarine groundwater discharge, balance model, tidal pumping, Dafengjiang River Estuary

**Citation:** Wang Xilong, Su Kaijun, Du Juan, Li Linwei, Lao Yanling, Ning Guizhen, Bin Li. 2021. Estimating submarine groundwater discharge at a subtropical river estuary along the Beibu Gulf, China. Acta Oceanologica Sinica, 40(9): 13–22, doi: 10.1007/s13131-021-1862-7

## 1 Introduction

One of the main manifestations of human activities in coastal ecosystems is the land-ocean interaction process. Among these interactions, submarine groundwater discharge (SGD) is an important but often overlooked process, which has been prominent in the global water cycles. Since many ingredients exhibit higher concentrations, such as nitrate, in groundwater than in seawater, SGD can be regarded as an important carrier of nutrients and other substances along coastal areas. At the same time, SGD-driven materials can change the composition and structure of offshore substances so as to change the traditional pattern of the biogeochemical cycles of coastal waters (Johannes, 1980; Maher et al., 2013; Kwon et al., 2014; Chen et al., 2020, Zhao et al., 2021).

SGD includes all flow of water on continental margins from the seabed to the coastal ocean, which contains both the fresh groundwater discharge and the recirculated seawater discharge (Burnett et al., 2003). Because of its underground and non-intuitive characteristics, it is generally difficult to directly measure. For instance, the physical measurement data can only partially reflect the SGD, and hydrogeological models require detailed hydrogeological analysis and reliable parameters. However, geochemical tracers have proven to be an effective method for SGD estimation and require relatively minimal effort; among these tracers, the radium (Ra) isotope is considered to be one of the most efficient ways (Beck et al., 2007; Colbert and Hammond, 2008; Moore et al., 2011; Zhang et al., 2020). There are four naturally occurring Ra isotopes, $^{223}$Ra ($T_{1/2}$=11.4 d), $^{224}$Ra ($T_{1/2}$=3.6 d), $^{226}$Ra ($T_{1/2}$=1 600 a), and $^{228}$Ra ($T_{1/2}$=5.75 a). Because of the large variation in the rates of their generation and decay, these four isotopes can be used to study the biogeochemical processes at different time scales.

The Beibu Gulf is considered to be the last clean sea area in China, and its marine environment is healthier than that of other coastal areas (Guo, 2020). However, owing to the rapid develop-

Foundation item: The National Natural Science Foundation of China under contract No. 41906150; the Natural Science Foundation of Guangxi under contract No. 2018GXNSFBA281051; the Science and Technology Plan Projects of Guangxi Province under contract Nos Gui Science AD19245147 and Gui Science AB18126098; the Research Fund of Guangxi Education Department under contract No. 2018KY0616; the Research Startup Fund of Beibu Gulf University under contract No. 2018KYQD09.
*Corresponding author, E-mail: xuanfeng698547@126.com

*Acta Oceanol. Sin.*, 2022, Vol. 41, No. 1, P. 30–38
https://doi.org/10.1007/s13131-021-1812-4
http://www.aosocean.com
E-mail: ocean2@hyxb.org.cn

# Improved method for measuring the $\delta^{15}N$ compound-specific amino acids: Application on mesopelagic fishes in the South China Sea

Fuqiang Wang[1, 2, 3], Ying Wu[1]*, Lin Zhang[3], Jie Jin[1], Zuozhi Chen[4, 5], Jun Zhang[4, 5], Wing-man Lee[3]

[1] State Key Laboratory of Estuarine and Coastal Research, East China Normal University, Shanghai 200241, China

[2] Center for Blue Life, Pilot National Laboratory for Marine Science and Technology (Qingdao), Qingdao 266237, China

[3] Department of Physical and Environmental Science, Texas A&M University-Corpus Christi, Texa 78412, USA

[4] Key Field Scientific Experimental Station of South China Sea Fishery Resource and Environment, Ministry of Agriculture and Rural Affairs, Guangzhou 510300, China

[5] South China Sea Fisheries Research Institute, Chinese Academy of Fishery Sciences, Guangzhou 510300, China

Received 14 October 2020; accepted 19 January 2021



**Abstract**

Compound-specific stable isotope analysis of individual amino acids (CSIA-AA) has been widely used in ecological and biogeochemical studies. It has been proven to be powerful in tracing the diet sources and trophic interactions. However, assessing the N sources of mesopelagic fishes has been inconclusive because the mesopelagic fishes' unique domain (water depth ranged from 0 to 1 000 m) and unresolved nitrogen isotopes of various forms. This study proposes a new method for coupling instruments (ion chromatography and Precon-IRMS) and chemical method of oxidation-reduction of amino acids, and also combined $\delta^{15}N$ of AAs with $\delta^{13}C$ of fatty acids (FAs) to analyze the trophic interactions of mesopelagic fishes in the South China Sea (SCS). AAs were isolated by ion chromatography with high peak resolution and collected by an automated fraction collector. The chemical method then converted the AAs into $N_2O$ with a robust oxidation yields and suitable molar ratio of $NH_2OH$ to $NO_2^-$. Finally, the $\delta^{15}N$ of AAs at 20 nmol were measured with a reasonable precision (<0.6‰). With this method, this study report the first batch high precision $\delta^{15}N$ of AAs and $\delta^{13}C$ of FAs of mesopelagic fishes collected from SCS. *Diaphus luetkeni*, *Chauliodus minimus* and *Bathygadus antrodes* showed similar $\delta^{13}C$ values of 20:4n-6 (~ −28‰), while *Argyropelecus affinis* and *Stomias* had similar values (~ −32‰). These results reflect that mesopelagic fishes had complex diet sources. An increase of 4‰ in $\delta^{15}N$ of glutamic acid (Glu) was found between piscivorous and planktivorous fishes, which might suggest a trophic discrimination factor of mesopelagic fishes in the SCS. This study used $\delta^{13}C$ of 20:4n-6 to reveal the diet sources of mesopelagic fishes and $\delta^{15}N$ of Glu to clarify trophic level between piscivorous and planktivorous fishes. Thus, this combinative method could therefore ultimately be applied in a variety of deep-sea ecosystem.

**Key words:** $\delta^{13}C$ of fatty acids, $\delta^{15}N$ of amino acids, ion chromatography, mesopelagic fishes, Precon-IRMS

**Citation:** Wang Fuqiang, Wu Ying, Zhang Lin, Jin Jie, Chen Zuozhi, Zhang Jun, Lee Wing-man. 2022. Improved method for measuring the $\delta^{15}N$ compound-specific amino acids: Application on mesopelagic fishes in the South China Sea. Acta Oceanologica Sinica, 41(1): 30–38, doi: 10.1007/s13131-021-1812-4

## 1 Introduction

Compound-specific stable isotope analysis of individual amino acids (CSIA-AA) has become an important tool for resolving questions regarding source, transformation, and biogeochemical cycling of nitrogen (Arthur et al., 2014; McCarthy et al., 2013; McClelland and Montoya, 2002; Sherwood et al., 2011, 2014), with applications extending from archeology (Broek et al., 2013; Sherwood et al., 2014; Styring et al., 2010) to trophic ecology (Chikaraishi et al., 2009; Hetherington et al., 2017). The $\delta^{15}N$ of amino acids (AAs) in particular has emerged as a powerful new proxy of food web study. Because the AAs can be separated into two specific groups for undergoing different $\delta^{15}N$ fractionation with trophic transfer. One group of AAs maintains relatively unchanged $\delta^{15}N$ values along the trophic transfer (termed as "source" AAs), whereas the second group undergoes predictable isotope fractionation (termed as "trophic" AAs) (Chikaraishi et al., 2009; Popp et al., 2007). Within these two groups, the "trophic" AAs have been used to indicate the extent of trophic transfer, and the "source" AAs have provided the original $\delta^{15}N$ values of primary production (McMahon and McCarthy, 2016). Therefore, measuring $\delta^{15}N$ values of "source" and "trophic" AAs together overcomes a basic problem in the interpretation of bulk $\delta^{15}N$ data, because this approach requires no assumptions about baseline $\delta^{15}N$ values. Thus, CSIA-AA typically revealed more de-

Foundation item: The National Basic Research Program (973 Program) of China under contract No. 2014CB441502; the National Natural Science Foundation of China under contract No. 41876074; the Cross-research Center Project by QNLM under contract No. JCZX202007.

*Corresponding author, E-mail: wuying@sklec.ecnu.edu.cn

*Acta Oceanol. Sin.*, 2021, Vol. 40, No. 7, P. 183–197
https://doi.org/10.1007/s13131-021-1721-6
http://www.aosocean.com
E-mail: ocean2@hyxb.org.cn

# Multi-beam and seismic investigations of the active Haima cold seeps, northwestern South China Sea

Bin Liu[1], Jiangxin Chen[2, 3]*, Li Yang[1], Minliang Duan[2, 4], Shengxuan Liu[1], Yongxian Guan[1], Pengcheng Shu[4]

[1] Key Laboratory of Marine Mineral Resources, Guangzhou Marine Geological Survey, Ministry of Natural Resources, Guangzhou 510760, China

[2] Key Laboratory of Gas Hydrate, Qingdao Institute of Marine Geology, Ministry of Natural Resources, Qingdao 266071, China

[3] Laboratory for Marine Mineral Resources, Pilot National Laboratory for Marine Science and Technology (Qingdao), Qingdao 266071, China

[4] Key Laboratory of Submarine Geosciences and Prospecting Techniques of Ministry of Education, Ocean University of China, Qingdao 266100, China

Received 10 October 2020; accepted 11 December 2020



**Abstract**

To confirm the seabed fluid flow at the Haima cold seeps, an integrated study of multi-beam and seismic data reveals the morphology and fate of four bubble plumes and investigates the detailed subsurface structure of the active seepage area. The shapes of bubble plumes are not constant and influenced by the northeastward bottom currents, but the water depth where these bubble plumes disappear (630–650 m below the sea level) (mbsl) is very close to the upper limit of the gas hydrate stability zone in the water column (620 m below the sea level), as calculated from the CTD data within the study area, supporting the "hydrate skin" hypothesis. Gas chimneys directly below the bottom simulating reflectors, found at most sites, are speculated as essential pathways for both thermogenic gas and biogenic gas migrating from deep formations to the gas hydrate stability zone. The fracture network on the top of the basement uplift may be heavily gas-charged, which accounts for the chimney with several kilometers in diameter (beneath Plumes B and C). The much smaller gas chimney (beneath Plume D) may stem from gas saturated localized strong permeability zone. High-resolution seismic profiles reveal pipe-like structures, characterized by stacked localized amplitude anomalies, just beneath all the plumes, which act as the fluid conduits conveying gas from the gas hydrate-bearing sediments to the seafloor, feeding the gas plumes. The differences between these pipe-like structures indicate the dynamic process of gas seepage, which may be controlled by the build-up and dissipation of pore pressure. The 3D seismic data show high saturated gas hydrates with high RMS amplitude tend to cluster on the periphery of the gas chimney. Understanding the fluid migration and hydrate accumulation pattern of the Haima cold seeps can aid in the further exploration and study on the dynamic gas hydrate system in the South China Sea.

**Key words:** fluid escape, cold seep, natural gas hydrate, bubble plume, Qiongdongnan Basin, South China Sea

**Citation:** Liu Bin, Chen Jiangxin, Yang Li, Duan Minliang, Liu Shengxuan, Guan Yongxian, Shu Pengcheng. 2021. Multi-beam and seismic investigations of the active Haima cold seeps, northwestern South China Sea. Acta Oceanologica Sinica, 40(7): 183–197, doi: 10.1007/s13131-021-1721-6

## 1 Introduction

Cold seeps are areas where gases and fluids leak into the ocean water column from the seafloor sediments (Judd and Hovland, 2007; Foucher et al., 2009). The word "cold" is used to distinguish them from the hydrothermal vents. Unlike hydrothermal vents that mostly occur near the ocean ridges where a new crust is formed or derived from magmatism in the sedimentary basins, cold seeps are widespread globally (Judd and Hovland, 2007). Cold seeps have attracted considerable attention because of their potential role in the global methane budget (Judd, 2003; Etiope, 2012) and their association with natural gas hydrates and seafloor ecosystems (Foucher et al., 2009; Suess, 2014).

The cold seeps can be verified by the presence of gas bubble plumes that can be detected using high-frequency acoustic methods. Gas bubble plumes often manifest themselves as gas flares in acoustic images that have been observed in most of the oceans around the world, such as the Hydrate Ridge (Bangs et al., 2011), Barbados (Barnard et al., 2015), Costa Rica (Crutchley et al., 2014), Hikurangi margin (Klaucke et al., 2010), Gulf of Mexico (Solomon et al., 2009), Mediterranean (Prinzhofer and Deville, 2013), Black Sea (Greinert et al., 2006), U.S. Atlantic margin (Brothers et al., 2013, 2014; Skarke et al., 2014), sub-Antarctic island (Römer et al., 2014) and the Svalbard continental margin (Westbrook et al., 2009).

Foundation item: The Shandong Province "Taishan Scholar" Construction Project; the fund of the Laboratory for Marine Mineral Resources, Pilot National Laboratory for Marine Science and Technology (Qingdao) under contract No. MMRKF201810; the National Natural Science Foundation of China under contract No. 41606077; the National Key R&D Program of China under contract No. 2018YFC0310000.

*Corresponding author, E-mail: jiangxin_chen@sina.com

*Acta Oceanol. Sin.*, 2021, Vol. 40, No. 8, P. 78–88
https://doi.org/10.1007/s13131-021-1803-5
http://www.aosocean.com
E-mail: ocean2@hyxb.org.cn

# The influence of coupling mode of methane leakage and debris input on anaerobic oxidation of methane

Rui Xie[1, 2, 3], Daidai Wu[1, 3, 4*], Jie Liu[1], Guangrong Jin[1], Tiantian Sun[1], Lihua Liu[1], Nengyou Wu[4, 5]

[1] Key Laboratory of Gas Hydrate, Guangzhou Institute of Energy Conversion, Chinese Academy of Sciences, Guangzhou 510640, China

[2] Guangzhou Marine Geological Survey, China Geological Survey, Ministry of Natural Resources, Guangzhou 510075, China

[3] Institution of South China Sea Ecology and Environmental Engineering, Chinese Academy of Sciences, Guangzhou 510301, China

[4] Evaluation and Detection Technology Laboratory of Marine Mineral Resources, Pilot National Laboratory for Marine Science and Technology (Qingdao), Qingdao 266237, China

[5] Key laboratory of Gas Hydrate, Ministry of Natural Resources, Qingdao 266071, China

Received 6 July 2020; accepted 9 December 2020



**Abstract**

Anaerobic oxidation of methane (AOM) is an important biogeochemical process, which has important scientific significance for global climate change and atmospheric evolution. This research examined the $\delta^{34}S$, terrigenous clastic indices of $TiO_2$ and $Al_2O_3$, and times for formation of the Ba front at site SH1, site SH3 and site 973-4 in the South China Sea. Three different coupling mechanisms of deposition rate and methane flux were discovered. The different coupling mechanisms had different effects on the role of AOM. At site 973-4, a high deposition rate caused a rapid vertical downward migration of the sulphate–methane transition zone (SMTZ), and the higher input resulted in mineral dissolution. At site SH3, the deposition rate and methane flux were basically in balance, so the SMTZ and paleo-SMTZ were the most stable of any site, and these were in a slow process of migration. At site SH1, the methane flux dominated the coupled mode, so the movement of the SMTZ at site SH1 was consistent with the general understanding. Understanding the factors influencing the SMTZ is important for understanding the early diagenesis process.

**Key words:** methane seep, terrestrial detrital material, anaerobic oxidation of methane, gas hydrate

**Citation:** Xie Rui, Wu Daidai, Liu Jie, Jin Guangrong, Sun Tiantian, Liu Lihua, Wu Nengyou. 2021. The influence of coupling mode of methane leakage and debris input on anaerobic oxidation of methane. Acta Oceanologica Sinica, 40(8): 78–88, doi: 10.1007/s13131-021-1803-5

## 1 Introduction

Methane is an important greenhouse gas in the atmosphere, and its greenhouse effect is 25 times that of $CO_2$. The concentration of methane in the atmosphere has increased by 150% since 1975 and continues to grow at a rate of 1.0%–1.2% per year (Kotelnikova, 2002). The ocean is the largest methane reservoir on the planet. It is estimated that about 5 000 Gt (according to carbon) of methane is contained in oceanic anaerobic sediments. Most of this methane (3 000 Gt (according to carbon)) is consolidated in hydrates, but 2 000 Gt (according to carbon) is stored as free gas (Dong et al, 2019). Although there is a large amount of methane in the ocean, the ocean contributes only 2% to the methane in the atmosphere. In 1992, the Intergovernmental Panel on Climate Change (IPCC) pointed out that the actual amount of methane produced in marine sediments is much higher than the annual methane content released into the atmosphere by the ocean. Research has shown that the methane produced by marine sediments is almost completely consumed by anaerobic oxidation of methane (AOM) and that 90% of this methane is consumed by anaerobic microorganisms in anoxic sediments (Wankel et al, 2012; Lloyd et al, 2006).

In the South China Sea (SCS), many studies have examined the relationship between methane leakage and AOM and also the operational mechanism of AOM (Li et al, 2008; Tong et al, 2013; Feng and Chen, 2015; Zhang et al, 2017). Wu et al (2011) studied the change of sulphate and methane concentrations in the pore water and indicated that the sulphate–methane transition zone (SMTZ) in the Shenhu area is basically around 20 m depth, which is generally consistent with the internationally common SMTZ of 10–50 m, indicating moderate leaking of methane in the northern part of the SCS. Li et al, (2017) considered that the flux of methane leakage has an important influence on the SMTZ in sediment. When the methane leakage flux is large, the SMTZ in the sediment is relatively shallow; and when the methane leakage is small, the SMTZ in the sediment is relatively deep. Therefore, the depth of the SMTZ in sediment can be used as an indicator of bottom methane leakage. Meanwhile, the SMTZ is also the sedimentary interval where methane driven authigenetic carbonate

Foundation item: The Guangdong Basic and Applied Basic Research Fund Project under contract No. 2021A1515011509; the Municipal Science and Technology Program of Guangzhou under contract No. 201904010311; the Special Project for Marine Economy Development of Guangdong Province under contract No. GDME-2018D002.
*Corresponding author, E-mail: wudd@ms.giec.ac.cn

*Acta Oceanol. Sin.*, 2021, Vol. 40, No. 9, P. 33–42
https://doi.org/10.1007/s13131-021-1898-8
http://www.aosocean.com
E-mail: ocean2@hyxb.org.cn

# Tectonic unit divisions based on block tectonics theory in the South China Sea and its adjacent areas

Zhengxin Yin[1], Zhourong Cai[2, 3*], Cheng Zhang[2, 3], Xiaofeng Huang[2, 3], Qianru Huang[2, 3], Liang Chen[1, 4]

[1] South China Sea Marine Survey and Technology Center, State Oceanic Administration, Guangzhou 510275, China

[2] School of Marine Sciences, Sun Yat-sen University, Zhuhai 519082, China

[3] Southern Laboratory of Ocean Science and Engineering (Zhuhai), Zhuhai 519082, China

[4] Key Laboratory of Marine Environmental Survey Technology and Application, Ministry of Natural Resources, Guangzhou 510275, China

Received 8 January 2021; accepted 20 May 2021



**Abstract**

Identifying distinct tectonic units is key to understanding the geotectonic framework and distribution law of oil and gas resources. The South China Sea and its adjacent areas have undergone complex tectonic evolution processes, and the division of tectonic units is controversial. Guided by block tectonics theory, this study divide the South China Sea and its adjacent areas into several distinguished tectonic units relying on known boundary markers such as sutures (ophiolite belts), subduction-collision zones, orogenic belts, and deep faults. This work suggests that the study area is occupied by nine stable blocks (West Burma Block, Sibumasu Block, Lanping-Simao Block, Indochina Block, Yangtze Block, Cathaysian Block, Qiongnan Block, Nansha Block, and Northwest Sulu Block), two suture zones (Majiang suture zone and Southeast Yangtze suture zone), two accretionary zones (Sarawak-Sulu accretionary zone and East Sulawesi accretionary zone), one subduction-collision zone (Rakhine-Java-Timor subduction-collision zone), one ramp zone (Philippine islands ramp zone), and six small oceanic marginal sea basins (South China Sea Basin, Sulu Sea Basin, Sulawesi Sea Basin, Banda Sea Basin, Makassar Basin, and Andaman Sea Basin). This division reflects the tectonic activities, crustal structural properties, and evolutionary records of each evaluated tectonic unit. It is of great theoretical and practical importance to understand the tectonic framework to support the exploration of oil and gas resources in the South China Sea and its adjacent areas.

**Key words:** South China Sea, block tectonics, tectonic units, suture zone

**Citation:** Yin Zhengxin, Cai Zhourong, Zhang Cheng, Huang Xiaofeng, Huang Qianru, Chen Liang. 2021. Tectonic unit divisions based on block tectonics theory in the South China Sea and its adjacent areas. Acta Oceanologica Sinica, 40(9): 33–42, doi: 10.1007/s13131-021-1898-8

## 1 Introduction

The South China Sea and its adjacent areas have long been subjected to tectonic movements caused by interactions with the Eurasian Plate, the Philippine Sea-Pacific Plate, and the Indo-Australian Plate (Fig. 1). Influenced by different tectonic stresses, many phases of Cenozoic tectonic processes, such as tension, rupture, convergence, and collision, result in the formation of various crustal and lithospheric fragments in these areas (Yin et al., 2015; Liu et al., 2002a; Yao et al., 2012). A large number of geotectonic units and the diversity of crustal properties complicate our understanding of both the tectonic history of the South China Sea and the location of the oil and gas resources in these areas. Accurate demarcation of the different tectonics is an effective way to understand the distribution law of oil and gas resources. Previous studies have attempted to divide the different tectonic units in the South China Sea and its adjacent areas based on the theory of faulted block tectonics, plate tectonics, layered block tectonics, microblock tectonics and historical geotectonics (Zhang, 1984; Liu, 1993; Li et al., 2018, 1995a; Wu, 1998; Liu et al., 2002a, 2004a, 2018; Yao et al., 2010; Metcalfe, 2013; Yang et al., 2015; Zhang et al., 2018). These division schemes have different emphases and reflect different geotectonic perspectives within a certain historical period. However, they also have certain limitations because the tectonic unit often mixes stable zones and active zones in these schemes. It is difficult to distinguish the differences in the tectonic activities, crustal tectonic properties and evolutionary history of the region. This study utilizes a new scheme for the tectonic unit division of the South China Sea and its adjacent areas (approximate research scope: 10°S–25°N, 90°–130°E) based on block tectonic theory.

The term “block” was formerly used to describe the mass of a surface unit, such as an avalanche or a landslide. The concept of blocks or terranes was first proposed in an early study of continental tectonics (William, 1972). Zhu (1983) and Liu (1993) defined blocks as stable geotectonic units that share similar evolutionary histories. Conversely, suture zones or active zones are defined as geotectonic units that have undergone multiple tectonic movements and are typically distributed along the borders

Foundation item: The National Natural Science Foundation of China under contract Nos 41706055, 41776072, 41602092, 4106035 and 41776072; the Natural Science Foundation of Guangdong Province under contract Nos 2018A030313168 and 2018B030311030; the National Marine Geology Special Project under contract Nos DD20160147 and DD20189643.
*Corresponding author, E-mail: caizhr@mail.sysu.edu.cn

*Acta Oceanol. Sin.*, 2021, Vol. 40, No. 11, P. 162–175
https://doi.org/10.1007/s13131-021-1833-z
http://www.aosocean.com
E-mail: ocean2@hyxb.org.cn

# Tracking historical storm records from high-barrier lagoon deposits on the southeastern coast of Hainan Island, China

Liang Zhou[1, 2, 3], Xiaomei Xu[4], Yaping Wang[3], Jianjun Jia[3], Yang Yang[5], Gaocong Li[6], Changliang Tong[2], Shu Gao[2, 4*]

[1] School of Geography, Geomatics, and Planning, Jiangsu Normal University, Xuzhou 221116, China

[2] Hainan Key Laboratory of Marine Geological Resources and Environment, Haikou 570206, China

[3] State Key Laboratory of Estuarine and Coastal Research, East China Normal University, Shanghai 200046, China

[4] Ministry of Education Key Laboratory for Coast and Island Development, Nanjing University, Nanjing 210023, China

[5] School of Marine Science and Engineering, Nanjing Normal University, Nanjing 210046, China

[6] Department of Marine Technology, Guangdong Ocean University, Zhanjiang 524088, China

Received 5 February 2021; accepted 10 March 2021



**Abstract**

The relationship between storm activity and global warming remains uncertain. To better understand storm–climate relationships, coastal lagoon deposits are increasingly being investigated because they could provide high-resolution storm records long enough to cover past climate changes. However, site-specific sediment dynamics and high barriers may bias storm reconstructions. Here, we aimed to investigate these factors through the reconstruction of five distinct storm records (XCL-01, XC-03, XC-06, XC-07, XC-08) from different water depths in a lagoon with a high barrier (i.e., Xincun Lagoon of Hainan Island). Sediment cores were characterized using high-resolution grain size and XRF measurements, to identify storm events. These data were coupled with a numerical simulation to obtain bed shear stress data with high-spatial resolution to better understand storm-induced sediment transport mechanisms. $^{210}$Pb dating and Pb pollution chronostratigraphic markers indicated that the chronology of the storm deposit sequences of the cores span the period between 117 a and 348 a. The grain size and XRF results indicated numerous, highly variable and short-duration fluctuations, suggesting that storm-induced coarse-grained sediments were deposited at these core sites. The inconsistent storm events recorded in these cores suggest that these sites have different preservation potentials for storm deposits. However, the consistence between storm sediment records and historical documents for Core XCL-01 indicates that high-barrier lagoons could provide long-term storm event records with high preservation potential.

**Key words:** storm deposits, preservation potential, sediment dynamics, high-barrier lagoon, Hainan Island

**Citation:** Zhou Liang, Xu Xiaomei, Wang Yaping, Jia Jianjun, Yang Yang, Li Gaocong, Tong Changliang, Gao Shu. 2021. Tracking historical storm records from high-barrier lagoon deposits on the southeastern coast of Hainan Island, China. Acta Oceanologica Sinica, 40(11): 162–175, doi: 10.1007/s13131-021-1833-z

## 1 Introduction

Global warming is expected to increase the frequency and intensity of storm events in the future (IPCC, 2013). This issue has attracted wide social attention, because storms often trigger large waves and storm surges, which may severely affect coastal geomorphology (Wang et al., 2009; Almeida et al., 2012; Liu et al., 2019) and ecosystems (Greening et al., 2006; Zheng and Tang, 2007; Li et al., 2014; Chen et al., 2018), and may result in catastrophic losses of life and resources. However, the brevity of tide gauge records on the scale of several decades or incomplete historical records on the last centuries make the assessment of long-term trends in storm events difficult (e.g., Donnelly and Woodruff, 2007; Woodruff et al., 2009; Lane et al., 2011). Thus, the extraction of long-term storm information from sedimentary records is essential.

Previous paleostorm studies have widely been conducted in low energy environments (e.g., lagoons, lakes, and ponds). These environments, where the background sedimentation primarily by fine-grained sediments occurs, are usually protected by sand barriers (Liu and Fearn, 1993; Sabatier et al., 2008; Woodruff et al., 2009), which are very effective in trapping storm-induced coarse-grained sediments. Among them, back-barrier lagoons with low-lying barriers (top elevation lower than that of the local extreme storm surge) have been recognized as one of the most suitable environments to preserve overwash deposits of storm events, which has greatly improved the interpretation of the long-term evolution of coastal systems and the understanding of the response of intense storm activities to climatic changes (Sabatier et al., 2008; Switzer and Jones, 2008; Degeai et al., 2015; Rouina et al., 2016). Sand layers in lagoon deposits are con-

Foundation item: The National Natural Science Foundation of China under contract Nos 41706096 and 41530962; the Research Start-up Project of Jiangsu Normal University under contract No. 19XSRX006; the Opening Foundation of Hainan Key Laboratory of Marine Geological Resources and Environment under contract No. HNHYDZZYHJKF005; the High-level Talent Program of Basic and Applied Basic Research Programs (Field of Natural Science) in Hainan Province under contract No. 2019RC349; a project funded by the Priority Academic Program Development of Jiangsu Higher Education Institutions.
*Corresponding author, E-mail: sgao@sklec.ecnu.edu.cn

*Acta Oceanol. Sin.*, 2022, Vol. 41, No. 8, P. 22–30
https://doi.org/10.1007/s13131-021-1917-9
http://www.aosocean.com
E-mail: ocean2@hyxb.org.cn

# Last glacial terrestrial vegetation record of leaf wax *n*-alkanols in the northern South China Sea: Contrast to scenarios from long-chain *n*-alkanes

Shengyi Mao[1, 2], Guodong Jia[3], Xiaowei Zhu[2, 4], Nengyou Wu[5, 6], Daidai Wu[1], Hongxiang Guan[1], Lihua Liu[1*]

[1] CAS Key Laboratory of Gas Hydrate, Guangzhou Institute of Energy Conversion, Chinese Academy of Sciences, Guangzhou 510640, China

[2] Southern Marine Science and Engineering Guangdong Laboratory (Guangzhou), Guangzhou 511458, China

[3] State Key Laboratory of Marine Geology, Tongji University, Shanghai 200092, China

[4] Key Laboratory of Ocean and Marginal Sea Geology, South China Sea Institute of Oceanology, Chinese Academy of Sciences, Guangzhou 510301, China

[5] Key Laboratory of Gas Hydrate of Ministry of Natural Resources, Qingdao Institute of Marine Geology, Qingdao 266237, China

[6] Laboratory for Marine Mineral Resources, Pilot National Laboratory for Marine Science and Technology (Qingdao), Qingdao 266237, China

Received 14 January 2021; accepted 3 July 2021



**Abstract**

Long-chain *n*-alkanols and *n*-alkanes in core sediments from the northern South China Sea (SCS) were measured to make a comparison during terrestrial vegetation reconstruction from ~42 ka to ~7 ka. The results showed that terrestrial vegetation record from long-chain *n*-alkanes matched well with previous studies in nearby cores, showing that more $C_4$ plants developed during the Last Glacial Maximum (LGM) and $C_3$ plants dominated in the interglacial period. However, these scenarios were not revealed by terrestrial vegetation reconstruction using long-chain *n*-alkanols, which showed $C_3$ plant expansion during the LGM. The discrepancy during the interglacial period could be attributed to the aerobic degradation of functionalized long-chain *n*-alkanols in the oxygen-rich bottom water, resulting in poor preservation of terrestrial vegetation signals. On the other hand, the different advantages of functionalized *n*-alkanols and non-functional *n*-alkanes to record local and distal vegetation signals, respectively, may offer a potential explanation for the contradiction during the LGM when the SCS was characterized by low-oxygen deep water. Nevertheless, large variations on *n*-alkyl lipid compositions in $C_3$/$C_4$ plants could play a part in modulating sedimentary long-chain *n*-alkanols and *n*-alkanes toward different vegetation signals, thereby suggesting that caution must be taken in respect to the terrestrial vegetation reconstruction using long-chain *n*-alkanes and long-chain *n*-alkanols.

**Key words:** South China Sea, long-chain *n*-alkanols, long-chain *n*-alkanes, Last Glacial Maximum, terrestrial vegetation record

**Citation:** Mao Shengyi, Jia Guodong, Zhu Xiaowei, Wu Nengyou, Wu Daidai, Guan Hongxiang, Liu Lihua. 2022. Last glacial terrestrial vegetation record of leaf wax *n*-alkanols in the northern South China Sea: Contrast to scenarios from long-chain *n*-alkanes. Acta Oceanologica Sinica, 41(8): 22–30, doi: 10.1007/s13131-021-1917-9

## 1 Introduction

Long-chain (>$C_{24}$) *n*-alkyl compound classes, i.e., $C_{27–31}$ odd carbon-numbered *n*-alkanes and $C_{28–32}$ even carbon-numbered *n*-alkanols and *n*-fatty acids (FAs), are major components of epicuticular waxes of vascular higher plant leaves (Eglinton and Hamilton, 1967). Different photosynthetic plant types generally possess diverse chain length distributions and contain variable carbon isotopes ($\delta^{13}C$) in long-chain *n*-alkyl lipids (e.g., Diefendorf and Freimuth, 2017, and references therein). Therefore, chain length-dependent proxies such as carbon preference index (CPI) and average chain length (ACL), together with $\delta^{13}C$ compositions have been widely applied to the terrestrial, atmospheric and aquatic environments for terrestrial vegetation reconstruction (e.g., Diefendorf and Freimuth, 2017, and references therein). However, few studies were reported for the application of long-chain *n*-alkanols and/or *n*-FAs. This is surpris-

Foundation item: The Key Special Project for Introduced Talents Team of Southern Marine Science and Engineering Guangdong Laboratory (Guangzhou) under contract No. GML2019ZD0104; the Science and Technology Program of Guangzhou, China under contract No. 201804010264; the Guangdong MEPP Fund under contract No. GDOE[2019]A41; the National Natural Science Foundation of China under contract No. 41706059; the Fund of Institution of South China Sea Ecology and Environmental Engineering, Chinese Academy of Sciences under contract No. ISEE2020YB05; the State Key R&D Project under contract No. 2016YFA0601104.

*Corresponding author, E-mail: liulh@ms.giec.ac.cn

*Acta Oceanol. Sin.*, 2022, Vol. 41, No. 9, P. 86–106
https://doi.org/10.1007/s13131-022-1992-6
http://www.aosocean.com
E-mail: ocean2@hyxb.org.cn

# Distribution characteristics of delta reservoirs reshaped by bottom currents: A case study from the second member of the Yinggehai Formation in the DF1-1 gas field, Yinggehai Basin, South China Sea

Shuo Chen[1], Renhai Pu[1]*, Huiqiong Li[2], Hongjun Qu[1], Tianyu Ji[3], Siyu Su[1], Yunwen Guan[1], Hui Zhang[4]

[1] State Key Laboratory of Continental Dynamics (Northwest University), Xi'an 710069, China

[2] Research Institute of Yanchang Petroleum Group Co. Ltd., Xi'an 710065, China

[3] Research Institute of Petroleum Exploration and Development, Beijing 100083, China

[4] Research Institute of Zhanjiang Branch of China National Offshore Oil Corporation, Zhanjiang 524057, China

Received 6 May 2021; accepted 10 November 2021



**Abstract**

The Dongfang1-1 gas field (DF1-1) in the Yinggehai Basin is currently the largest offshore self-developed gas field in China and is rich in oil and gas resources. The second member of the Pliocene Yinggehai Formation (YGHF) is the main gas-producing formation and is composed of various sedimentary types; however, a clear understanding of the sedimentary types and development patterns is lacking. Here, typical lithofacies, logging facies and seismic facies types and characteristics of the YGHF are identified based on high-precision 3D seismic data combined with drilling, logging, analysis and testing data. Based on 3D seismic interpretation and attribute analysis, the origin of high-amplitude reflections is clarified, and the main types and evolution characteristics of sedimentary facies are identified. Taking gas formation upper II (IIU) as an example, the plane distribution of the delta front and bottom current channel is determined; finally, a comprehensive sedimentary model of the YGHF second member is established. This second member is a shallowly buried "bright spot" gas reservoir with weak compaction. The velocity of sandstone is slightly lower than that of mudstone, and the reflection has medium amplitude when there is no gas. The velocity of sandstone decreases considerably after gas accumulation, resulting in an increase in the wave impedance difference and high-amplitude (bright spot) reflection between sandstone and mudstone; the range of high amplitudes is consistent with that of gas-bearing traps. The distribution of gas reservoirs is obviously controlled by dome-shaped diapir structural traps, and diapir faults are channels through which natural gas from underlying Miocene source rocks can enter traps. The study area is a delta front deposit developed on a shallow sea shelf. The lithologies of the reservoir are mainly composed of very fine sand and coarse silt, and a variety of sedimentary structural types reflect a shallow sea delta environment; upward thickening funnel type, strong toothed bell type and toothed funnel type logging facies are developed. In total, 4 stages of delta front sand bodies (corresponding to progradational reflection seismic facies) derived from the Red River and Blue River in Vietnam have developed in the second member of the YGHF; these sand bodies are dated to 1.5 Ma and correspond to four gas formations. During sedimentation, many bottom current channels (corresponding to channel fill seismic facies) formed, which interacted with the superposed progradational reflections. When the provenance supply was strong in the northwest, the area was dominated by a large set of delta front deposits. In the period of relative sea level rise, surface bottom currents parallel to the coastline were dominant, and undercutting erosion was obvious, forming multistage superimposed erosion troughs. Three large bottom current channels that developed in the late sedimentary period of gas formation IIU are the most typical.

**Key words:** South China Sea, Yinggehai Basin, second member of the Yinggehai Formation, bottom current transformation, sedimentary model

**Citation:** Chen Shuo, Pu Renhai, Li Huiqiong, Qu Hongjun, Ji Tianyu, Su Siyu, Guan Yunwen, Zhang Hui. 2022. Distribution characteristics of delta reservoirs reshaped by bottom currents: A case study from the second member of the Yinggehai Formation in the DF1-1 gas field, Yinggehai Basin, South China Sea. Acta Oceanologica Sinica, 41(9): 86–106, doi: 10.1007/s13131-022-1992-6

## 1 Introduction

The Yinggehai Basin (YGHB), located in the South China Sea (SCS), is one of the world's eight offshore overpressurized basins and contains abundant natural gas resources. After more than 30 years of exploration, several commercial natural gas reservoirs and petroliferous structures have been found in the basin, including Dongfang (DF)1-1, DF29-1, DF1-13-1, and DF1-13-2 in the DF area and Ledong (LD)15-1 and LD22-1 in the Ledong area. The main gas reservoirs discovered to date are the shallow Yinggehai and Ledong formations at normal temperatures and

Foundation item: The National Natural Science Foundation of China's Major Project "Research on Geophysical Theories and Methods of Unconventional Oil and Gas Exploration and Development", Task I: "China's Tight Oil and Gas Reservoir Geological Characteristics, Classification and Typical Geological Model Establishment" under contract No. 41390451.
*Corresponding author, E-mail: purenhai@126.com

*Acta Oceanol. Sin.*, 2022, Vol. 41, No. 9, P. 107–116
https://doi.org/10.1007/s13131-022-2002-8
http://www.aosocean.com
E-mail: ocean2@hyxb.org.cn

# Mounded seismic units in the modern canyon system in the Shenhu area, northern South China Sea: Sediment deformation, depositional structures or the mixed system?

Xishuang Li[1, 2*], Chengyi Zhang[1], Baohua Liu[3], Lejun Liu[1]

[1] First Institute of Oceanography, Ministry of Natural Resources, Qingdao 266061, China

[2] Laboratory for Marine Geology, Pilot National Laboratory for Marine Science and Technology (Qingdao), Qingdao 266237, China

[3] National Deep Sea Center, Ministry of Natural Resources, Qingdao 266237, China

Received 22 November 2020; accepted 5 February 2022



**Abstract**

The canyon system, including 17 small slope-confined canyons in the Shenhu area, northern South China Sea, is significantly characterized by mounded or undulating features on the canyon flanks and canyon heads. However, the mechanism underlying the formation of these features has yet to be elucidated. In previous studies, most of them were interpreted as sediment deformation on the exploration seismic profiles. In this paper, we collected high-resolution bathymetric data, chirp profiles and geotechnical test data to investigate their detailed morphology, internal structures, and origin. The bathymetric data indicated that most mounded seismic units have smooth seafloors and are separated by grooves or depressions. The distance between two adjacent mounded units is only hundreds of meters. On chirp profiles, mounded seismic units usually exhibit chaotic reflections and wavy reflections, of which the crests migrate upslope. The slope stability analysis results revealed that the critical angle of the soil layers in the study area tends to be 9°, indicating that most mounded seismic units on the canyon flanks and heads are stable at present. The terrain characteristics and seismic configurations combined with the slope stability analysis results indicated that most mounded seismic units are not sediment deformation but depositional structures or mixed systems composed of deformation and depositional structures.

**Key words:** northern South China Sea, submarine canyons, mounded seismic units, chirp profile, slope stability

**Citation:** Li Xishuang, Zhang Chengyi, Liu Baohua, Liu Lejun. 2022. Mounded seismic units in the modern canyon system in the Shenhu area, northern South China Sea: Sediment deformation, depositional structures or the mixed system?. Acta Oceanologica Sinica, 41(9): 107–116, doi: 10.1007/s13131-022-2002-8

## 1 Introduction

As one of the intensive sediment deformations, submarine landslides are widely distributed on continental margins worldwide and strongly shape marginal landforms and contribute to slope architecture (Bøe et al., 2000; Canals et al., 2004; Klaucke and Cochonat, 1999; Vanneste et al., 2006). Submarine landslides usually include a series of erosional and depositional processes that lead to a diversity of seismic signatures from chaotic sediment depocenters to well-stratified layers (O'Leary, 1991; Carlson et al., 1991; Hampton et al., 1996; Lee and Chough, 2001; Canals et al., 2004; Haflidason et al., 2004). Therefore, in many cases, it is difficult to distinguish between landslides and depositional structures, such as sediment waves and contourite drifts (Lee et al., 2002; Rebesco et al., 2009, 2014; Ribó et al., 2016). For example, the "Humboldt slide" on the Eel River continental margin in northern California was previously considered a slide (Gardner et al., 1999) and later considered as sedimentary waves caused by bottom currents (Lee et al., 2002). The origin of the seafloor wavy structures on the Adriatic shelf (Correggiari et al., 2001) and an extensive depositional body with nearly flat lying to slightly landward-dipping reflections in the Gulf of Alaska (Lee and Baraza, 1999) were once considered large landslides.

Seventeen small slope-confined canyons developed in the Shenhu area, north of the South China Sea (SCS), and cover water depths from ~300 m to ~2 000 m. These small canyons initiated in the middle Miocene (~13.8 Ma) and are characterized by periodic erosion-filling structures inside and thalweg migration eastward during their geological evolution (Zhu et al., 2010; Gong et al., 2013; Zhou et al., 2015; Jiang et al., 2017). Another significant phenomenon is that the seafloor in the canyon system is rough and rugged (Fig. 1), with complex topographic features (i.e., scarps, mounded units, depressions and grooves (Li et al., 2016)). Previous studies on the basis of exploration seismic data suggest that the undulated seafloor is mainly attributed to landslides or sediment creeps, which often exhibit mounded seismic units (He et al., 2014; Ma et al., 2015; Qiao et al., 2015). However, Li et al. (2019) grouped seafloor undulations, mounded seismic units with layer-ed reflections, into three types and considered undulations on canyon flanks as a result of sediment creeping and those on canyon heads and bottoms as a result of turbidity currents and internal waves. It is of great significance to clarify whether mounded units are sediment deformations or depos-

Foundation item: The National Natural Science Foundation of China under contract No. 41876061; the National Key Research and Development Program under contract No. 2016YFC0301403.
*Corresponding author, E-mail: lxs@fio.org.cn

*Acta Oceanol. Sin.*, 2021, Vol. 40, No. 4, P. 116–126
https://doi.org/10.1007/s13131-021-1783-5
http://www.hyxb.org.cn
E-mail: ocean2@hyxb.org.cn

# The role of biocrusts in nitrogen cycling on the tropical reef islands, South China Sea

Lin Wang[1, 2], Si Zhang[1, 3], Jie Li[1, 3*]

[1] CAS Key Laboratory of Tropical Marine Bio-resources and Ecology, South China Sea Institute of Oceanology, Chinese Academy of Sciences, Guangzhou 510301, China

[2] University of Chinese Academy of Sciences, Beijing 100049, China

[3] Innovation Academy of South China Sea Ecology and Environmental Engineering, Chinese Academy of Sciences, Guangzhou 510301, China

Received 27 November 2019; accepted 30 June 2020



**Abstract**

Harboring polyextremotolerant microbial topsoil communities, biological soil crusts (biocrusts) occur across various climatic zones, and have been well studied in the terrestrial drylands. However, little is known about the functional metabolic potential of microbial communities involved in the biogeochemical processes during the early succession of biocrusts on the tropical reef islands. We collected 26 biocrusts and bare soil samples from the Xisha Islands and Nansha Islands, and applied a functional gene array (GeoChip 5.0) to reveal nitrogen (N) cycling processes involved in these samples. Both physicochemical measurement and enzyme activity assay were utilized to characterize the soil properties. Results revealed the composition of N-cycling functional genes in biocrusts was distinct from that in bare soil. Additionally, microorganisms in biocrusts showed lower functional potential related to ammonification, denitrification, N assimilation, nitrification, N fixation, and dissimilatory nitrate reduction to ammonium compared to bare soils. Although the abundance of *nifH* gene was lower in biocrusts, nitrogenase activity was significantly higher compared to that in bare soils. Precipitation, soil physicochemical properties (i.e., soil available copper, soil ammonia N and pH) and soil biological properties (i.e., $\beta$-glucosidase, fluorescein diacetate hydrolase, alkaline protease, urease, alkaline phosphatase, catalase and chlorophyll *a*) correlated to the N-cycling functional genes structure. Nitrate N and ammonia N were more abundant in biocrusts than bare soil, while pH value was higher in bare soil. Our results suggested biocrusts play an important role in N-cycling in coral sand soil, and will be helpful in understanding the development and ecological functions of biocrusts on tropical reef islands.

**Key words:** biocrusts, microbial functional structure, metabolic potential, nitrogen cycling, tropical reef islands

**Citation:** Wang Lin, Zhang Si, Li Jie. 2021. The role of biocrusts in nitrogen cycling on the tropical reef islands, South China Sea. Acta Oceanologica Sinica, 40(4): 116–126, doi: 10.1007/s13131-021-1783-5

## 1 Introduction

Biological soil crusts (biocrusts) are polyextremotolerant microbial topsoil communities, consisting of algae, bacteria, archaea, fungi, lichen and mosses in varying proportions that colonize the soil surface and get embedded together within a matrix of extracellular polymeric substance and soil particles to form a surface crust (Belnap et al., 2001, 2016). Biocrusts show different colors, ranging from white through green to black hues, depending on the different successional stages, reflected by the different dominating photoautotrophic organisms, including cyanobacterium-, lichen-, and moss-dominated types (Bowker et al., 2006; Büdel et al., 2009; Weber et al., 2012). As multifunctional communities, biocrusts play important ecological functions in various ecosystems that promote soil formation by increasing its nutrient and water contents (Evans and Johansen, 1999; Belnap, 2006; Pointing and Belnap, 2012), stabilize the soil and reduce soil erosion effectively by producing polysaccharides (Van Den Ancker et al., 1985; Belnap et al., 2001). These functions have a positive influence on seed germination, establishment and performance of plants, and population and behavior of animals (Evans and Johansen, 1999; Belnap et al., 2001; Lan et al., 2015; Guan et al., 2018).

Nitrogen (N) is an essential macronutrient that is initially low in the soil and a vital limiting factor that influences productivity in arid terrestrial and rangeland ecosystems (Hooper and Johnson, 1999; Vitousek et al., 2010). Thus, N supply is one of the most important factors for further development of the initial ecosystem. Diverse N input processes (biological fixation and dust capture) and direct N loss processes (dissolution, vaporisation and erosion) have been found in the biocrusts developed in arid and semiarid ecosystems (Barger et al., 2016). Biological fixation of atmospheric N is an omnipresent biogeochemical transformation in the biological soil crusts. It possibly contributes to the dominant source of N in low-nutrient environments with few symbolic vascular plant N fixers (Evans and Ehleringer, 1993; Evans and Lange, 2001). Furthermore, N fixation by biocrusts leads to N re-

Foundation item: The Strategic Priority Research Program of the Chinese Academy of Sciences under contract Nos XDA13020301 and XDA13010500; the Fund of Innovation Academy of South China Sea Ecology and Environmental Engineering, Chinese Academy of Sciences under contract No. ISEE2018PY01.

*Corresponding author, E-mail: lijietaren@scsio.ac.cn

*Acta Oceanol. Sin.*, 2022, Vol. 41, No. 3, P. 24–33
https://doi.org/10.1007/s13131-021-1925-9
http://www.aosocean.com
E-mail: ocean2@hyxb.org.cn

# Influences of fisheries management measures on biological characteristics of threadfin bream (*Nemipterus virgatus*) in the Beibu Gulf, South China Sea

Kui Zhang[1, 2, 3], Ping Geng[1], Jiajun Li[1, 2], Youwei Xu[1, 2], Muhsan Ali Kalhoro[4], Mingshuai Sun[1, 2], Dengfu Shi[1], Zuozhi Chen[1, 2, 3*]

[1] South China Sea Fisheries Research Institute, Chinese Academy of Fishery Sciences, Guangzhou 510300, China

[2] Key Laboratory for Sustainable Utilization of Open-sea Fishery, Ministry of Agriculture and Rural Affairs, Guangzhou 510300, China

[3] Southern Marine Science and Engineering Guangdong Laboratory (Guangzhou), Guangzhou 511458, China

[4] Faculty of Marine Sciences, Lasbela University of Agriculture, Water and Marine Sciences, Uthal 90150, Pakistan

Received 26 April 2021; accepted 12 May 2021



**Abstract**

Long-term variations in population structure, growth, mortality, length at median sexual maturity, and exploitation rate of threadfin bream (*Nemipterus virgatus*) are reported based on bottom trawl survey data collected during 1960–2012 in the Beibu Gulf, South China Sea. Laboratory-based analyses were conducted on 16 791 individuals collected quarterly in eight different sampling years. Average body length, estimated asymptotic length, and percentage of large individuals have decreased significantly with the growth of marine catch and fishing power, indicating individual miniaturization of this fish species. Estimated exploitation rates indicate that the *N. virgatus* stock in the Beibu Gulf was moderately exploited in 1960 and 1962 and overexploited after 1992. This stock was taking a good turn in status in 2012, with the lowest exploitation rate since 1992 and ceased downward trend in length indexes. These results suggest that management measures to reduce fishing pressure may have a positive influence on the biological characteristics of this commercial fish species. Biological characteristics of most commercial fish species have phenotypic plasticity and might change over years in response to fisheries management. Therefore, attentions should be paid on variations in fish biological characteristics, when evaluating the effectiveness of current measures to control the total catch for all fisheries.

**Key words:** growth, mortality, length at median sexual maturity, fishing pressure, phenotypic plasticity

**Citation:** Zhang Kui, Geng Ping, Li Jiajun, Xu Youwei, Kalhoro Ali Muhsan, Sun Mingshuai, Shi Dengfu, Chen Zuozhi. 2022. Influences of fisheries management measures on biological characteristics of threadfin bream (*Nemipterus virgatus*) in the Beibu Gulf, South China Sea. Acta Oceanologica Sinica, 41(3): 1–10, doi: 10.1007/s13131-021-1925-9

## 1 Introduction

Coastal fisheries provide a major source of food and livelihoods for inhabitants of coastal areas. The total catch of coastal fisheries is more than $5\times10^7$ t annually, accounting for about half of global marine landings (Palomares and Pauly, 2019). However, there are still catch shortfalls in developed or rapidly developing countries due to the growing popularity of seafood (Pauly and Zeller, 2016). The sustainability of fisheries should be based on scientific and effective management, otherwise the benefits to people and ecosystems would be severely compromised (Costello et al., 2012; Pauly et al., 2005).

The Beibu Gulf (17°–21.75°N, 105.67°–110.17°E) is a semi-closed bay in the northwestern South China Sea (SCS). This local gulf is highly productive and rich in fishery resources, benefiting from its favorable geomorphological and climatic conditions (Chen et al., 2009). As reported to date, 960 fish species inhabit in this ecosystem, which belong to 475 genera and 162 families. About 80% of these species are demersal and the rest as pelagic (Khanh et al., 2013). As one of China's four major fishing grounds, this gulf has been extensively fished for many decades. Therefore, the Beibu Gulf has been playing an important role in food security, economy, and employment (Chen et al., 2009). The main types of fishing gears used in this system include trawls, purse seines, gill nets, hooks, and set nets, and the trawl fishery usually contributes to more than 70% of the total catch (Zhang et al., 2020a). Since China's reform and opening up, the economy in coastal areas has developed rapidly and the demand for seafood has increased with fast growth in the economy of coastal areas. Rapid growth in the number of marine fishing vessels and catches from the 1970s to the 1990s (Shen and Heino, 2014) has resulted in decreasing catch rates and shifts in fish community structure from high trophic level fish species such as crimson snapper (*Lutjanus erythropterus*) and large yellow croaker (*Larimichthys crocea*) to lower trophic level species (Qiu et al., 2010). Over-exploitation

Foundation item: The National Key R&D Program of China under contract No. 2018YFD0900906; the National Natural Science Foundation of China under contract No. 31602157; the Key Special Project for Introduced Talents Team of Southern Marine Science and Engineering Guangdong Laboratory under contract No. GML2019ZD0605; the Central Public-Interest Scientific Institution Basal Research Fund under contract Nos 2020TD05 and 2021SD01.
*Corresponding author, E-mail: chenzuozhi@scsfri.ac.cn

*Acta Oceanol. Sin.*, 2022, Vol. 41, No. 3, P. 70–75
https://doi.org/10.1007/s13131-021-1928-6
http://www.aosocean.com
E-mail: ocean2@hyxb.org.cn

# The environmental adaptability and reproductive properties of invasive green alga *Codium fragile* from the Nan'ao Island, South China Sea

Lanping Ding[1, 2, 3], Xulei Wang[2], Bingxin Huang[1, 2, 3*], Weizhou Chen[2], Shanwen Chen[2]

[1] College of Life Sciences, Tianjin Normal University, Tianjin 300387, China

[2] Marine Biology Institute, Shantou University, Shantou 515063, China

[3] Tianjin Key Laboratory of Animal and Plant Resistance, Tianjin 300387, China

Received 16 February 2021; accepted 24 March 2021



**Abstract**

It has been widely recognized that biological invasion has become one of the greatest threats to the ecosystem. *Codium fragile* is an invasive species which exhibits a variety of attributes like parthenogenesis, winter fragment, and vegetative reproduction; and therefore, it has become a successful invader, colonizing most subtropical regions. In China's southeast coastal aquaculture waters, the green algal bloom caused by *C. fragile* will probably become a serious problem. In order to understand more details about the species, an experiment focused on its reproductive characteristics was conducted using culture established from a sample collected in the aquaculture raft of the Nan'ao Island in the South China Sea. The results showed that there were two types of gametes resembling aplanospores and zoospores respectively, both of which were able to germinate. During the gametes liberation, a long mucilage tube was formed out of the mouth of the gametangium assisting dispersal of gametes away from the parent plant. This tube was adapted not only to its surrounding flowing water environment but also to its parent plant's outer gelatinous structure. In general, the optimum temperature for gametes release and germination was 15–20°C and 15°C, respectively, which corresponded to the local offshore marine water. The plant was observed to produce vegetative buds under favourable reproductive conditions which were called propagules. They were capable of developing into filamentous thalli. The results will provide some scientific evidences for revealing the biological mechanism of bloom and control strategies of invasive green algae.

**Key words:** *Codium fragile*, gametes, propagules, mucilage tube, temperature, environmental adaptation

**Citation:** Ding Lanping, Wang Xulei, Huang Bingxin, Chen Weizhou, Chen Shanwen. 2022. The environmental adaptability and reproductive properties of invasive green alga *Codium fragile* from the Nan'ao Island, South China Sea. Acta Oceanologica Sinica, 41(3): 70–75, doi: 10.1007/s13131-021-1928-6

## 1 Introduction

As one of the most invasive species, now the geographical expansion of *Codium fragile,* which originated in Japan, has colonized in the northeast and northwest Atlantic coast, southern England, the Mediterranean Sea, Australia, New Zealand, and Chile (Bird et al., 1993; Carlton and Scanlon, 1985; Chapman, 1998; Churchill and Moeller, 1972; Dromgoole, 1975; Neill et al., 2006; Silva, 1955; Trowbridge, 1995). Invasive species have become widely recognized as one of the greatest threats to the ecosystem (Vitousek et al., 1997), and coastal marine eco-systems are among the most impacted aquatic systems (Grosholz, 2002; Ruiz and Hewitt, 2002).

What are the probable reasons for the invasive success of *C. fragile*? Many researchers have investigated this phenomenon. Several attributes have been proposed for potentially successful invaders of this genus: high growth rates over the summer and early fall (Malinowski and Ramus, 1973), broad physiological tolerance (Benson et al., 1983; Hanisak, 1979a; Hanisak and Harlin, 1978; Yang et al., 1997), potyphagia (Hanisak, 1979b), and minimal grazing (Trowbridge, 1995). Though seaweeds grow generally by attaching to hard substrates such as rocky shores or fouling communities, they also survive by inhabiting soft-bottom environments (Williams, 2007). All of the above attributes are beneficial for the survival of *C. fragile*.

From the perspective of vegetative propagation, the filamentous thalli of *C. fragile* could be formed from isolated utricles, medullary filaments, propagules, or parthenogenetic female gametes, as spongy thallus of *C. fragile* formed from filamentous thallus had been observed in the field (Arasaki et al., 1955; Yotsui and Migita, 1989). In the northwest Atlantic, *C. fragile* reproduces parthenogenetically, the swarmers settle, and could develop into a dichotomously branching adult thallus (Churchill and Moeller, 1972; Malinowski and Ramus, 1973). In addition, Fralick and Mathieson (1972) reported that maximum fragmentation occurred predominately in winter in New England, Scheibling and Melady (2008) provided evidence that the producing segments were capable of dispersal and reattachment to the substratum. Mature thalli also produced lateral, vegetative "buds" (~1 cm to 10 cm

Foundation item: The National Natural Science Foundation of China under contract Nos 31970216 and 31670199; the Science and Technology Plan Project of Guangdong Province under contract No. 2012A020200007; the Scientific Research Plan of Tianjin Municipal Education Committee under contract No. JW1705; the Research Fund for Talented Scholars of Tianjin Normal University (2016).

*Corresponding author, E-mail: skyhbx@tjnu.edu.cn

*Acta Oceanol. Sin.*, 2022, Vol. 41, No. 12, P. 1–15
https://doi.org/10.1007/s13131-022-2047-8
http://www.aosocean.com
E-mail: ocean2@hyxb.org.cn

# Construction and analysis of a coral reef trophic network for Qilianyu Islands, Xisha Islands

Xiaofan Hong[1, 2, 3], Zuozhi Chen[1, 2*], Jun Zhang[1, 2], Yan'e Jiang[1, 2], Yuyan Gong[1, 2], Yancong Cai[1, 2], Yutao Yang[1, 2, 3]

[1] Key Laboratory for Sustainable Utilization of Open-sea Fishery of Ministry of Agriculture and Rural Affairs, South China Sea Fisheries Research Institute, Chinese Academy of Fishery Sciences, Guangzhou 510300, China

[2] Southern Marine Science and Engineering Guangdong Laboratory (Guangzhou), Guangzhou 510300, China

[3] College of Marine Sciences, Shanghai Ocean University, Shanghai 201306, China

Received 20 August 2021; accepted 22 April 2022



**Abstract**

Qilianyu Islands coral reefs (QICR), located in the northeastern part of the South China Sea, has been affected by human activities and natural disturbance. To characterize the trophic structure, ecosystem properties and keystone species of this region, a food-web model for the QICR is developed using methods involving a mass-balance approach with Ecopath with Ecosim software. Trophic levels range from 1.00 for detritus and primary producers to 3.80 for chondrichthyes. The mean trophic transfer efficiency for the entire ecosystem is 13.15%, with 55% of total energy flow originating from primary producers. A mixed trophic impact analysis indicates that coral strongly impacts most components of this ecosystem. A comparison of our QICR model with that for other coral reef ecosystems suggests that the QICR ecosystem is immature and/or is degraded.

**Key words:** South China Sea, Qilianyu Islands, coral reef, Ecopath model, food webs, ecosystem characteristic

**Citation:** Hong Xiaofan, Chen Zuozhi, Zhang Jun, Jiang Yan'e, Gong Yuyan, Cai Yancong, Yang Yutao. 2022. Construction and analysis of a coral reef trophic network for Qilianyu Islands, Xisha Islands. Acta Oceanologica Sinica, 41(12): 1–15, doi: 10.1007/s13131-022-2047-8



## 1 Introduction

The complex habitat composed of reef-building corals in the coral reef ecosystem is the main reason for its extremely high level of biodiversity and primary productivity (Knowlton, 2001). The large number of shelters, breeding grounds and nursery grounds in the ecosystem of coral reefs provide suitable habitats for various marine organisms with different living habits (Botha et al., 2013). However, coral reefs are currently under threat and deteriorating worldwide due to numerous influences of anthropogenic activities and climate change (Hoegh-Guldberg et al., 2007), which has prompted multifaceted conservation and restoration efforts (Baums, 2008).

Coral reefs in the South China Sea (SCS) cover an area of approximately $3.72\times10^4$ km$^2$, with tropical reefs therein accounting for nearly 5% of the total global area of coral reefs (Wang and Guan, 2020). The richness of corals in this region (571 species) is comparable to that in the "Coral Triangle" (Huang et al., 2015). Coral reef ecosystems in the SCS have abundant biological resources, with at least 3 600 fish species (Shao et al., 2008) (more than one-third of these are reef fish) having been reported from them. Coral reefs on the Xisha Islands of the central part of SCS are located more than 400 km from mainland China and are isolated from terrestrial nutrient influence via runoff through rivers and drains. As the main tropical fishing ground in China, there are more than 400 species of oceanic fish and coral reef fish in the coral reefs of the Xisha Islands, it is the important fishing ground for catching commercial fish such as tuna, mackerel, snapper, bonito, flying fish, shark and grouper. Moreover, as part of Xisha Islands, Qilianyu Islands also as the site of the largest spawning ground for green turtle (*Chelonia mydas*) in China (Zhang et al., 2020b), more than 40 species of birds occur there, and the surrounding waters are rich in high-quality and valuable seafoods (Yang, 2017). Despite all of this, the numbers and density of coral reef fish in the waters surrounding the Qilianyu Islands have recently trended down because of anthropogenic disturbance and natural environment variation (Li et al., 2017), such as overfishing, destructive fishing, ocean acidification, ocean warming, typhoon damage, and outbreaks of crown-of-thorns starfish (Wu et al., 2011), these factors also chiefly responsible for serious declines in SCS coral reef fishery resources (Zhang et al., 2020a). Continuing degradation of coral reef ecosystems has generated substantial interest in how management and restoration can support reef resilience (MacNeil et al., 2015). Many measures can be taken to reduce the threats affecting coral reef ecosystems. Confronting large-scale threats requires a major scaling-up of management and restoration efforts based on an improved understanding of the ecological processes that underlie reef resilience (Bellwood et al., 2004). Focusing in ecosystem assessment of coral reef, the lack of knowledge of the structure and function about coral reef ecosystems is one of the main problems for conserving

Foundation item: The National Key Research and Development Program of China under contract No. 2018YFC1406502; the National Natural Science Foundation of China under contract No. 31902374; the Key Special Project for Introduced Talents Team of Southern Marine Science and Engineering Guangdong Laboratory (Guangzhou) under contract No. GML2019ZD0605; the Central Public-Interest Scientific Institution Basal Research Fund of Chinese Academy of Fishery Sciences under contract No. 2020TD05.
*Corresponding author, E-mail: chenzuozhi@scsfri.ac.cn

*Acta Oceanol. Sin.*, 2022, Vol. 41, No. 4, P. 109–118
https://doi.org/10.1007/s13131-021-1943-7
http://www.aosocean.com
E-mail: ocean2@hyxb.org.cn

# The model of tracing drift targets and its application in the South China Sea

Yang Chen[1, 2], Shouxian Zhu[1, 2*], Wenjing Zhang[3], Zirui Zhu[2], Muxi Bao[4]

[1] Key Laboratory of Marine Hazards Forecasting of Ministry of Natural Resources, Hohai University, Nanjing 210098, China

[2] College of Oceanography, Hohai University, Nanjing 210098, China

[3] College of Meteorology and Oceanography, National University of Defense Technology, Nanjing 211101, China

[4] Nanjing Maritime Safety Administration, Nanjing 210009, China

Received 28 November 2020; accepted 27 July 2021



**Abstract**

A Leeway-Trace model was established for the traceability analysis of drifting objects at sea. The model was based on the Leeway model which is a Monte Carlo-based ensemble trajectory model, and a method of realistic traceability analysis was proposed in this study by using virtual spatiotemporal drift trajectory prediction. Here, measured data from a drifting buoy observation experiment in the northern South China Sea in April 2019, combined with surface current data obtained from the finite volume community ocean model (FVCOM), were used for the traceability analysis of humanoid buoys. The results were basically consistent with the observations, and the assimilation of measured current data can significantly improve the accuracy of the traceability analysis. Several sensitive experiments were designed to discuss the effects of wind and tide on the traceability analysis, and their results showed that the wind-driven current and the wind-induced leeway drift are both important to the traceability analysis. The effect of tidal currents on traceability could not be ignored even though they were much weaker than the residual currents in the experimental area of the northern South China Sea.

**Key words:** South China Sea, FVCOM, Leeway-Trace model, traceability analysis

**Citation:** Chen Yang, Zhu Shouxian, Zhang Wenjing, Zhu Zirui, Bao Muxi. 2022. The model of tracing drift targets and its application in the South China Sea. Acta Oceanologica Sinica, 41(4): 109–118, doi: 10.1007/s13131-021-1943-7

## 1 Introduction

The South China Sea (SCS) is an important international maritime transport corridor with heavy ship and aircraft traffic. It is abundant in fishery resources and there are many fishing vessels on the sea. The frequency of typhoons and other natural disasters in the SCS has posed serious dangers to ships and has affected the safety of aircrafts, and the statistics show that the China Maritime Search and Rescue Centre deals with more than 2 000 maritime accidents every year in the SCS (Zhu et al., 2019). The trajectory prediction of drifting object and the traceability analysis for drift target are two important issues that need to be resolved urgently for maritime security in the SCS (Cho et al., 2014; Zhou et al., 2019).

Over the last few decades, many international drift trajectory prediction models for search and rescue (SAR) have been developed, such as the Canadian CANSARP model (Abi-Zeid and Frost, 2005), the American HACSALV model (Allen, 2005), the Norwegian Leeway model (Breivik and Allen, 2008). The models of trajectory prediction for drifting object have also been studied in China. Jiang et al. (2011) established the domestic search area determination model based on the Monte Carlo method, and Xiao et al. (2013) constructed the East China Sea search and rescue path prediction system. The methods of trajectories prediction for drifting objects commonly adopt Lagrangian particle tracking models. The Lagrangian particle tracking method, which is also frequently used in seawater motion studies, describes the characteristics of seawater motion based on drifting particle trajectories (Chorin, 1973; Abi-Zeid and Frost, 2005; Chen, 2005). However, the trajectory prediction of buoyant objects, such as people in water (PIW), is more complex than the simulation of water particle trajectory (Fraser et al., 2009). The motion of a drifting object on the sea surface is affected by the ambient current, but its drifting velocity is not identical to the current velocity (Davidson et al., 2009; Coppini et al., 2016). The force of wind on the overwater structure of the object should not be ignored, and Breivik et al. (2011) defined it wind-induced leeway. The wind-induced motion needs to consider the differences in leeway coefficients for different types of objects, as well as the uncertainty in the direction of the leeway angle and the forecast errors in wind fields (Breivik et al., 2012; Brushett et al., 2017). The trajectories prediction of drifting object in actual maritime accident needs to consider the inaccuracy of the information regarding the time of accidents and the last known position (LKP) of the object on the sea (Richardson, 1997; Breivik et al., 2013). Traceability analysis of drifting object found after a maritime accident requires a reverse Lagrangian particle tracking method. Similar to the prediction of the drifting trajectory of buoyant objects, the traceability analysis should not only consider the effect of current velocity but also the effect of wind-induced leeway drift (including the differences in leeway coefficients for different types of objects, uncertainties in the direction of leeway angle, errors in wind field) and the error of the initial traceability information

Foundation item: The National Natural Science Foundation of China under contract Nos 41376012, 41076048 and 41275029.
*Corresponding author, E-mail: zhushouxian@vip.sina.com

*Acta Oceanol. Sin.*, 2022, Vol. 41, No. 7, P. 153–165
https://doi.org/10.1007/s13131-022-1991-7
http://www.aosocean.com
E-mail: ocean2@hyxb.org.cn

# Statistics of underwater ambient noise at high sea states arisen from typhoon out zones in the Philippine Sea and South China Sea

Qiulong Yang[1, 2, 3*], Kunde Yang[1, 2*], Shunli Duan[1, 2], Yuanliang Ma[1, 2]

[1] School of Marine Science and Technology, Northwestern Polytechnical University, Xi'an 710072, China

[2] Key Laboratory of Ocean Acoustics and Sensing, Ministry of Industry and Information Technology, Xi'an 710072, China

[3] Key Laboratory of Marine Environmental Information Technology, Ministry of Natural Resources, Tianjin 300171, China

Received 31 December 2020; accepted 10 November 2021



**Abstract**

Oceanic noise is the background interference in sonar performance prediction and evaluation at high sea states. Statistics of underwater ambient noise during Typhoons Soulik and Nida were analyzed on the basis of experimental measurements conducted in a deep area of the Philippine Sea and the South China Sea. Generated linear regression, frequency correlation matrix (FCM), Burr distribution and Gumbel distribution were described for the analysis of correlation with environmental parameters including wind speed (WS), significant wave height (SWH), and the inter-frequency relationship and probability density function of noise levels (NLs). When the typhoons were quite close to the receivers, the increment of NLs exceeded 10 dB. Whilst ambient noise was completely dominated by wind agitation, NLs were proportional to the cubic and quintic functions of WS and SWH, respectively. The fitted results between NLs and oceanic parameters were different for "before typhoon" and "after typhoon". The fitted slopes of linear regression showed a linear relationship with the logarithm of frequency. The average observed typhoon-generated NLs were 5 dB lower than the Wenz curve at the same wind force due to the insufficiently developed sea state or the delay between NLs and WS. The cross-correlation coefficient of FCM, which can be utilized in the identification of noise sources in different bands, exceeded 0.8 at frequencies higher than 250 Hz. Furthermore, standard deviation increased with frequency. The kurtosis was equal to 3 at >400 Hz approximately. The characteristics of NLs showed good agreement with the results of FCM.

**Key words:** statistics, underwater acoustics, cruise-measured ambient noise, typhoon, Philippine Sea, South China Sea, deep ocean

**Citation:** Yang Qiulong, Yang Kunde, Duan Shunli, Ma Yuanliang. 2022. Statistics of underwater ambient noise at high sea states arisen from typhoon out zones in the Philippine Sea and South China Sea. Acta Oceanologica Sinica, 41(7): 153–165, doi: 10.1007/s13131-022-1991-7

## 1 Introduction

Successfully forecasting typhoon intensity is of paramount importance in ensuring minimal damage to lives and properties. The knowledge on ambient noise at high sea states is useful in optimizing sonar performance and acquiring the Green function and sound speed profile (SSP) in an ocean waveguide (Brooks and Gerstoft, 2009). The highly complex physical processes associated with typhoon ocean interactions were investigated in the impact of typhoons on the ocean in the Pacific systematically (Pun et al., 2011; D'Asaro et al., 2014). Cyclonic eddies tend to promote upwelling, mixing and sea surface temperature (SST) cooling. SST cooling or wind wave agitation accumulates over time within the tropical cyclone inner-core (Jullien et al., 2014). Sound of short and long period double frequencies lower than 0.5 Hz are induced by the wave interaction generated by typhoons. Gravity wave interacts with the seafloor and couples into wind-generated seismic surface and body waves (Lin et al., 2017; Gerstoft and Bromirski, 2016).

The relationship between noise and environmental parameters has been extensively measured and researched over the past decades. Noise levels (NLs) during extreme wind conditions were measured in the northern Gulf of Mexico during the summers of 2001 and 2002 with three environmental acoustic recording systems deployed by the Littoral Acoustic Demonstration Center (Newcomb et al., 2004). Underwater noise data on typhoon intensities were collected by passive aquatic listeners on possible typhoon paths (Ma and Yang, 2009). NLs show a better correlation with wind speed (WS) than wave height during cyclone crossing (Sanjana et al., 2014). The correlation coefficient between ocean ambient NLs and WS during a typhoon event is

Foundation item: The Project of Global Change and Air-Sea Interaction under contract No. D5120210106; the Open Fund Project of Key Laboratory of Marine Environmental Information Technology, Ministry of Natural Resources of the People's Republic of China under contract No. D5110200611; the Fundamental Research Funds for the Central Universities under contract No. 3102019HHZY030011; the China Postdoctoral Science Foundation under contract No. 2019M663822; the National Natural Science Foundation of China under contract Nos 11574251 and 11704313.

*Corresponding author, E-mail: yangqiulong@nwpu.edu.cn; ykdzym@nwpu.edu.cn

*Acta Oceanol. Sin.*, 2022, Vol. 41, No. 6, P. 137–145
https://doi.org/10.1007/s13131-022-2015-3
http://www.aosocean.com
E-mail: ocean2@hyxb.org.cn

# Assessment of theoretical approaches to derivation of internal solitary wave parameters from multi-satellite images near the Dongsha Atoll of the South China Sea

Huarong Xie[1], Qing Xu[2]*, Quanan Zheng[3], Xuejun Xiong[4], Xiaomin Ye[5], Yongcun Cheng[6, 7]

[1] Key Laboratory of Marine Hazards Forecasting of Ministry of Natural Resources, Hohai University, Nanjing 210098, China

[2] College of Marine Technology, Faculty of Information Science and Engineering, Ocean University of China, Qingdao 266100, China

[3] Department of Atmospheric and Oceanic Science, University of Maryland, College Park, Maryland 20742, USA

[4] First Institute of Oceanography, Ministry of Natural Resources, Qingdao 266061, China

[5] National Satellite Ocean Application Service, State Oceanic Administration, Beijing 100081, China

[6] Southern Marine Science and Engineering Guangdong Laboratory (Guangzhou), Guangzhou 511458, China

[7] PIESAT Information Technology Co., Ltd., Beijing 100195, China

Received 15 March 2021; accepted 8 May 2021



**Abstract**

This study assesses the accuracy and the applicability of the Korteweg-de Vries (KdV) and the nonlinear Schrödinger (NLS) equation solutions to derivation of dynamic parameters of internal solitary waves (ISWs) from satellite images. Visible band images taken by five satellite sensors with spatial resolutions from 5 m to 250 m near the Dongsha Atoll of the northern South China Sea (NSCS) are used as a baseline. From the baseline, the amplitudes of ISWs occurring from July 10 to 13, 2017 are estimated by the two approaches and compared with concurrent mooring observations for assessments. Using the ratio of the dimensionless dispersive parameter to the square of dimensionless nonlinear parameter as a criterion, the best appliable ranges of the two approaches are clearly separated. The statistics of total 18 cases indicate that in each 50% of cases, the KdV and the NLS approaches give more accurate estimates of ISW amplitudes. It is found that the relative errors of ISW amplitudes derived from two theoretical approaches are closely associated with the logarithmic bottom slopes. This may be attributed to the nonlinear growth of ISW amplitudes as propagating along a shoaling thermocline or topography. The test results using three consecutive satellite images to retrieve the ISW propagation speeds indicate that the use of multiple satellite images (>2) may improve the accuracy of retrieved phase speeds. Meanwhile, repeated multi-satellite images of ISWs can help to determine the types of ISWs if mooring data are available nearby.

**Key words:** internal solitary waves, KdV equation, NLS equation, South China Sea, satellite images

**Citation:** Xie Huarong, Xu Qing, Zheng Quanan, Xiong Xuejun, Ye Xiaomin, Cheng Yongcun. 2022. Assessment of theoretical approaches to derivation of internal solitary wave parameters from multi-satellite images near the Dongsha Atoll of the South China Sea. Acta Oceanologica Sinica, 41(6): 137–145, doi: 10.1007/s13131-022-2015-3

## 1 Introduction

The ocean internal waves (IWs) play a significant role in the nutrient transport, underwater acoustic propagation, offshore engineering, and submarine navigation (Osborne and Burch, 1980; Jackson, 2007; Xu et al., 2008; Guo and Chen, 2014; Zhao et al., 2014; Alford et al., 2015; Dong et al., 2016; Huang et al., 2016; Xie et al., 2016). Satellite observations show that the IWs are broadly distributed in the northern South China Sea (NSCS) from the Luzon Strait to Hainan Island, especially near the Dongsha Atoll and generally propagate westward in the form of internal solitary wave (ISW) packets (Hsu and Liu, 2000; Zhao et al., 2004; Zheng et al., 2008, 2020; Wang et al., 2013; Zheng, 2017). Before reaching the continental shelf, the ISWs typically have the trans-basin evolution and dissipate almost all their energy (Chang et al., 2006; Dai et al., 2011; Xie et al., 2019). These waves are more active from April to July and occur less frequently in winter owing to the deep surface mixed layer and weaker stratification (Zheng et al., 2007; Ramp et al., 2010). Three types of ISWs with different re-appearance periods have been observed in the NSCS. Type-A ISWs re-appear regularly at the same time each day, while type-B and type-C waves re-appear one hour later and earlier each day, respectively (Ramp et al., 2004; Chen et al., 2018).

Previous investigators have addressed that satellite remote sensing technology is an important tool for observing ISWs. Besides the spatial and temporal distribution characteristics, the quantitative data of dynamic parameters, such as the amplitude,

Foundation item: The National Key Project of Research and Development Plan of China under contract No. 2016YFC1401905; the National Natural Science Foundation of China under contract No. 41976163; the Key Special Project for Introduced Talents Team of Southern Marine Science and Engineering Guangdong Laboratory (Guangzhou) under contract No. GML2019ZD0602; the Guangdong Special Fund Program for Marine Economy Development under contract No. GDNRC[2020]050.
*Corresponding author, E-mail: xuqing@ouc.edu.cn

*Acta Oceanol. Sin.*, 2022, Vol. 41, No. 2, P. 26–40
https://doi.org/10.1007/s13131-021-1903-2
http://www.aosocean.com
E-mail: ocean2@hyxb.org.cn

# Assimilating satellite SST/SSH and *in-situ T*/*S* profiles with the Localized Weighted Ensemble Kalman Filter

Meng Shen[1], Yan Chen[1], Pinqiang Wang[1], Weimin Zhang[1, 2*]

[1] College of Meteorology and Oceanology, National University of Defense Technology, Changsha 410073, China

[2] Laboratory of Software Engineering for Complex Systems, Changsha 410073, China

Received 5 March 2021; accepted 27 July 2021



**Abstract**

The Localized Weighted Ensemble Kalman Filter (LWEnKF) is a new nonlinear/non-Gaussian data assimilation (DA) method that can effectively alleviate the filter degradation problem faced by particle filtering, and it has great prospects for applications in geophysical models. In terms of operational applications, along-track sea surface height (AT-SSH), swath sea surface temperature (S-SST) and *in-situ* temperature and salinity (*T*/*S*) profiles are assimilated using the LWEnKF in the northern South China Sea (SCS). To adapt to the vertical S-coordinates of the Regional Ocean Modelling System (ROMS), a vertical localization radius function is designed for *T*/*S* profiles assimilation using the LWEnKF. The results show that the LWEnKF outperforms the local particle filter (LPF) due to the introduction of the Ensemble Kalman Filter (EnKF) as a proposal density; the RMSEs of SSH and SST from the LWEnKF are comparable to the EnKF, but the RMSEs of *T*/*S* profiles reduce significantly by approximately 55% for the *T* profile and 35% for the *S* profile (relative to the EnKF). As a result, the LWEnKF makes more reasonable predictions of the internal ocean temperature field. In addition, the three-dimensional structures of nonlinear mesoscale eddies are better characterized when using the LWEnKF.

**Key words:** data assimilation, Localized Weighted Ensemble Kalman Filter, northern South China Sea, sea surface height, sea surface temperature, temperature and salinity profiles, mesoscale eddy

**Citation:** Shen Meng, Chen Yan, Wang Pinqiang, Zhang Weimin. 2022. Assimilating satellite SST/SSH and *in-situ T*/*S* profiles with the Localized Weighted Ensemble Kalman Filter. Acta Oceanologica Sinica, 41(2): 26–40, doi: 10.1007/s13131-021-1903-2

## 1 Introduction

Data assimilation (DA) is playing an increasingly important role in the numerical prediction of atmosphere and ocean. It can improve the analysis and prediction effects of a model by continuously integrating observations (Shen et al., 2016) and can also be used to optimize parameters of the model.

The most widely used ocean DA methods are variational methods and the ensemble Kalman filter (EnKF). The four-dimensional variational (4D-Var) method is a variational method that obtains the best trajectory by minimizing the cost function. Compared with 4D-Var, the EnKF does not need to construct the tangent linear or adjoint operators of the model and can estimate the background error covariance matrix using an ensemble. The limitations of the EnKF lie in the implicit assumption of model linearity in the background error covariance matrix calculation and Gaussian distributions of model error and observation error. Thus, in theory, the EnKF may not be applicable to strong nonlinear/non-Gaussian systems. In earlier studies, oceanographers assumed that changes in the ocean occurred slowly and thus that the evolution of the ocean involved a weakly nonlinear process. However, mesoscale eddies have strong nonlinear characteristics (Zhang et al., 2020). To better characterize nonlinear evolution in the ocean, nonlinear DA methods such as the particle filter (PF) have received increasing attention.

Both the PF and EnKF are based on the statistical estimation theory. Compared with the EnKF, the PF is not limited by the linear model, linear/weak nonlinear observations or the hypothesis of Gaussian-distributed error and can be applied to any nonlinear/non-Gaussian dynamic system in theory. In the PF, the probability density function (PDF) of states is approximated by the weighted mean of the particles. The observations affect the weights of the particles rather than the values of the particles. With assimilation progress, most particles cannot obtain meaningful weights (close to 0) due to the large gap between them and observations, which is known as filter degeneracy in the PF. To alleviate or overcome filter degeneracy, four main techniques were introduced to the PF, including proposal density, transportation, localization and hybridization (van Leeuwen et al. 2019).

The basic idea of localization is calculating particle weights locally. The PF localization techniques can be divided into two categories (Farchi and Bocquet, 2018). One is state-domain localization, which independently analyzes grid points using only the observations in a localized region. This approach is easy to implement in parallel but may lead to an imbalance between state variables. The related studies include Rebeschini and van Handel (2015), Penny and Miyoshi (2016), Lee and Majda (2016), and Chustagulprom et al. (2016). The other is sequential-observation localization. In this method, each observation is sequentially assimilated. An analysis is implemented at each observation site, and only the model variables near the observation site are up-

Foundation item: The National Key Research and Development Program of China under contract No. 2018YFC1406202; the National Natural Science Foundation of China under contract No. 41830964.
*Corresponding author, E-mail: wmzhang104@139.com

*Acta Oceanol. Sin.*, 2022, Vol. 41, No. 9, P. 149–157
https://doi.org/10.1007/s13131-022-1988-2
http://www.aosocean.com
E-mail: ocean2@hyxb.org.cn

# Optical flow-based method to estimate internal wave parameters from X-band marine radar images

Jinghan Wen[1], Zhongbiao Chen[1], Yijun He[1, 2*]

[1] School of Marine Sciences, Nanjing University of Information Science & Technology, Nanjing 210044, China

[2] Key Laboratory of Space Ocean Remote Sensing and Applications, National Satellite Ocean Application Service, Beijing 100081, China

Received 5 August 2021; accepted 18 January 2022



**Abstract**

The velocity and direction of internal waves (IWs) are important parameters of the ocean, however, traditional observation methods can only obtain the average parameters of IWs for a single location or large area. Herein, a new method based on optical flow is proposed to derive the phase velocity vectors of IWs from X-band marine radar images. First, the X-band marine radar image sequence is averaged, and ramp correction is used to reduce the attenuation of gray values with increasing radial range. Second, the average propagation direction of the IWs is determined using the two-dimensional Fourier transform of the radar images; two radial profiles along this direction are selected from two adjacent radar images; and then, the average phase velocity of the IWs is estimated from these radial profiles. Third, the averaged radar images are processed via histogram equalization and binarization to reduce the influence of noise on the radar images. Fourth, a weighting factor is determined using the average phase velocity of a reference point; the phase velocities on the wave crest of the IWs are subsequently estimated via the optical flow method. Finally, the proposed method is validated using X-band marine radar image sequences observed on an oil platform in the South China Sea, and the error of the phase velocity is calculated to be 0.000 3–0.073 8 m/s. The application conditions of the proposed method are also discussed using two different types of IW packets.

**Key words:** internal wave, X-band marine radar, optical flow, phase velocity

**Citation:** Wen Jinghan, Chen Zhongbiao, He Yijun. 2022. Optical flow-based method to estimate internal wave parameters from X-band marine radar images. Acta Oceanologica Sinica, 41(9): 149–157, doi: 10.1007/s13131-022-1988-2

## 1 Introduction

Internal waves (IWs) are ubiquitous in the ocean and play important roles in energy transfer, biological processes, marine production activities, and ocean engineering. Because IWs frequently occur in the South China Sea (SCS), observing these waves in this region is highly significant (Huang et al., 2016).

*In-situ* observations, such as acoustic Doppler current profiles and conductivity–temperature–depth, are widely used to observe IWs. These strategies enable the observation of the amplitude, period, phase velocity, polarity, and other characteristics of IWs with high accuracy (Briscoe, 1975) but are usually limited to specific locations. Moreover, they cannot determine the characteristics of IWs at different locations.

Developments in satellite remote sensing have enabled the observation of IWs using optical and microwave satellite images. Synthetic aperture radar (SAR) can obtain high-resolution (several meters) sea surface images, rendering it suitable for observing IWs (Yang et al., 2001); additionally, it has the advantage of being able to conduct all-day, all-weather operations. Alpers (1985) presented a fundamental radar imaging theory of IWs for SAR in 1985, i.e., IW leads to sea-surface convergence or divergence, which changes the surface roughness, thereby affecting the gray level of the radar image. Many characteristics of IWs have been estimated in the literature based on this study, such as the velocity of IWs (Li et al., 2000), the characteristic half-widths of IWs (Zheng et al., 2001), the amplitudes of IWs (Jia et al., 2019), and the spatial distribution of IWs (Liu et al., 1998; Ning et al., 2020). The moderate resolution imaging spectroradiometer (MODIS) has a large swath area of several hundred kilometers, fine spatial resolution, and near-daily global coverage; hence, it is commonly used to study the IWs, in particular, to study characteristics such as the occurrence frequency (Jackson, 2007; Wang et al., 2011), propagation and sources (Sun et al., 2019; Wang et al., 2013), and spatial distribution (Zhou et al., 2016) of IWs.

X-band marine radar has high spatiotemporal resolution and can obtain sea surface images in real-time. Thus, this technology may help determine the evolution of an IW packet (Kropfli et al., 1999). The imaging mechanism of X-band marine radar is similar to that of SAR; specifically, it detects modulations in sea surface roughness associated with currents induced by IWs (Xue et al., 2013). Watson and Robinson (1990) studied the evolution of IWs in the Strait of Gibraltar using X-band marine radar images. Orr and Mignerey (2003) used X-band marine radar to track IWs in the SCS. Ramos et al. (2009) used Radon transform to calculate IW parameters, such as the propagation direction of IWs, their nonlinear velocity, the distance between solitary waves, and the number of solitary waves in each packet, from radar backscatter images. Lü et al. (2010) employed Radon transform to re-

Foundation item: The National Natural Science Foundation of China under contract Nos 41620104003 and 42027805; the National Natural Science Youth Foundation of China under contract No. 41506199.
*Corresponding author, E-mail: yjhe@nuist.edu.cn

*Acta Oceanol. Sin.*, 2022, Vol. 41, No. 9, P. 182–191
https://doi.org/10.1007/s13131-022-1994-4
http://www.aosocean.com
E-mail: ocean2@hyxb.org.cn

# A hybrid forecasting model for depth-averaged current velocities of underwater gliders

Yaojian Zhou[1], Yonglai Zhang[1]*, Wenai Song[1], Shijie Liu[2], Baoqiang Tian[3]

[1] Software School, North University of China, Taiyuan 030051, China

[2] State Key Laboratory of Robotics, Shenyang Institute of Automation, Chinese Academy of Sciences, Shenyang 110016, China

[3] School of Mechanical Engineering, North China University of Water Resources and Electric Power, Zhengzhou 450045, China

Received 2 August 2021; accepted 20 December 2021



**Abstract**

In this paper, we propose a hybrid forecasting model to improve the forecasting accuracy for depth-averaged current velocities (DACVs) of underwater gliders. The hybrid model is based on a discrete wavelet transform (DWT), a deep belief network (DBN), and a least squares support vector machine (LSSVM). The original DACV series are first decomposed into several high- and one low-frequency subseries by DWT. Then, DBN is used for high-frequency component forecasting, and the LSSVM model is adopted for low-frequency subseries. The effectiveness of the proposed model is verified by two groups of DACV data from sea trials in the South China Sea. Based on four general error criteria, the forecast performance of the proposed model is demonstrated. The comparison models include some well-recognized single models and some related hybrid models. The performance of the proposed model outperformed those of the other methods indicated above.

**Key words:** *:* underwater glider, hybrid forecasting model, depth-averaged current velocities (DACVs)

**Citation:** Zhou Yaojian, Zhang Yonglai, Song Wenai, Liu Shijie, Tian Baoqiang. 2022. A hybrid forecasting model for depth-averaged current velocities of underwater gliders. Acta Oceanologica Sinica, 41(9): 182–191, doi: 10.1007/s13131-022-1994-4

## 1 Introduction

Underwater gliders are excellent autonomous mobile ocean observation platforms (Webb et al., 2001; Eriksen et al., 2001; Sherman et al., 2001; Rudnick, 2016; Liu et al., 2020b). Compared with other platforms, underwater gliders have incomparable advantages such as low cost, long endurance, and convenient recovery. In recent years, they have been widely used in the observation of complex ocean phenomena such as air-sea interactions (Qiu et al., 2015) and mesoscale eddies (Qiu et al., 2019; Li et al., 2020) and achieved some significant results. However, buoyancy drive features make them highly sensitive to ocean currents, resulting in their failure to follow an arbitrary trajectory to a predetermined location (Rudnick et al., 2018). Therefore, it is essential to know the ocean flow information in advance in the environment where the glider will travel. However, being influenced by *in situ* observation capability, numerical ocean model forecast technology, and data storage technology, the existing ocean dynamics models for current forecasting possess many problems, such as low spatial resolution and a large number of errors, which means that the forecast values cannot satisfy the underwater glider application demand. Moreover, due to the limited carrying capacity and power, unless specifically required, underwater gliders are not equipped with current meters or acoustic Doppler current profilers (Zhou et al., 2017; Sun et al., 2020). Fortunately, the depth-averaged current (DAC) of underwater gliders can solve the above contradiction: the integration value of different types of ocean currents in glider profiles can be calculated directly by gliders rather than external current forecast models or ocean current sensors. The details of how to calculate the depth-averaged current velocity (DACV) can be seen in Zhou et al. (2017) and Merckelbach et al. (2008). Because DACV is an important and unique characteristic of underwater glider, its research is of great significance to the development of underwater glider. In particular, the study of DAC research can improve the ability of underwater gliders to perform observation missions and facilitate the development of other related ocean observation platforms.

Depth-averaged current velocities (DACVs) can be used to assist the navigation and path planning of underwater gliders in their deployments (Merckelbach et al., 2008; Chang et al., 2015). In addition, DACVs have many other applications, such as current equipment, and ocean model calibration. However, it is not easy to measure the DACV accurately, which depends on many factors, such as the pitch, measurement heading, and repeatable hydrodynamic shape (Rudnick et al., 2018).

In terms of actual utility, we care more about the predicted value of DACVs than its real-time measurement at most times because only the former can provide the glider with information about environmental currents in advance. However, compared with real-time measurement, predicting DACVs is even more challenging. Only a few scholars have studied DACVs prediction, and there are many limitations in their forecasting schemes. For

Foundation item: The National Natural Science Foundation of China under contract Nos U1709202 and 51809127; the Natural Science Foundation of Shanxi Province, China under contract No. 201901D211248.
*Corresponding author, E-mail: zhangyonglai@nuc.edu.cn

*Acta Oceanol. Sin.*, 2022, Vol. 41, No. 10, P. 154–170
https://doi.org/10.1007/s13131-022-2018-0
http://www.aosocean.com
E-mail: ocean2@hyxb.org.cn

# Remote sensing survey and research on internal solitary waves in the South China Sea-Western Pacific-East Indian Ocean (SCS-WPAC-EIND)

Junmin Meng[1, 2*], Lina Sun[1, 2], Hao Zhang[1, 2], Beilei Hu[1, 2], Fucheng Hou[1, 2], Sude Bao[1, 2]

[1] First Institute of Oceanography, Ministry of Natural Resources, Qingdao 266061, China

[2] Technology Innovation Center for Ocean Telemetry, Ministry of Natural Resources, Qingdao 266061, China

Received 29 November 2021; accepted 8 March 2022



**Abstract**

Internal solitary waves (ISWs) are common mesoscale dynamic processes in the ocean that are spread throughout the world's oceans. The South China Sea (SCS), Western Pacific (WPAC) and Indian Ocean (EIND) (SCS-WPAC-EIND) are areas where ISWs frequently occur. In particular, in the northern part of the South China Sea, Sulu Sea, Celebes Sea, Andaman Sea, Lombok Strait and northeastern part of Taiwan Island, ISWs exist almost year-round. Remote sensing is an important technique to carry out investigations and research on ISWs on a large scale. In particular, optical sensors represented by the Moderate Resolution Imaging Spectroradiometer (MODIS) can observe ISWs for a long time and on a large scale, while SAR sensors such as Sentinel-1 A/B can compensate for the deficiencies in optical sensors and comprehensively observe ISWs. Based on many years of remote sensing surveys of ISWs, this paper uses MODIS and Sentinel-1 satellite remote sensing images of more than 70 000 scenes from 2010 to 2020 to carry out survey studies of ISWs in the SCS-WPAC-EIND. The survey systematically gives the temporal and spatial distribution characteristics of ISWs in the SCS-WPAC-EIND and focuses on the analysis of the ISW characteristics in main areas in the SCS-WPAC-EIND, thereby providing basic data for further research on ISWs.

**Key words:** internal solitary waves, SCS-WPAC-EIND, remote sensing, MODIS, Sentinel-1A/B

**Citation:** Meng Junmin, Sun Lina, Zhang Hao, Hu Beilei, Hou Fucheng, Bao Sude. 2022. Remote sensing survey and research on internal solitary waves in the South China Sea-Western Pacific-East Indian Ocean (SCS-WPAC-EIND). Acta Oceanologica Sinica, 41(10): 154–170, doi: 10.1007/s13131-022-2018-0

## 1 Introduction

Internal solitary waves (ISWs) are an important marine dynamic process with large amplitudes, short periods, and fast velocities. ISWs referred to in this paper are usually generated by the interaction between internal tides and terrain, such as sea sills, and undergo nonlinear evolution. They have an important impact on material transportation, vertical mixing, sound propagation and the safety of submarine navigation in the ocean. ISWs have a large scale and a wide range of effects, covering all major oceans in the world (Jackson, 2007). Especially in the South China Sea (SCS), Western Pacific (WPAC) and Indian Ocean (EIND) (SCS-WPAC-EIND) adjacent to China's surrounding areas, ISWs are more common. Among them, the SCS is a sea area in which ISWs occur most frequently in the world. It is known as a natural test site for researching ISWs, and ISWs with the largest amplitudes have been detected in this area (Fang and Du, 2005; Huang et al., 2016). The Sea of Japan in the WPAC and the seas of northeastern Taiwan Island are also areas where ISWs frequently occur (Sun et al., 2018b; Meng, 2002). Due to the influence of tides and topography, the morphological characteristics of ISWs are complicated. ISWs in the Andaman Sea and the Lombok Strait in the EIND have large scales and relatively regular shapes; these areas have become important areas of research on ISWs in recent years.

As ISWs propagate through the ocean, they modulate the redistribution of microscale waves on the sea surface, thereby changing the distribution of sea surface roughness, and thus can be observed from the air. At present, the methods commonly used in ISW research include field observations, numerical simulations and remote sensing observations. In contrast, although remote sensing observations are affected by the environment, they can record the changes in the sea surface when ISWs pass by on a larger scale and can invert the underwater parameters of ISWs based on related models. ISW remote sensing research can basically be divided into three categories: optical remote sensing, which mainly has the advantages of a large swath width and short revisit period; synthetic aperture radar (SAR) remote sensing, which actively emits microwaves and has the advantages of high spatial resolution and all-day weather observations; and actively emitting microwave altimeters, which can detect changes in sea surface height caused by ISWs but usually cannot produce images.

With the rapid development of satellite and sensor technology, researchers have used various remote sensing images to study the characteristics of ISWs and reveal their interactions with the surrounding environment. For ISW optical remote sens-

Foundation item: The National Natural Science Foundation of China under contract No. 42006164; the Global Change and Air-Sea Interaction Program of China under contract Nos GASI-02-SCS-YGST2-04, GASI-02-IND-YGST2-04 and GASI-02-PAC-YGST2-04.
*Corresponding author, E-mail: mengjm@fio.org.cn

*Acta Oceanol. Sin.*, 2021, Vol. 40, No. 6, P. 129–130
https://doi.org/10.1007/s13131-021-1875-2
http://www.aosocean.com
E-mail: ocean2@hyxb.org.cn

**News and Views**

# The first near real-time inverted echo sounder observation in the South China Sea

Ruixiang Zhao[1, 2], Xiaohua Zhu[1, 2, 3]*, Chuanzheng Zhang[1, 2], Hua Zheng[1, 3]

[1] State Key Laboratory of Satellite Ocean Environment Dynamics, Second Institute of Oceanography, Ministry of Natural Resources, Hangzhou 310012, China

[2] Southern Laboratory of Ocean Science and Engineering (Zhuhai), Zhuhai 519082, China

[3] School of Oceanography, Shanghai Jiao Tong University, Shanghai 200030, China

Received 18 May 2021; accepted 14 June 2021



We report the first near real-time inverted echo sounder (IES) observation in the South China Sea (Fig. 1). Although the first IES observation in the South China Sea was in 2005, and the near real-time IES observation module was first developed in 2012 (http://www.po.gso.uri.edu/dynamics/IES/hist.html), the real-time IES has never been deployed in the South China Sea until the reporting of observations in this study. IES is a bottom-mounted mooring that records the round-trip acoustic travel time from the bottom to the surface and back ($\tau$), bottom pressure, and near bottom velocities (eastward component $\vec{u}$ and westward component $\vec{v}$). To achieve near real-time observations, four Popeye data-shuttles (PDSs) contained in a float sphere were deployed around the IES. The PDSs are the add-on devices of IES, and can serve as a data carrier. When the PDS was activated at its scheduled time, the IES transmitted its data by generating a non-propagating magnetic field around its housing. The PDS equipped with a magnetic field detector converted the amplitude modulations of the field into digital signals and recorded the IES data. After complete data download, the PDS was released from the anchor and it floated on the surface. Subsequently, the PDS accessed the Iridium Short Burst Data (SBD) service and transmitted IES observation data to the email address of the user. Each PDS-IES system can achieve four near real-time data transmissions before recovery.

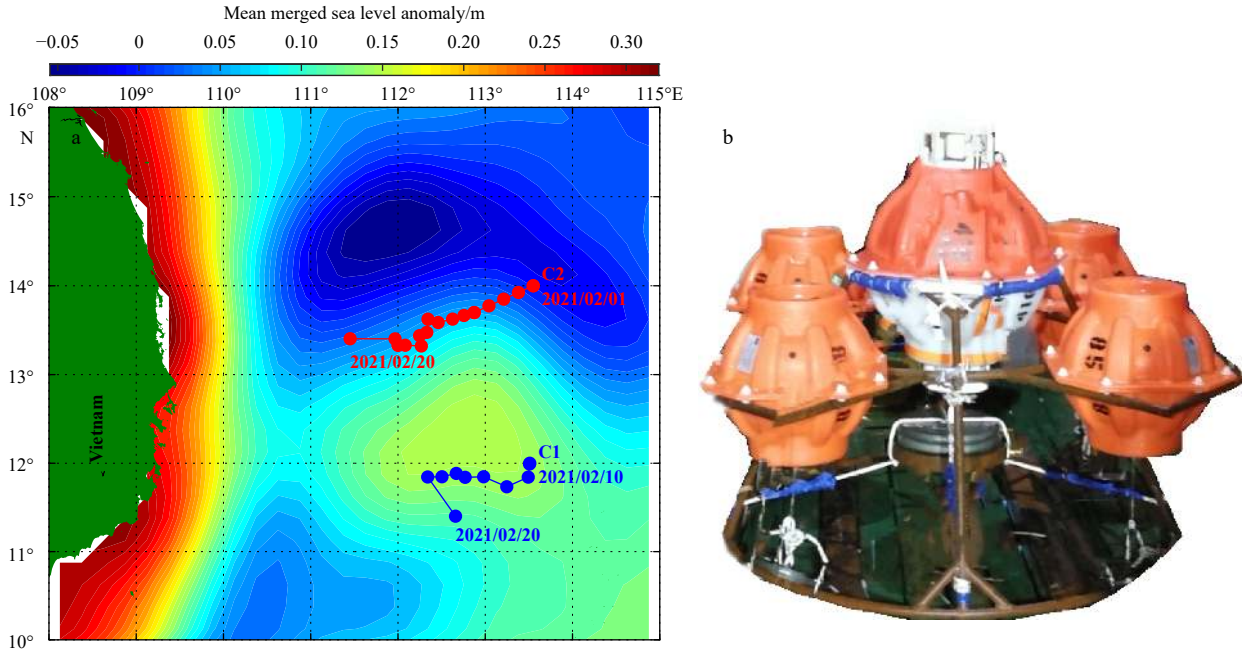


**Fig. 1.** Location map of the PDS-IES stations (C1 and C2) and trajectories of PDSs after reaching the surface (February 10 and 1 for C1 and C2, respectively) (a), and a photo of PDS-IES before deployment (b). The instrument in the middle is IES, which is surrounded by four PDSs.

Foundation item: The Scientific Research Fund of Second Institute of Oceanography, MNR, under contract Nos QNYC2102, JZ2001 and JT1801; the National Natural Science Foundation of China under contract Nos 41920104006, 41906023, 41806020, 41776107, 41906024 and 41976001; the Project of State Key Laboratory of Satellite Ocean Environment Dynamics, SIO, under contract No. SOEDZZ2106.

*Corresponding author, E-mail: xhzhu@sio.org.cn

*Acta Oceanol. Sin.*, 2021, Vol. 40, No. 11, P. 196–199
https://doi.org/10.1007/s13131-021-1963-3
http://www.aosocean.com
E-mail: ocean2@hyxb.org.cn

**News and Views**

# Advances in interscale and interdisciplinary approaches to the South China Sea

Lingling Xie[1, 2, 3], Yi Guan[1, 2, 3]*, Jianyu Hu[4], Quanan Zheng[5]

[1] Laboratory of Coastal Ocean Variation and Disaster Prediction, College of Ocean and Meteorology, Guangdong Ocean University, Zhanjiang 524088, China

[2] Key Laboratory of Climate, Resources and Environments in Continent Shelf Sea and Deep Ocean, Zhanjiang 524088, China

[3] Key Laboratory of Space Ocean Remote Sensing and Applications, Ministry of Natural Resources, Beijing 100081, China

[4] State Key Laboratory of Marine Environmental Science, College of Ocean and Earth Sciences, Xiamen University, Xiamen 361005, China

[5] Department of Atmospheric and Oceanic Science, University of Maryland, College Park 20742, USA

Received 1 November 2021; accepted 10 November 2021



The South China Sea (SCS) connects the Pacific Ocean and the Indian Ocean, and acts as an important part in regional and global climate systems (e.g., Qu et al., 2009; Wang et al., 2009). Multi-scale dynamic and biogeochemical processes in the SCS, comprising a hot spot in marginal sea studies, have attracted great attentions from researchers (e.g., Chen et al., 2020; Hu et al., 2020). The South China Sea Annual Meeting (SCSAM) 2021, recently held on October 22–24 in Zhanjiang, China, focused on academic exchanges of the newly research results and progresses in the interdisciplinary multi-scale processes in the SCS. The SCSAM 2021 is the eighth international workshop of the series, which started in April 2013 (Zhu, 2013) and renamed as SCSAM in 2018. There were 90 oral presentations and 57 posters in the meeting this year, which attracted attentions of more than 2 000 audiences both on line and on site. This short article summaries the cutting-edge advances in interscale and interdisciplinary approaches to the SCS from the meeting presentations and the associated research.

Three-dimensional (3D) basin circulation provides the basic and important dynamic environment for processes in the SCS. Previous investigators have revealed that the large-scale three-layer ocean circulation in the SCS is featured by cyclonic/anticyclonic circulation in the upper layer, anticyclonic in the middle layer, and cyclonic in the deep layer (e.g., Gan et al., 2016; Cai and Gan, 2021). The new findings further show the meridional overturning circulation in the upper layer (Lan and Jiang, 2021) and the variability of the deep circulation in the SCS (Zhu et al., 2021). Meanwhile, intra-seasonal variations of currents in the upper and deep layers of the northern SCS were observed and attributed to the topographic Rossby waves (Zheng et al., 2021b; Shu et al., 2021). Subseasonal variability in the SCS was revealed by numerical simulations (Xie et al., 2020). In terms of energy and vorticity balances, Huang (2021) diagnosed the roles played in regulating the SCS circulation by the SCS throughflow, the local wind stress, the deep overflow through the Luzon Strait, the local thermohaline forcing and the meso/submeso-scale eddies, and concluded that the contribution from the open ocean plays a dominant role.

The interaction between the SCS with its adjacent open oceans attracts more input from many research teams. Wei and Xu (2021) summarized couplings within a system consisting of the Pacific Ocean, the SCS and the Indian Ocean, indicating that the interannual variations in the Pacific and Indian Oceans change the monsoon-derived circulation in the SCS, the freshwater transport by the SCS throughflow into the Indonesian seas significantly influences the Indonesian Throughflow (ITF), and the SCS summer monsoon contributes to the development of the Indian Ocean Dipole (IOD). Susanto et al. (2021) reported the tidal mixing in controlling the ITF and regional circulation. Wu et al. (2021a), Zhou and Liu (2021) and Zhou (2021) investigated the multiscale variations of the main currents in the North Pacific, and Gong (2021) presented the variation of the deep circulation in the Pacific in the paleoclimate. Zhong et al. (2020) evidenced the Kuroshio intrusion into the SCS as a form of interaction between the SCS and the Pacific.

The mesoscale eddies are quite active and energetic in the SCS. Recently, the interscale interactions of meoscale eddies and other processes have become a research hot spot. The reported new results include modulation of eddies to small-scale processes such as sea surface waves (Tan et al., 2021), internal tides (Deng and Xie, 2021) and turbulent mixing (Liu and Liao, 2021). Besides, Sun et al. (2021b) studied abnormal eddies, i.e., cyclonic warm-core eddies and anticyclonic cold-core eddies, in the northeastern SCS associated with the Kuroshio intrusion. Sun et al. (2021a) found a strong Kuroshio intrusion into the SCS and its accompanying cold-core anticyclonic eddy in winter 2020–2021. Dong et al. (2021a) analyzed the symmetric instability, gravitational instability and centrifugal instability in the surface mixed layer of an anticylonic eddy and found that the symmetric instability dissipation plays a key role in the eddy kinetic energy budget. Xie (2021) revealed the seasonal reversal of eddy polarity distribution (PDR) in the SCS and

Foundation item: The National Natural Science Foundation of China under contract Nos 41776034 and 91958203; the Innovation Team Plan in Universities of Guangdong Province under contract No. 2019KCXTF021; the Guangdong Province First-Class Discipline Plan under contract No. CYL231419012.
*Corresponding author, E-mail: yiguan@gdou.edu.cn

# Acta Oceanologica Sinica

## Introduction

*Acta Oceanologica Sinica* is a monthly academic journal founded in 1982, which publishes the most recent scientific achievements and results as well as papers in the field of ocean sciences.

**Scope:**

Physical oceanography, marine physics, marine chemistry, marine geology, marine biology, marine meteorology, ocean engineering, marine remote sensing, and marine environment sciences

**Column:**

Original research papers, review articles, and research notes. News and views are also included.

**Journal information:**

Editor-in-Chief: Chen Dake
Govern Body: China Association for Science and Technology
Sponsor: Chinese Society of Oceanography
Publisher: China Ocean Press
ISSN: 0253-505X (print version)
ISSN: 1869-1099 (electronic version)
E-mail: ocean1@hyxb.org.cn; ocean2@hyxb.org.cn
Tel.: +86-10-62179976
Address: Editorial Office of Acta Oceanologica Sinica, No. 8 Dahuisi Road, Haidian District, Beijing 100081, China
Website: http://www.hyxb.org.cn
Online Submission: https://mc03.manuscriptcentral.com/actaos
Distributed abroad by Springer-Verlag

**Abstracted/indexed in:**

Science Citation Index Expanded (SCI search), Journal Citation Reports/Science Edition, SCOPUS, INSPEC, Chemical Abstracts Service (CAS), Google Scholar, EBSCO, CSA, Academic OneFile, ASFA, Chinese Science Citation Database, Current Contents/Physical, Chemical and Earth Sciences, Environment Index, INIS Atomindex, OCLC, SCImago, Summon by Serial Solutions, VINITI-Russian Academy of Science, Zoological Record